

ELECTRICAL STIMULATION IN BONE CELL CULTURE MEDIA

ELECTRICAL STIMULATION IN BONE CELL CULTURE MEDIA

By TAYLOR DEVET B.ENG

A Thesis Submitted to the School of Graduate Studies in Partial Fulfilment of the
Requirements for the Degree Master of Applied Science

McMaster University © Copyright by Taylor deVet, November 2020

MASTER OF APPLIED SCIENCE (2020) McMaster University
School of Biomedical Engineering, Hamilton, Ontario
TITLE: Electrical Stimulation in Bone Cell Culture Media
AUTHOR: Taylor deVet, B.Eng. (McMaster University)
SUPERVISOR: Gregory R. Wohl, Ph. D., P.Eng.
NUMBER OF PAGES: xiv, 154

Lay Abstract

Osteocytes are the least understood bone cells and the way that they communicate with the bone matrix and other cells is widely debated. It is assumed that osteocytes sense mechanical stresses within the bone matrix through electrical charges that develop in areas of increased strain. External electrical stimuli have been shown to increase bone formation indicating that the cells are electrically sensitive. The electrical sensitivity of the osteocytes specifically is under-researched causing a gap in knowledge of the behaviour of the cell in the remodelling process. To study the effects of electrical stimulation on osteocytes, an experimental apparatus must be designed to deliver stimulation to the cells *in vitro* and maintain a stable environment. A culture medium is needed to keep cells alive *in vitro* To do this, the electrical characteristics of the cell culture medium must be understood in attempts to maintain homeostatic conditions for the cells.

Abstract

Osteocytes are the most abundant bone cells, however, they are also the least understood. They sense mechanical stress within the bone matrix to control remodelling, but there is debate about the way that this occurs. The bone matrix experiences changes in electrical charge through stress generated potentials in the canaliculi, and piezoelectricity of the collagen-hydroxyapatite junctions. External electrical stimulation (ES) has been shown to increase bone formation, indicating that the cells involved in remodelling are electrically sensitive. However, the effects of ES on osteocytes specifically are under-researched.

Before applying ES *in vitro* the electrical characteristics of the culture media need to be understood to see if it will negatively impact cells in culture. ES in culture media causes pH changes and gas formation as well as precipitate formation directly on the electrode surface. The resistance of the media increases rapidly upon application of the electrical stimulus and plateaus after 100 - 200 minutes. The pH gradient disperses around the same time frame, with most stimulating currents causing no permanent change to the media pH. Stimulation parameters that cause minimal side effects will be better for the health of cells in culture. This should also make it more clear which outcomes are a result of the electrical stimulation and which come from the electrochemical reactions that are present in the media due to the ES.

Acknowledgements

A huge thank you to Dr. Wohl for teaching me not to take oneself too seriously, and that academia can be fun if you choose to make it fun. I hope to carry that mentality forward into my own career in academia. Oh, and also the valuable lesson of being able to say **no!**

Thank you to Dr. deBruin for introducing me to the wild world of electrical and biomedical engineering, and that no matter how long you are in a field, you always have new things to learn.

Thank you to everyone in the Wohl lab who made the past three years fun, and especially to Roshan and Alec for helping with CAD and graphs when I reached the end of my abilities and patience. Thank you to my parents, for supporting me through my journey of being a “professional student” and the constant reminder that one day I will actually have to get a job... one day. And finally, thank you to all the friends I’ve collected along the way. Whether that was through trivia beers at the Phoenix or bonding over our TAship woes, your support and friendship made the past seven years a blast.

Table of Contents

1. Introduction.....	1
1.1. Signal Type	3
1.2. Bulk Piezoelectricity	4
1.3. Fracture vs maintenance.....	5
1.4. Reproducibility.....	5
1.5. Thesis Motivation.....	6
1.5.1. Electrode Development.....	7
1.5.2. Media Electrical Stimulation	7
1.5.3. Cell Electrical Stimulation	8
2. Background.....	9
2.1. Bone Tissue Composition	9
2.2. Stress Generated Potentials (SGPs).....	10
2.3. Fracture Repair	11
2.4. Electrical Stimulation.....	12
2.4.1. Whole Bone (<i>in vivo</i>)	12
2.4.2. Cell Stimulation (<i>in vitro</i>).....	16
2.5. Electrical Stimulation Side Effects	20
2.6. Cell Culture Media	23
2.7. Media Composition	24
2.7.1. pH.....	25
2.7.2. Additives	28
2.8. Dulbecco's Modified Eagle's Medium	29
2.9. McCoy's 5A Modified Medium.....	30
3. Electrode Design and Setup.....	31
3.1. Intro	31
3.1.1. Chapter Motivation	32
3.1.2. Material Selection	32
3.1.3. Electrode Shape	33
3.2. Materials and Methods	34
3.2.1. Bar Electrodes	34
3.2.2. L Shaped Electrodes	35

3.2.3.	Electrode Holder Design.....	36
3.3.	Results	36
3.3.1.	Bar Electrodes.....	36
3.3.2.	L-Shaped Electrodes	38
3.3.3.	Electrode Holder Design.....	39
3.4.	Discussion	40
3.4.1.	Electrode Design.....	40
3.4.2.	Experimental Design.....	41
3.5.	Conclusion.....	42
4.	Electrical Stimulation in Media.....	44
4.1.	Introduction	44
4.1.1.	Chapter Motivation	45
4.1.2.	Media Stimulation.....	46
4.1.3.	Electrode Polarity.....	48
4.1.4.	Chlorine.....	50
4.1.5.	pH.....	50
4.1.6.	Signal Shape.....	51
4.1.7.	Hydrogen Peroxide	52
4.2.	Constant Voltage Materials and Methods	53
4.2.1.	Voltage Divider Circuit Design	53
4.2.2.	Various Constant Voltage Setups	56
4.3.	Constant Voltage Results	59
4.3.1.	AC Stimulation	60
4.3.2.	Square Wave Stimulation	60
4.3.3.	DC Simulation	61
4.4.	Constant Voltage Discussion	64
4.4.1.	Precipitate Formation.....	64
4.4.2.	Solder	65
4.4.3.	Stimulation shape.....	65
4.4.4.	Field Strength.....	66
4.5.	Constant Current Materials and Methods.....	67
4.5.1.	Constant Current Circuit Design.....	67

4.5.2.	DMEM vs McCoy's Testing.....	71
4.5.3.	Data Analysis	72
4.6.	Constant Current Results.....	73
4.6.1.	DMEM Medium.....	Error! Bookmark not defined.
4.6.2.	McCoy's Medium	Error! Bookmark not defined.
4.7.	Constant Current Discussion	96
4.7.1.	Temporal Behaviour	97
4.7.2.	pH split.....	98
4.7.3.	Electrodes.....	99
4.7.4.	IR Relationship	100
4.7.5.	Circuitry Limitations.....	102
4.8.	Conclusion.....	102
5.	Osteoblast-like Cell Testing	104
5.1.	Intro	104
5.1.1.	Chapter Motivation	104
5.1.1.	Cell Electrical Stimulation	104
5.2.	Materials and Methods	105
5.3.	Results	108
5.4.	Discussion	113
5.4.1.	Field Strength Uniformity.....	114
5.4.2.	Constant Current vs Constant Voltage.....	115
5.4.3.	Statistical Significance.....	115
5.5.	Conclusion.....	115
6.	Conclusion	117
6.1.	Future steps	118
7.	Appendices	129
7.1.	Media Composition	129
7.2.	Constant Voltage Experiments.....	131
7.2.1.	DC Stimulation	131
7.2.2.	AC Stimulation	134
7.2.3.	Square Wave	135
7.2.4.	McCoy's Medium	Error! Bookmark not defined.

7.3.	Predicted Resistances	138
7.4.	Cell Microscopy Images.....	139
7.5.	Cell Stimulation Resistance Graphs (Well 1 and 2).....	141
7.6.	TECAN Plate Reader Settings	143
7.7.	Alamar Blue Assay Results.....	144
7.8.	Normalized DMEM Graphs	145
7.9.	Normalized McCoy's Graphs.....	148
7.10.	Reviewed Studies on ES of Whole Bone	151
7.11.	Reviewed studies on <i>in vitro</i> stimulation of cells.....	152

List of Figures

Figure 1: DMEM Phenol red range in DMEM Medium [105]	27
Figure 2: Absorbance and pH graphs for media over time [103].....	30
Figure 3: Electrodes alignment in a single well of 24-well plate.....	34
Figure 4: L-Shaped Electrodes alignment in a single well of 24-well plate	35
Figure 5: Electrode holder, Oblique view, Top view.....	36
Figure 6: Electrode deterioration and precipitate formation	38
Figure 7: Precipitate buildup on L-shaped electrodes.....	38
Figure 8: Experimental Circuit Setup	54
Figure 9: Flowchart of Experimental Setup	55
Figure 10: UNO R3 Code Flowchart Off State, On state	58
Figure 11: Precipitate (blue) Gas formation (yellow)	63
Figure 12 Electrode gas formation 10 min, 210 Minutes, 420 Minutes.....	64
Figure 13: Electrode precipitate and gas formation	64
Figure 14: Circuit Schematic [117].....	68
Figure 15: Media pH gradient.....	76
Figure 16: DMEM Medium 100 μ A stimulation 365 minutes.	77
Figure 17: DMEM Medium 100 μ A stimulation 648 minutes	78
Figure 18: DMEM Medium 150 μ A stimulation 489 minutes	78
Figure 19: DMEM Medium 200 μ A stimulation 728 minutes.	79
Figure 20: DMEM Medium 250 μ A stimulation 361 minutes	79
Figure 21: DMEM Medium 350 μ A stimulation 915 minutes	80
Figure 22: DMEM Medium 400 μ A stimulation 1061 minutes	81
Figure 23: DMEM Medium 525 μ A stimulation 791 minutes	82
Figure 24: DMEM Medium 600 μ A stimulation 552 minutes	83
Figure 25: DMEM Medium 650 μ A stimulation 660 minutes	84
Figure 26: DMEM Medium 750 μ A stimulation 24 minutes	84
Figure 27: DMEM Medium Current vs Resistance graph	86
Figure 28: Media colour changes.....	88
Figure 29: McCoy's Medium 100 μ A stimulation 494 minutes.....	89
Figure 30: McCoy's Medium 250 μ A stimulation 360 minutes.....	90
Figure 31: McCoy's Medium 350 μ A stimulation 371 minutes.....	91
Figure 32: McCoy's Medium 450 μ A stimulation 1253 minutes.....	92
Figure 33: McCoy's Medium 600 μ A stimulation 360 minutes.....	93
Figure 34: McCoy's Medium 800 μ A	94
Figure 35: McCoy's Medium IR Characteristics	95
Figure 36: Saos-2 cells 1-day stimulation.....	109
Figure 37: Saos-2 cells, 2 days stimulation	109
Figure 38: Saos-2 cells, 3 days of stimulation	110

Figure 39: Fluorescence readings from TECAN plate reader.....	111
Figure 40: Preliminary Variable Field Test	131
Figure 41: Variable Field Strengths: 0.25, 0.5, 1, 2V/cm for 120 minutes	131
Figure 42: DC Extended Time Test	132
Figure 43: DC Test with the introduction of FBS.....	132
Figure 44: DC Test with the introduction of FBS, reduced spacing to increase field strength	133
Figure 45: Manual measurements AC Test.....	134
Figure 46: AC Test.....	134
Figure 47: Biphasic Square Wave Test.....	135
Figure 48: Square Wave Test.....	136
Figure 49: McCoy's Medium Test.....	137
Figure 50: McCoy's Medium Testing Halved Spacing	137

List of Tables

Table 1: Average Fluorescence Values for nine reading locations within the circular well.....	111
Table 2: T-Tests	112
Table 3: Predicted Resistances.....	138
Table 4: Reviewed Studies on in vivo Electrical Stimulation on Whole Bone.....	151
Table 5: Reviewed studies on in vitro stimulation of cells	152

List of Abbreviations and Symbols

A	Amp
AC	Alternating current
ADC	Analog to Digital convertor
BMD	Bone mineral density
BMP	Bone morphogenetic proteins
CBS	Calf bovine serum
CSV	comma-separated value
CX43	Connexin 43
DC	Direct current
DMEM	Dulbecco's Modified Eagles Medium
EM	Electromagnetic fields
ES	Electrical stimulation
FBS	Fetal bovine serum
H ₂ O ₂	Hydrogen peroxide
IC	Integrated circuit
kOhm, k Ω	Kiloohm, 1000 ohms
McCoy's Medium	McCoy's Modified 5A Medium
Media	A general term for a substance, plural
Medium	One single type of substance, singular
MSC	Mesenchymal stem cell
Op-Amp	Operational Amplifier
OPG	Osteoprotegerin
OVX	Ovariectomized
PEMF	Pulsed Electromagnetic fields
PFM	Protein free media
PLA	Polylactic acid
RANKL	Receptor activator of nuclear factor kappa-B ligand
RMS	Root mean square
ROS	Reactive oxygen species
SGP	Stress generated potential
Spp1	Secreted phosphoprotein 1, codes for osteopontin
V	Volt
Voltage, Potential, Potential difference	Electrical pressure that propels charge carriers

Declaration of Academic Achievement

I, Taylor deVet, completed a literature review, designed the experimental setup as well as CAD models used for electrodes and am solely responsible for the content in this thesis. I also performed all of the electrical stimulation experiments. My supervisor, Dr. Gregory Wohl, provided expertise on bone biomechanics, supervised, and guided in this work. Dr. Hubert de Bruin provided guidance for the electrical design and setup, following designs used in the thesis of Akiv Jhirad. Alec Fernback aided in chart construction and Roshan Bashar provided her expertise in CAD modelling. Bryan Lee provided guidance and expertise in cell culturing.

1. Introduction

The effect of electrical stimulation (ES) on bone tissue and bone healing has been of great interest since Fukada and Yasuda reported load-induced electrical potentials in the late 1950s [1]. The deformation of the bone tissue has a direct correlation to the electrical signal created on either side of the bend. Bone surfaces under compression producing negative potentials that cause tissue formation and areas under tension produce positive potentials that cause resorption [1]–[4]. The loading rate and magnitude of the load directly correlate to the magnitude of the generated charges [1]–[3]. The electric field generated due to stress is reduced to almost zero when there is no weight-bearing occurring, and in cases like this, the bones will start to deteriorate [2]. This was directly related to earlier studies by Becker et al. that showed that misaligned fractures in children had new bone deposited on the concave side, while the older bone was removed from the convex side, allowing the misalignment to straighten with time [3]. Many studies since have demonstrated that electrical stimulation has a significant effect on outcomes in fracture healing [5], spinal fusion [6], [7] the healing of osteotomies [8], as well as aiding in delayed unions post-fracture [9].

It has since been hypothesized that the bone cells can sense mechanical force in the extracellular network through an induced electrical signal, causing cell proliferation and cytodifferentiation [10], [11]. It has also been proposed that bone cells are electrically sensitive with a positive charge inducing chemotaxis in osteoblasts and attracting them for bone-building to occur [12]. There are a few theories that describe what the cells are sensing to initiate this movement. Firstly, most cells have negative membrane potentials

that allow DC electrical stimulation to propel them in one direction, referred to as galvanotaxis [13]. The side of the membrane facing the anode gets hyperpolarized and attracts free calcium ions, which causes the membrane to contract to propel the cell towards the cathode [14]. Secondly, the cells may be able to sense the movement of ions in their environment, allowing them to migrate and reorient themselves accordingly [14]. The movement of ions due to fluid flow creates a stress generated potential (SGP) in the extracellular matrix and a change in charges around the cells. The change in charge distribution is a factor in the calcium response theory, indicating the cell's reaction is most likely a combination of these two phenomena.

Due to the potential ability for electrical signals to influence bone cell behaviour, ES became a popular research topic for applications in bone repair [5], [6], [8], [9], [15]–[18] and for mitigating bone loss [19]–[26]. However, this research has not progressed as far as expected as the osteocyte response remains largely misunderstood.

Based on the published studies on the electrical nature of bone tissue, the ability of bone cells to sense external stimuli, and the response of whole bone to ES, there is an abundance of evidence to support the hypothesis that osteocytes respond to electrical stimuli. It makes sense that an electrical signal like the endogenous electrical charge in the tissue created *in vivo* could activate the cells in the same way if applied *in vitro*. The ability to do so would allow us to further our understanding of the osteocyte and how it can maintain bone homeostasis through the control of surrounding cells. As cells showed no adverse effects due to the application of electrical charge [27], interestingly, there is not more research into this area for osteocytes.

There seems to be a wide range of research that uses direct ES of cells but none on osteocytes specifically. The work on the electrical behaviour of osteocytes primarily uses pulsed electromagnetic fields (PEMF) as the stimulus, and none use direct DC stimulation. This is an area that should be explored further to try and understand osteocyte responses to electrical charge, and further, what are the characteristics of the electrical signal (magnitude, frequency) that the osteocyte sees *in vivo*? There is potential to improve and broaden therapeutic applications of ES for bone healing and mitigation of bone loss. ES methods have potential applications in the treatment of bone loss, improving fracture healing, and improving outcomes for osseointegration into implantable medical devices. This will require a better understanding of the bone cellular environment from an electrical perspective, and the cellular responses to electrical stimulation.

1.1. Signal Type

Some overarching issues arise out of studies on ES of bone cells. An important issue is a need for consistency of stimulation parameters, whether mechanical, fluid-induced, or electrical. The general lack of consistency or missing data on parameters makes it difficult to compare results when none are doing similar enough procedures to do a direct comparison. With ES, in particular, there is very little consistency when it comes to signal parameters, and this seems to be partly because researchers are unsure of which parameters are important for cell stimulation [28]. There seems to be a consensus that DC stimulation is preferred over rapid AC signals [10], [29], but there is controversial support when it comes to signals such as cyclical DC signals or low-frequency AC signals [30]. It

has been theorized that alternating electrical signals could act as a pump to move ions and waste towards and away from cells with little to no vasculature [2]. AC signals are commonly looked at to mimic endogenous signals but there is no evidence showing that this is better as charge seems to be the more important factor, not signal shape [31]. Oscillating fields have also been shown to inhibit cAMP responses, rendering cells less productive [10], and altering the mechanical deformation rate results in a significant decrease in the cellular response indicating that there is an effect of loading rate on the cells [32].

1.2. Bulk Piezoelectricity

While it is agreed that bone tissue has strong bioelectric properties, looking at the tissue from the view of the cells has a very different outcome. Different components combined interact to create an overall piezoelectric response that generates local potential differences of up to 6 mV [33]. But, the generators of the signal are very small, to the point of being not measurable [2], and this makes it very difficult to determine exactly how much of the tissue response each cell will see. Free ions move along fracture concentration gradients, creating local electrical fields of 1-2V/cm as the ions move into surrounding cells [10]. When bone is loaded, the shear experienced at the cellular surface is 0.8-3Pa indicating that only a small fraction of the forces exerted on the tissue make it to the cells [32]. If this principle is extended to electrical signals, the amount of charge that gets through to the cells is a small fraction of the local electric field. Due to the minuscule nature of this value, there has been limited research into the actual electrical environment that the cell sees. The cells are presumably very sensitive to their

environment and could be very sensitive to the type of signals that they sense and respond to. The lack of research in this area may be part of the reason that osteocyte behaviour is still not well understood. Additional work is needed to try to characterize the electrical signal environment of the cells and to determine the nature of electrical signals that they receive *in situ*.

1.3. Fracture vs maintenance

While there is overlap in the mechanics of bone maintenance and fracture healing, the processes involved in fracture healing and bone remodelling are much different. The presence of a strong electrically negative site to attract cells and ions in a fracture is not present in remodelling to the same magnitude. This may be one of the reasons why ES for fracture healing has been so successful compared to direct stimulation for bone maintenance. The smaller electrical stimuli present in habitual bone remodelling processes are harder to try to enhance as the stimulus is likely just locally activating osteocytes, and not at a strength to cause cellular migration. Additionally, the fractures studied most are osteotomies or critical fracture – the most severe cases. The extreme nature of these injuries indicates a stronger electrical response will be present, which is easier to try to enhance with exogenous ES with few adverse effects occurring.

1.4. Reproducibility

Cells are very sensitive to their environment making it very difficult to reproduce the same results even when using consistent ES on bone cells [12]. The medium that the cells are grown in is not created with electrical properties in mind and the addition of electrical current causes fluctuations in the medium to which the cells react quickly. While most

studies do not report on precipitates in cell media, there is evidence to support that various calcium deposits occur [13], [34], which leads to a change in the free ions in the medium. This, coupled with the ion movement from convection currents, can alter the local pH and greatly affect the cells independent of electrical current effects [34].

Additionally, bone adaptation seems to be controlled by the recruitment of more cells, not by altering the response of an individual cell making it an all or nothing type of process [35]. If the number of cells in a study is not very closely controlled, the results can be vastly different. This may be why early studies that harvested cells from bone, rather than experimenting on immortalized cell lines have so much variability. The amount and type of cells harvested from the tissue can vary significantly from study to study and even within the same experiment [36].

1.5. Thesis Motivation

To do direct stimulation on cells, there needs to be a safe way to provide stimulation to cells in culture. One of the big unknowns in this situation, however, is the behaviour of the cell culture media with the introduction of electrical stimuli. Due to the complex chemistry of the media, many faradaic and non-faradaic reactions occur driven by electric charge. These are under-reported in cell stimulation studies with few reporting any issues coming from the media at all. However, it is important to understand the behaviours of the media before the introduction of cells to be able to decipher if cells are reacting to electrical stimuli or chemical byproducts of the stimulation. This may also involve understanding the electrical properties of the media to understand how the media changes instantaneously but also over time. This will provide insight into what stimulation

parameters – both temporal and electrical power – create unstable media environments that may be detrimental to cellular health. These factors can then be taken into account when designing experimental protocols to maintain the most stable conditions possible to minimize variability in cell culture ES experiments.

1.5.1. **Electrode Development**

The first step in designing ES experiments involves creating inert electrodes that do not cause cell death. Any material that is in contact with the cell culture media, is by extension in contact with cells in culture. This creates challenges with design as the electrodes have to be made of inert material and have to be robust enough to maintain their shape and positioning without support material directly around them. This involved designing an electrode holder to maintain positioning, that fit snugly onto a well plate but was able to be removed easily for performing cell culture procedures.

Preliminary tests showed that solder was the main cause of electrochemical reactions and resulted in the design of electrodes to keep solder far enough away from the media that even excessive gas and foam formation would not result in an interaction.

1.5.2. **Media Electrical Stimulation**

A lot of studies on the electrical stimulation of cells and biological tissues use a constant electric field model. To mimic this using direct electrical stimulation, a constant voltage should be applied across the electrodes. This was done as a preliminary step to test different voltages and signal shapes to see how the media would react. The wide range of

input parameters resulted in insights into the behaviour of the media resistance over time as well as the generation of precipitates due to poor electrode construction.

To look at a more constant delivery of charge, a constant current setup can be used. Using results from constant voltage experiments, the stimulation can be altered to decrease the presence of gas and precipitate formation. To be able to provide maximum stimulation to cells in culture, electrochemical reactions must be reduced to keep the culture environment as stable as possible. This optimal level of stimulation can be explored by using a range of stimulating currents.

1.5.3. **Cell Electrical Stimulation**

As cell culture media are not designed to have electrical stimulation running through them, it is unknown how the electrochemical reactions will impact the cells. Very few cell ES studies report these byproducts and their impacts on the cells. Using stimulation parameters from other published cells from bone cell lineages, SaOs-2 osteoblast-like cells were stimulated to see if it increases or decreases cellular activity. This could also present as increased or decreased cellular proliferation or apoptosis.

2. Background

2.1. Bone Tissue Composition

Bone tissue is comprised of a mineral phase of hydroxyapatite and an organic phase of collagen, water, proteins, and cells [37]. While studies have confirmed that the electrical effect in bone is not entirely biological [1], [3], the exact cause of the bioelectric effect is still under debate. Both collagen and hydroxyapatite are piezoelectric tissues in specific settings and have a unique bioelectric effect when they interact. The properties of dry bone are almost identical to that of dry collagen [38], [39] as it makes up the bulk of the organic portion of the tissue. Typically bone is only considered piezoelectric when it is dry; that is because collagen behaves piezoelectrically when dry and the piezoelectricity drops drastically when it becomes wet [40]. As collagen gets saturated with water, it aligns more symmetrically and the electric potentials get short-circuited [38]–[41]. *In situ*, the hydroxyapatite limits the amount of water that collagen can absorb and allows it to maintain some of its piezoelectricity while saturated, as it alters the orientation of fibres [38]. Collagen has an abundance of electrons whereas hydroxyapatite has very few, and it is proposed that the bending of the junction between the two generates an electric potential as it behaves similarly to a p-n junction in a semiconductor [2].

When hydroxyapatite is removed from the bone matrix, the amount of electricity generated by deformation significantly decreases but does not disappear, indicating that the hydroxyapatite carries the bulk of the load but collagen still experiences an increase in strain under compressive loads [1], [2], [32]. Collagen is an important component for the cells as it allows them to detect the *direction* of the stress within the matrix as opposed to just the magnitude from hydroxyapatite [1]. This indicates that the electricity generated

from mechanical deformation in the bone comes from a combination of the stress on the collagen fibres and the hydroxyapatite crystals, in addition to the creation of these p-n junctions [2].

2.2. Stress Generated Potentials (SGPs)

A secondary hypothesis on bone bioelectricity is the creation of stress generated potentials (SGPs), which were first reported in the 1960s, shortly after Yasuda and Fukada's initial breakthrough [32]. Interfaces that separate two different phases of material automatically create an electric potential, as one phase is usually more electronegative than the other [41]. When bone is compressed, a negative charge is spread throughout the matrix causing the cations in the interstitial fluid to be attracted to the negatively charged surfaces, leaving a net surplus of anions in the extracellular fluid [33]. These streaming potentials can be caused by differences in voltage, pressure, and concentration gradient within the channels of the bone [2], [13], [38], [42], [43] but are only referred to as SGPs when mechanically generated. To diffuse the built-up charge within the matrix, ions redistribute until the charges are balanced. This causes the current to dissipate and no net movement occurs [4], [42] as if there are no free ions left to create a streaming potential [39].

There is evidence that points to SGPs being a combination of the piezoelectricity of the matrix and streaming potentials [32], [44]. The SGP relaxation times are too long for classical piezoelectricity to be the dominant factor [32]. Conversely, if streaming potentials were dominant, the conductivity should affect the SGP relaxation time, which

is not the case either [32]. This demonstrates that both the anatomy and composition of bone play a role in its bioelectric behaviour.

2.3. Fracture Repair

A unique feature of bone tissue is its ability to repair from fracture. Any realignment, relocation, or even the introduction of an implant, initiates regeneration and osteoinduction [10], [45], which creates a combination of electrical, chemical, and mechanical stimuli on the tissue. Under normal conditions, the metaphyseal region of bone is electronegative while the midshaft is iso-polar [12]. When a fracture occurs, the entire bone becomes more electronegative, while the metaphysis remains the most electronegative [12]. The fracture site becomes very negatively charged as it collects electrons [11], [46] and anions, causing an ionic current flow to the injured area [47]. Free ions move along the concentration gradient, causing both a chemical and electrical shift, creating local electrical fields of 1-2V/cm as the ions move into surrounding cells [10]. This ion movement takes the form of current loops that enter through the injury site and exit through intact bone upstream [47].

Pulsed electromagnetic field (PEMF) and direct electric field stimulation have recently been used to speed up the rate of fracture healing. PEMFs have been shown to create more a more stable initial callus, resulting in faster healing [48] by recruiting more immature MSCs that will differentiate into pre-osteoblasts [45]. Direct ES has been shown to do the same, with callus that grows substantially thicker and forms weeks earlier when the cathode is on the injured bone [49]. As the cathode is the negative electrode, it causes the fracture site to become significantly more negative than normal,

presumably amplifying the flow of ions and cells to the site. With more cells and building materials present, the bone heal faster.

2.4. Electrical Stimulation

2.4.1. Whole Bone (*in vivo*)

2.4.1.1. Electrode Polarity

There has been a multitude of studies that have shown ES of whole bone produces osteogenesis at the cathode electrode [2], [34], [49]–[54], specifically in small areas closely surrounding the electrode [48]. These findings support those of the basic bone behaviour studies that found that areas of bone with the lowest electric potentials have the highest amounts of bone formation [55] and also agree with studies that show that the application of a negative charge to a fracture improves healing [49]. This phenomenon occurs as increased cell proliferation occurs at the cathode, with an increase in osteoid and new bone formation under the application of direct current [29], [56]. Electrical stimuli have been shown to cause bone formation that is fairly disorganized [50], [53], and similar to periosteal bone [29], [49], intramembranous bone [51], or a cartilaginous or fibrous type tissue that resembles metaplastic or osteoblastic type bone [52]. This indicates that the osteoblasts are more active with stimulation [29], [51], but also that other cell types are also more active. Throughout the stimulation process, the bone becomes more organized [57] as a controlled remodelling process occurs. When the stimulation ceases, the bone will be resorbed through osteolysis [50].

The activity at the anode has shown mixed results including bone destruction [29], [52] or no change in the tissue at the insertion site [2], [18]. Osteoclasts have been shown to

migrate towards a positive charge, which could explain increased bone resorption [13], but they have a higher membrane resistance when compared to osteoblasts, indicating that they are less electrically sensitive [27]. The osteoclast migration and increased necrosis around the anode may be linked as more remodelling occurs at the anode to eliminate the necrotic bone [29].

The lack of response at the anode has been hypothesized to be due to the electrical parameters of the signal. If the stimulating signal is not similar enough to the natural signal, the bone may not react similarly to the predicted *in vivo* behaviour [57]. The distribution of charge in growth or a healing environment in bone is focused on the relocation of negative charges at the injury site. The movement of positive charge is a means to counterbalance the negative charge. A large focus of positive charges in one location is inconsistent with the naturally occurring charge phenomenon, and so this could be why the accumulation of positive charge does not illicit a natural response in the same way that negative charge does.

2.4.1.2. **Signal Parameters**

While the overall consensus seems to be that 1-20 μA of current is optimal to stimulate bone formation [10], a review of several studies on *in vivo* whole bone stimulation suggests that there is a very wide range of current magnitude that can be used to achieve the same results. Studies using current magnitudes from as little as 20 pA, and up to as high as 100 mA have all shown the ability to stimulate the formation of bone, though sometimes poorly organized bone [34], [49], [50], [57]. However, others have demonstrated osteolysis due to excessive current above only 20 μA [18], [31], [49]. A

summary of studies can be found in **Table 4: Reviewed Studies on in vivo Electrical Stimulation on Whole Bone**, and this speaks to the need to control and carefully specify the parameters used in studies.

The amount of bone formed around the negative electrode is related to the current density and charge [54], rather than just the current itself. AC signals are commonly looked at to mimic endogenous signals but there is no evidence showing that an AC signal performs better than a DC signal as they deliver less charge overall [31]. Using equivalent current values, but altering the signal shape has been shown to have greater effects on the amount of bone formation with the results consistently showing that a DC signal is optimal [10], [29], [34], [54]. DC signal allows for the highest charge buildup at the cathodic site as well as the most consistent flow of ions resulting in the greatest formation of bone.

2.4.1.3. **Mitigation of Bone Loss**

Bone loss and the processes associated with bone remodelling are biologically different to fracture repair. Moreover, bone loss paradigms could respond differently based on the underlying mechanisms (e.g., disuse osteopenia versus postmenopausal osteoporosis, which is hormonally driven). Several different mechanisms have been tested to try to mitigate bone loss in different animal models including PEMF, direct ES, and capacitive coupling [20], [23]–[26]. PEMF employs the usage of two coils in a Helmholtz configuration, which induces an electromagnetic field in between them when an electric current is applied. Simple sinusoidal and complex PEMF waveforms were compared using the isolated (disuse) Turkey ulna model [25]. The simplest, lowest frequency sinusoidal waveform (15 Hz frequency, 0.08 mV amplitude) resulted in the greatest

increase in the cortical area relative to both an ES control group and the contralateral, intact ulnae within-group. A similar study was conducted to examine the effect of pulse power on the cortical bone area and demonstrated a maximum osteogenic effect between 0.01 and 0.04 T²/s [26]. Additionally, the within-group comparison of the contralateral ulnae of the study showed a -13% difference in the cortical area in the control group and a 12.3% difference in the group that underwent the 0.01 T²/s stimulation protocol. In a sciatic denervation rat model of disuse osteopenia, capacitively coupled electrical stimulation resulted in a significant reduction in the percent cortical porosity, increase cortical area, and increase the cortical thickness of the denervated bone when compared to the unstimulated, denervated control [24].

A common and well-established model of human postmenopausal osteoporosis is the ovariectomized (OVX) female rat [58]. Though the remodelling processes that lead to bone loss are similar to the disuse model, the underlying systemic hormonal mechanisms that drive the bone loss likely influence the bone responsiveness to electromagnetic (EM) stimulation. Nevertheless, studies using OVX rats have shown a positive response to EM stimulation. Using a 1 mT magnetic field signal at 50 Hz frequency, Sert et al. [20] reported a significant increase in the cortical thickness of tibial bone in OVX rats. Similarly, Chang and Chang used a 2 mV/cm electrical field at 7.5 Hz frequency and reported significant increases in trabecular bone volume fraction, trabecular thickness, and trabecular bone formation rate in the proximal tibial metaphysis of OVX rats [23]. The use of capacitive coupling has also been shown to have global effects on OVX rats that have had their whole body stimulated within a 1.5 MHz, 30 mW/cm² electric field

[19]. These experiments found an increase in the global bone mineral density (BMD), spinal BMD, and lower limb BMD in the treatment group compared to the control group. The same research group showed that low-intensity ES mitigated osteocyte apoptosis due to OVX in rats with the ES OVX rats having similar levels of osteocytes as the SHAM group that had the ovaries intact [59].

2.4.2. Cell Stimulation (*in vitro*)

Stimulation due to an external electric field results in a large voltage drop across a cell membrane but a small voltage drop in the cytoplasm as the plasma membrane gets polarized, creating a large local electric field at the membrane only [28]. This capacitive property of charge holding allows the cell to regulate its internal environment, shielding it from potentially damaging changes. The negative voltage of the cellular membrane makes almost all cells sensitive to ES and should cause migration towards the anode [57] but almost all bone cells exhibit migration towards the cathode [12] indicating other factors are controlling migration. A relatively important finding from an *in vitro* study was that bone adaptation seems to be controlled by the recruitment of more cells, not by altering the response of an individual cell – an all or nothing process [35] – and that bone cells seem to have a refractory period for stimulation, with specific frequencies being ideal for maximal stimulation response [30].

2.4.2.1. Osteoblasts

Most commonly, osteoblasts have been stimulated with PEMFs with some studies finding that there is a reduction in cell proliferation but an increase in ALP activity, collagen synthesis, and osteocalcin levels [60]–[62], as well as an increase in growth factors like

VEGF [63] using both direct current [64] and capacitive coupling [65] stimulation. The time of exposure to PEMF has also been shown to have a positive correlation with the expression levels of BMP-2 and BMP-4 from osteoblasts [66]. BMP-2 and BMP-4 are crucial factors in skeletal repair and regeneration [67], and their roles are complemented by VEGF without which there would be impaired bone formation and suppressed blood vessel development in bone [68]. Collectively, the increased expression of these biomolecules through the administration of ES could lead to an enhancement of bone formation and healing [69], along with mitigation of the loss of bone mass [70] *in vivo*.

Conversely, other studies have found that PEMFs increase osteoblast proliferation, but have no effect on cellular differentiation and cause a decrease in ALP activity [29], [71].

The extreme variance in these results shows how sensitive the cells are to electromagnetic stimulus as the waveform shape and duration greatly affects their behaviour. PEMFs can cause both positive, negative, and no change in cell activity depending on how they are applied. A summary of this can be seen in **Table 5: Reviewed studies on in vitro stimulation of cells**.

Direct ES can also be applied through the capacitive coupling of the culture environment. This has shown to have no adverse effects on osteoblasts, with numbers remaining stable through experiments [27]. Interestingly, the number and productivity of enzymes in the osteoblasts are higher on the side of the cell closest to the negative electrode, indicating asymmetrical activity [72]. Osteoblasts have been shown to move towards the negative charge of the cathode of a circuit [14], [27], [51], [57] and this is carried out through the growth of lamellipodia on the cathodic side of the cell [13], [27].

All methods of ES – capacitive, inductive, and magnetic coupling – cause increased DNA synthesis in pre-osteoblast cells, but capacitive coupling can maintain this increased activity throughout the duration of the stimulus [73]. This could be due to the different types of responses that come from each of these stimulation types. Capacitive coupling causes Ca^{2+} ion movement through voltage-gated channels whereas inductive coupling and EMFs cause Ca^{2+} to be released through intracellular stores. This intracellular release has been shown to increase cytosolic calcium concentrations and might involve the calcium/calmodulin pathway [73].

2.4.2.2. **Osteocytes**

Osteocytes are the most abundant type of cell within the bone tissue but while the basic structure and lineage are fairly well understood, there is a lot of debate regarding their behaviour [74]. Osteocytes are surrounded by tightly packed collagen fibres [75] and can control the structure of the bone up to one micron around the lacuna that they inhabit [2], [31]. The matrix directly around an osteocyte does not become fully mineralized forming the lacuna the cell resides in, to create an interconnected set of canaliculi channels [76]. They are presumed to be the cells that detect and communicate strain when subjected to shear stress by the movement of fluid past their cellular processes [74]. The osteocyte's sensory ability can be further confirmed based on the fact that the cellular processes are mainly on the mineralized side of the cell as opposed to the vascular side [75], indicating that communication is happening through the matrix and not through changes in blood flow. The cellular processes of neighbouring cells are connected through gap junctions

that are filled with fluid saturated with proteoglycans and ions to allow for communication [77].

Osteocytes communicate through gap junctions, which can be directly regulated by electric fields [60]. Although PEMFs have shown to not affect the number of cells present [78], they have been shown to affect the number of communication factors through the gap junctions. Osteocytes can have a twofold increase in PGE₂ and an overall increase of TGF-Beta 1 and NO²⁻ with exposure to a PEMF [60], [78]. Interestingly, the protein CX43 creates gap junctions and is produced in lower volumes with the application of PEMFs but is increased with shear stress [78]. This indicates that the PEMFs do not cause increased connectivity between cells but may increase the amount of communication between already connected cells.

PEMFs on MLO-Y4 at 5 Gauss (G) have been shown to inhibit cellular apoptosis and increase the length of the cellular dendrites while lowering RANKL levels and increasing the mRNA for OPG, both controllers for cellular apoptosis. A 5 G field strength was also found to lower the number of osteoclasts present, in addition to lowering their ability to resorb bone when using conditioned medium from the osteocyte-like cells [79]. This study proposed that the cell cilia are responsible for sensing the electrical environment around them, which corresponds to other theories that the cilia can respond to changes in the fluid flow around them.

2.4.2.3. **Osteoclasts**

Osteoclasts are very important in the maintenance of bone tissue but are not as closely related to osteocytes and osteoblasts. While osteoblasts and osteocytes are from the same lineage, osteoclasts are more closely related to macrophages and have different behavioural traits. While osteocytes and osteoblasts work together, osteocytes and osteoclasts usually counteract each other with osteoclasts being inhibited by osteocytes [80], [81] and in portions of bone with increased resorption, osteoclasts will degrade osteocytes [82].

The big difference in terms of ES is the migration direction of osteoclasts. They tend to migrate or collect at the anode, which could explain increased anodal bone resorption and remodelling [13], [27], [29], but they have a higher membrane resistance when compared to osteoblasts, indicating that they are less electrically sensitive [27]. PEMFs can cause cells collected from bone marrow to differentiate into osteoclasts[83]–[85], but the correct parameters must be used as extremely low PEMFs suppress osteoclast recruitment [85] and can also induce apoptosis [79], [84]. For example, Chang et al. demonstrated that 4.8 $\mu\text{V}/\text{cm}$ PEMF decreased the production of OPG and the recruitment of osteoclasts while increasing resorption area percentage and OPG production. Upping the strength to 12 $\mu\text{V}/\text{cm}$, had an opposite effect. [83]

2.5. **Electrical Stimulation Side Effects**

While cells seem to be directly sensitive to electrical stimulation *in vitro*, there is also speculation that the faradic byproducts created in the culture environment can influence cell responses. This involved the introduction of pH changes, hydrogen peroxide, reactive

oxygen species (ROS), and chlorine into the stimulation environment [86]. The introduction of an unbalanced electrical stimulus into an *in vivo* or *in vitro* environment can cause severe shifts in the pH [87], [88]. Specifically, while there may be no net pH change there is a pH decrease that occurs at the anode and a pH increase at the cathode [87], [89]–[91]. The pH changes are directly caused by the reactions that occur at the electrodes [88]. The electrodes cause both non-faradaic reactions, both using different methods to rebalance charge. Non-faradaic reactions have no electron transfer, but rather redistribute charged molecules in the electrolyte [92]. Faradaic reactions have electron transfer between the electrode and electrolyte, resulting in reduction or oxidation [92]. Hydroxide is created at the cathode of stimulation [91], [93], which then reduces water in the surrounding environment to create hydrogen peroxide [90], [93], [94]. In extreme cases, the cathode causes the formation of hydrogen gas, with the amount formed directly correlated to the voltage of the electrode [87], [88], [90]. In some medium types, a large amount of free chlorine is created through ES, which creates hypochlorite, a very strong oxidizing agent [87], [89].

The electrode selection is also very important as the faradaic reactions can cause them to dissolve releasing metal ions in the medium [88]. While platinum is used most often because of its stability, the side effects of high current stimulation with platinum electrodes on tissue are similar to tissues exposed to platinum salts, indicating that they may be dissolving [88]. Pt²⁺ ions are also powerful oxidizing agents, which can be reduced by organic species in the surrounding environment causing cellular necrosis [87].

The formation of hydrogen peroxide is of interest as it can stimulate VEGF production [95] and increase osteoblast activity and proliferation [91], [93]. Osteoblasts can experience an upregulation of factors like Runx2, SPP1, and BMP2 [94], and have been shown to initiate a transition towards an osteocyte like state with the formation of an osteocyte-like matrix when introduced to increased concentrations of hydrogen peroxide [91].

The effects of too much stimulation can directly affect the viability of cells, specifically through pH changes [94]. ES has been found to inhibit and kill bacteria around the electrodes potentially due to the pH changes or electrochemical reactions [86], [96]. Specifically, microampere DC stimulation is better than other ES for preventing bacteria around the cathode [97]. The amount of chlorine and byproducts created from ES has been shown to have the same potential to kill bacterial cells as the current itself, indicating that the chlorine may cause cell death, not the ES [89]. Osteoblasts can withstand more basic environments and at around pH 7.6, they increase their production of collagen, ALP, and thymidine [98], [99]. They also show an increase in DNA production from a pH of 7.0-7.2 and 7.6-7.8 [98]. Conversely, an increase in pH decreases osteoclastic p-glucuronidase creation [99]. This basic environment decreases the flow of calcium out of bone by decreasing osteoclastic activity and upregulating osteoblastic activity, which could explain increased osteoblast activity in more basic *in vitro* settings [99].

The generation of any of these side effects are important to consider when using ES, and the parameters of the stimulation signal need to be monitored to protect against faradaic

side-effects. The creation of hydrogen peroxide specifically is directly proportional to the pulse width, frequency, and voltage of the ES in the environment [100]. Changing the stimulus to a biphasic signal reduces the byproducts but does not fully eliminate them [88], [92]. Faradaic reactions that occur at the cathode are not direct reversal reactions to the electrode corrosion at the anode [92]. The length of the phases also affects how much of the reversible reactions can be reversed before the phase switches back [87]. Constant current, rather than voltage, controls the charge balance better to minimize the reactions [87].

2.6. Cell Culture Media

To investigate cells, they often have to be taken out of their natural environment and put into an artificial one while maintaining a lot of the *in situ* conditions [101]. A culture environment can be for prolonged or immediate survival or immortal growth of cells with a specialized function depending on the application [101]. To survive *in vitro*, cells need to have a controlled temperature, pH, concentration of growth factors, and osmolarity as well as the proper substrate to attach to [101].

Cell culture media contain nutrients for energy for cells to allow them to regulate their natural life cycle and contains amino acids, vitamins, inorganic salts, glucose, serum, hormones and attachment factors to do so [101]. Growth factors, cytokines and chemokines are all chemical messengers for cells but are generally unstable in media so are added just before use [102]. Carbohydrates are added for energy, usually in the form of glucose and galactose or maltose and fructose [101]. Additional proteins or peptides such as albumin can be added to bind water, salts, fatty acids, hormones and vitamins, or

transferrin for iron transport [101]. Vitamins are required for growth and proliferation, and while the cells can generate vitamins themselves, they are often supplemented because cells cannot create enough *in vitro* [101]. Fatty acids and lipids, hormones, and growth factors are usually present in serum but can also be supplemented if needed [101]. Finally, antibiotics are added to the media to try and prevent bacterial contamination from taking over [101].

Media can come from one of two backgrounds; natural media coming from biological fluids or tissue extracts, or artificial such as salt solutions, basal media or complex media [101]. Both medium types have their pros and cons with natural being optimal but difficult to achieve consistency with, and artificial being more consistent but difficult to manufacture well [101]. Artificial media has a standard base with varying amounts of nutrients, mineral salts, oxygen, carbon dioxide, serums, proteins, carbs and cofactors [101].

2.7. Media Composition

There are four main categories of cell culture media, each with its own application and composition; serum-containing, serum-free, chemically defined, and protein-free media [101]. A serum containing media generally has fetal bovine serum (FBS), which is the liquid component of clotted blood [101], [102]. To avoid composition inconsistencies and contamination risks, serum-free media can be used. Serum-free media contains the basic media and is substituted with albumin, insulin, selenium and transferrin instead of FBS [102]. This is usually implemented in immunological studies that omit the FBS but supplement the media with growth factors and proteins for cell health [101]. To further

reduce variability, chemically defined media avoids the risk of contamination from biologically derived serum and has inorganic and organic ingredients that are lab manufactured [101]. Lastly, if a study is trying to identify protein expression from a cell, protein-free media (PFM) can be implemented. PFM uses bacteria or yeast and genetic engineering with vitamins, amino and fatty acids to create a medium that maintains cell health with limited or no supplementary proteins [101].

2.7.1. pH

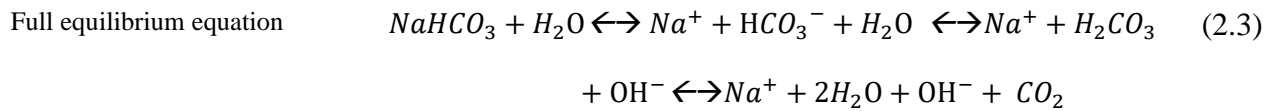
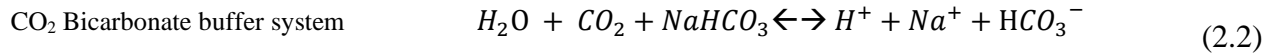
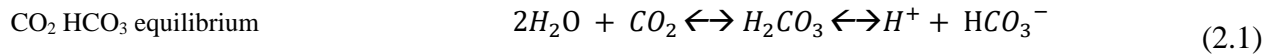
The pH of a culture environment is important as every cell has its own unique pH required to survive. Metabolic processes can cause changes in pH and cell death causes a large decrease in media pH [103].

2.7.1.1. Buffer System

Most mammalian cells naturally exist in environments at a pH that is close to neutral as arterial blood between a pH of 7.35 – 7.45 [102], [103]. This pH is maintained in the body through CO₂ exchange in the lung [103]. In media, this is replicated through a bicarbonate/ CO₂ buffer system. When the CO₂ from the air dissolves into the media it creates carbonic acid, which then reacts with the dissolved bicarbonate to maintain an equilibrium [101]–[104]. The process for this can be seen in Equation (2.1- Equation (2.3) [104]. Additionally, as the cells undergo metabolic activities they generate CO₂, which further decreases the pH [104]. The CO₃/HCO₃ system needs to be maintained in an incubator at 37°C and a 5% CO₂ concentration to maintain the pH in the media. Other buffer systems are less temperature-sensitive but come with the trade-off of being light-

sensitive [101], [102], [104]. The addition of serum can also aid in the buffering process.

[101].



2.7.1.2. Phenol Red

pH indicators are a simple way to analyze the pH of a solution without having to introduce an external sensor. In most cases, the indicator has a limited effect on the cells and allows the pH to be continuously monitored to allow for non-invasive monitoring of media integrity. For cell culture, the most common indicator is phenolsulfonphthalein or phenol red [101], [103]. This indicator goes from yellow to fuchsia from pH 6.2 to 8.2 with an ideal pH for cells being in the red state [101]–[103]. The indicator goes pale yellow below pH 6.2 or pale pink/colourless above 8.2, which indicates a toxic environment for cells [102], [103]. This colour range can be seen in Figure 1: DMEM Phenol red range. Phenol red acts as a zwitterion with a negatively charged sulphate group and a positively charged ketone group [103]. When the pH decreases the proton in the ketone is lost, causing the ion to turn yellow and when the pH increases hydrogen is lost from the hydroxyl group and the ion becomes red [103].

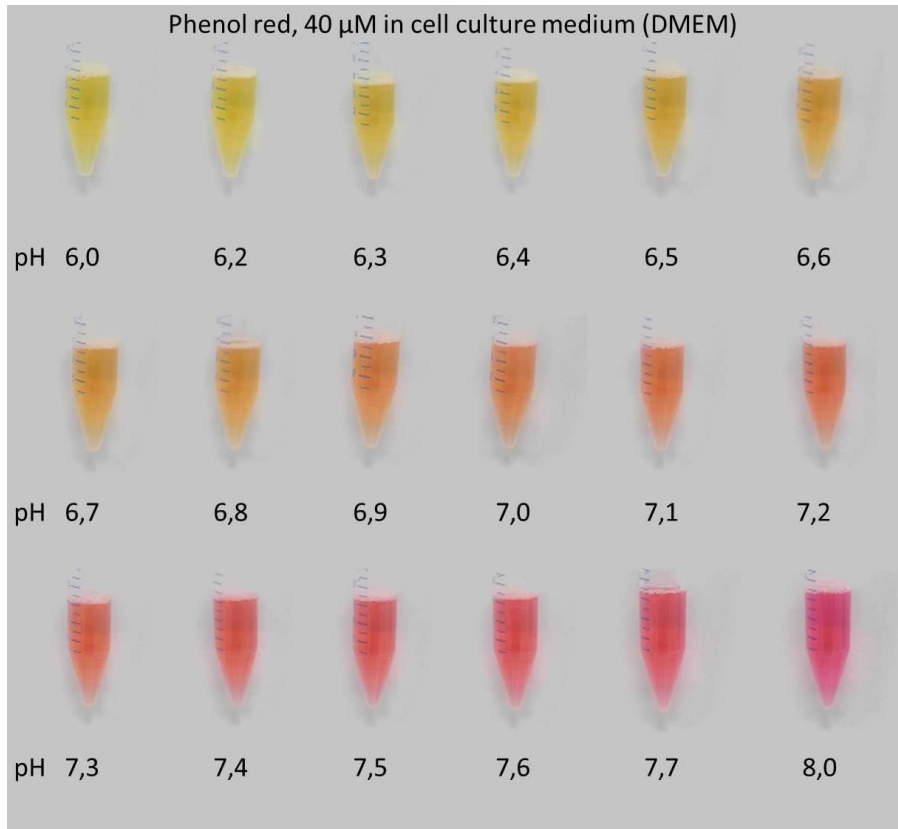


Figure 1: DMEM Phenol red range in DMEM Medium [105]¹

Some studies may choose to omit phenol red as it can mimic steroidal hormones such as estrogen, which can be detrimental in studies with cells that are estrogen-sensitive [101]–[103]. It interferes with Na-K homeostasis in these cells and is sometimes mitigated with the addition of bovine pituitary hormone [101].

¹ Reference is from a Wikipedia user Max Schwalbe who created a colour scale using DMEM Medium using varying amounts of acids and bases and measurement of pH using a calibrated pH meter. Due to shortened experimental timeline I was unable to complete a scale myself and have found this to be the only colorimetric pH scale for culture media available

2.7.2. Additives

2.7.2.1. Salts

A very important factor in culture media is the inorganic salts as they allow for basic cellular function and osmotic balance and membrane voltage maintenance [101]. The concentration and combination of salts vary with media but commonly contain H^+ , K^+ , and Ca^{2+} ions. [101]

2.7.2.2. Amino Acids

Culture media contain amino acids so the cells can produce the proteins that they need to function [101]. Non-essential amino acids are added to increase viability and proliferation [102]. The cells can create some amino acids themselves, but the addition reduces the side effects that occur when cells grow in environments with low levels of amino acids [102]. L-glutamine is commonly added to provide the nitrogen for NAD and NADPH and as a secondary energy source. However, due to its unstable nature, it is commonly added right before use to avoid harmful ammonia degradation products above $4^{\circ}C$ [101], [102]. In some cases, L-Alanyl-glutamine can be used in lieu as it is more stable than glutamine in culture, and cells can break the extra bonds to use it in the same way [102].

2.7.2.3. Serum

Serum supplements the media to allow for cellular growth and has chelators for the water-insoluble nutrients, hormones and growth factors as well as protease inhibitors and increases the media's ability to neutralize toxins [101], [102]. It also contains various amino acids, proteins, vitamins, carbohydrates, lipids and minerals [101], [102]. In some cases, calf bovine serum (CBS) is used as it has lower growth-promoting properties than

FBS and can be used for more controlled growth [101]. Some important factors of serum include albumin and transferrin, which are used to move molecules into the cells, and fibronectin which promotes cellular attachment [101].

In addition to providing nutrients, the serum increases the overall viscosity of the media, which protects the cells from mechanical damage when the medium is disturbed [101].

Cells *in vitro* are very sensitive to small changes and serum has to be properly treated as it can alter the uniformity of media and increases the risk of contamination [101], [102]. It also contains common cellular products and may make it difficult to isolate which products the cells are creating and which are pre-existing [101], [102].

2.8. Dulbecco's Modified Eagle's Medium

Dulbecco's Modified Eagle's Medium (DMEM) is one of the most common medium types in use [101], [102], [106]. DMEM stemmed from the basal Minimum Eagles Medium (MEM) that was developed by Eagle in 1959 using mouse fibroblasts, HeLa cells, and Chinese Hamster ovary cell lines [102], [106]. DMEM contains four times more amino acids and vitamins than basal media as well as additional components such as ferric nitrate and sodium pyruvate [101], [106]. It is commonly supplemented with 5-10% FBS for growth factors and proteins and needs a source of CO₂ to maintain its buffering system [101]. In an uncontrolled CO₂ environment the pH of the media will increase over time [103]. With DMEM Medium having more phenol red than other commonly used medium types such as McCoy's, the changes in colorimetric absorbance and therefore the colour is the greatest [103]. This can be seen in Figure 2 from Held et al. DMEM Medium can come with and without sodium pyruvate, however, it is essential to break down H₂O₂,

a common ES product [100]. The full composition and comparison against McCoy's Medium can be found in Appendix 7.1 Media Composition.



Figure 2: Absorbance and pH graphs for media over time [103]

2.9. McCoy's 5A Modified Medium

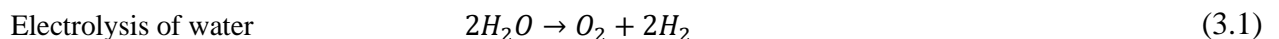
McCoy's modified 5A medium, or McCoy's Medium, was developed around the same time as DMEM Medium due to the different amino acid needs of Novikoff hepatoma cells [107]. It was originally used for primary cultures derived from bone marrow, skin, gingiva, lung, rat embryos, and other tissues. McCoy's Medium contains a small amount of ascorbic acid and reduced glutathione compared to DMEM [100]. This differing concentration of antioxidants alters how the medium deals with radicals and H_2O_2 in the medium. The concentration of phenol red is also about 40% less in McCoy's Medium than DMEM, creating less obvious colour changes that can be seen in Figure 2 above [107]. From this figure it can also be seen that McCoy's Medium is slightly more resilient to temporal pH changes, changing about 0.5 units less over 12 hours.

3. Electrode Design and Setup

3.1. Intro

For electrical stimulation procedures on humans, animals, or cells, it is important to use an inert metal for the electrodes to minimize the effect of harmful electrochemical side-effects such as the dissolution of the metal electrodes, the creation of reactive oxygen species (ROS), pH shifts, or the creation of H₂O₂ or chlorine [86]–[89], [92]–[94], [100]. Both faradaic and non-faradaic reactions can occur, where there is electron transfer or no electrons transfer between the electrode and electrolyte respectively [92]. Faradaic reactions cause reduction or oxidation of chemicals in the electrolyte and non-faradaic present as a redistribution of charged chemical species in the electrolyte [92]. Biphasic waveforms are often used to try to minimize these effects by balancing out charge, however, while some faradaic reactions are reversible, (i.e. cathodic oxygen reduction and anodic electrode corrosion) they are not inverses of each other and cannot be reversed [92]. To try and avoid this, electrodes should be designed with the electrochemical limits for metals in mind as in this range metal is neither oxidized nor reduced [108]. To try and balance charge with varying impedances at each electrode, a constant current supply should be used to further minimize permanent reactions [87].

At the cathode of stimulation, oxygen is reduced forming H₂O₂ and OH⁻ [93] [90], and with too high of a voltage, hydrogen gas can be created through the electrolysis of water as seen in equation (3.1) [90]. The electrolysis of water is a detrimental side effect because of the gas production and creation of a local pH increase near the electrode [87].



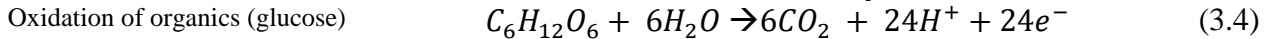
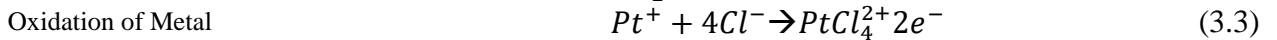
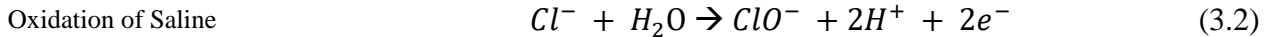
3.1.1. **Chapter Motivation**

The integrity of the electrodes throughout an electrical stimulation experiment is imperative to the success of the overall experiment. The electrodes should not change throughout the testing, both in composition and position. To avoid excessive electrochemical reactions and electrode deterioration, inert metal should be used. Platinum electrodes are expensive to create and decreasing the size allows for optimization of costs. Decreasing the size of the electrodes can be accomplished by soldering copper wire leads onto the electrodes which can then be connected to the stimulation circuitry. The behaviour of the solder and copper lead wires when interacting with the media and electrical stimulation was explored in preliminary constant voltage tests and was determined to be detrimental for maintaining stable media conditions. These experiments also were used to explore different stimulation strengths and shapes to see if these impacted the number of electrochemical reactions that occurred within the media. This was done by varying both the stimulating voltage and electrode displacement. Once an electrode spacing and size were decided on, an electrode holder was developed to maintain parallel spacing while ensuring the solder was fully isolated from the media.

3.1.2. **Material Selection**

Platinum is commonly used for electrodes for its inert properties; however, it is a very pliable metal and when it is stretched to small diameters, it is hard to maintain a rigid shape. To increase the stability, iridium is mixed with pure platinum to make an alloy that has an increased modulus but maintains the chemical stability of platinum. Despite being relatively stable, ES still causes disassociation of platinum and causes free platinum ions

to be released into the medium [87] [100]. This occurs through the oxidation of platinum by free chlorine in the medium [87]. Metal ions can be toxic to tissue and high-intensity ES with platinum electrodes has been shown to produce the same reactions in tissue through the introduction of platinum salts [88]. This indicates that platinum ions also display some toxicity. This is most likely due to Pt⁺ ions being reduced by organic species in the medium such as glucose, which can produce both toxic and non-toxic products [87]. The presence of saline, while vital for cells, causes the strong oxidizing agent ClO⁻ to form and is physiological toxic [87]. The reactions that occur with platinum electrodes and ES can be seen in equations (3.2) - (3.4) [87].



The electrochemical limits for metals as electrodes are also important to consider and for platinum-iridium alloys, the limits for both metals must be considered (0.1 - 0.35 mC/cm² and 1- 4 mC/cm² respectively) [108].

3.1.3. Electrode Shape

Previously, solder was composed of a tin-lead alloy but the health risks of lead have led to the creation of new lead-free alloys [109]. These new alloys now contain varying compositions of tin, copper, silver, bismuth, indium, zinc, and antimony as well as trace amounts of other metals [109]. With a solder connection between a platinum electrode and a copper lead wire are exposed to an electrolyte, a galvanic cell gets created causing decomposition of the various metals at differing rates. The influx of metal ions to a cell

culture environment is toxic to the cells and should be avoided as much as possible [88]. To keep only one type of metal in the electrolyte, studies have used L-shaped electrodes keeping a soldered connection point clear of the media [94], [110]–[112].

3.2. Materials and Methods

3.2.1. Bar Electrodes

To maximize the stimulation area within a 24 well cell culture plate (Corning, Corning NY), there is a trade-off between electrode length and spacing. With the wells being 15.6 mm in diameter, the electrodes were designed to be spaced 10 mm apart, allowing the 10 mm long electrodes to have space between the end of the electrodes and the well walls as seen in Figure 3. The platinum used for these experiments is a 90:10 platinum-iridium alloy (Alfa Aesar, Haverhill, MA) in 10 cm lengths. To maximize the number of electrodes that could be made from a 10 cm piece of platinum-iridium, 10 mm lengths were cut and soldered to an insulated copper wire (Allied Electronics, Fort Worth, TX) at a right angle on one end as illustrated in Figure 3.

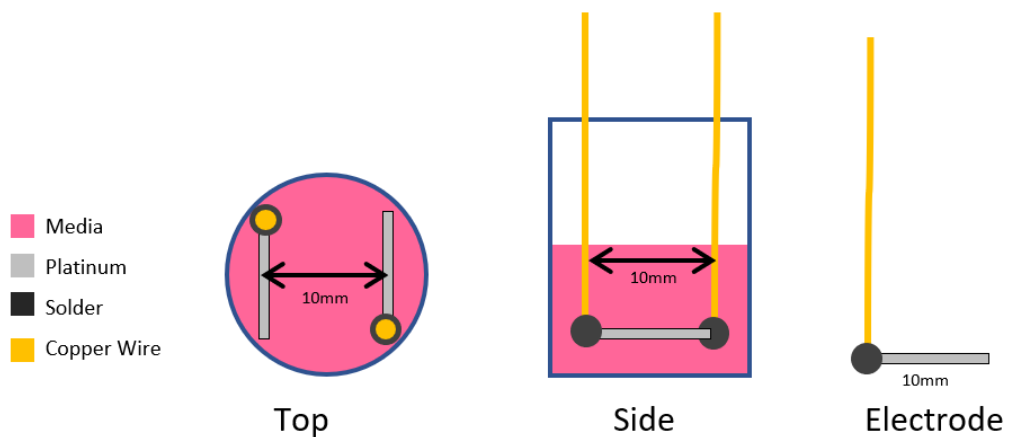


Figure 3: Electrodes alignment in a single well of 24-well plate

3.2.2. L Shaped Electrodes

The limitations of the bar electrodes (that will be discussed in section 3.3.1) led to a re-design of the electrode shape to keep the solder out of the media. This was accomplished through the design of L-shaped electrodes that kept the 10 mm active sites 10 mm apart, 5 mm off the bottom of the well. The solder point of the electrode could then be at the very top of the well, far from the media as can be seen illustrated in Figure 4. The insulated copper wire was soldered to the electrode and cut to 1 m in length to allow for the supply electronics to be kept out of biosafety cabinets or incubators. This new design was put in place once the experiments with the cells in culture were initiated (Chapter 5 -Osteoblast-like Cell Testing) and was used from that point forward for the constant current experiments (Chapters 4.5 Constant Current Materials and Methods - 4.7 Constant Current Discussion).

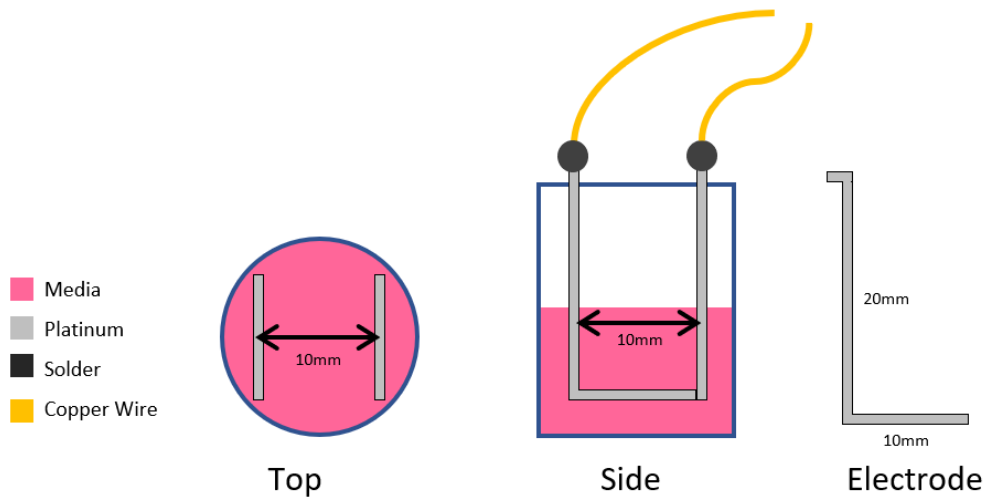


Figure 4: L-Shaped Electrodes alignment in a single well of 24-well plate

3.2.3. Electrode Holder Design

While the platinum electrodes are quite stiff due to their iridium composition, the copper wires they are attached to are quite pliable and difficult to control. This made it difficult to keep the electrodes at the correct placement for the experimental setup. To fix this, a 3D-printed plate was created to hold the electrodes in place (Figure 5). Channels on the top surface were included for the lead wires to stay in to keep them from getting tangled. As the stimulation experiments only used four of the 24 wells at a time, the plate was designed to hold electrodes over one row of wells, with one electrode being held on either side of a well.

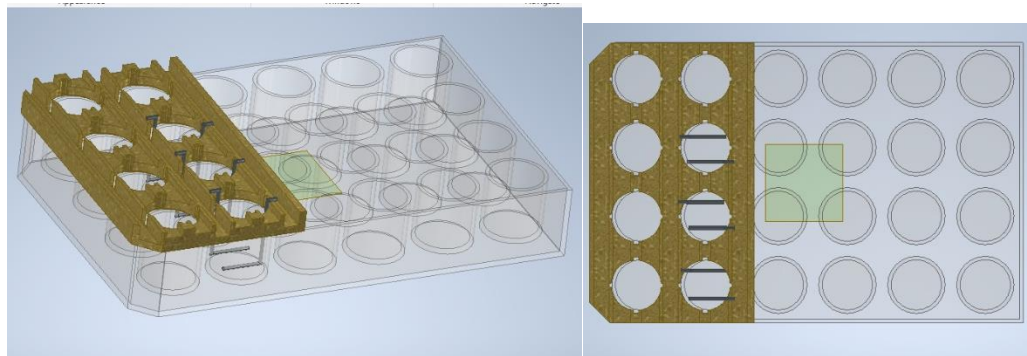


Figure 5: Electrode holder, Oblique view, Top view

3.3. Results

3.3.1. Bar Electrodes

The small 10 mm platinum electrodes were soldered to much longer lead wires to connect them to the stimulation apparatus. The length of the wires made it extremely difficult to maintain spacing between the electrodes and impossible to maintain parallel placement. To combat this, a wooden spacer was used to keep the electrodes parallel and 5mm apart.

This ended up being an issue as the wood absorbed medium and could be a potential contamination risk

Upon the completion of the constant voltage experiments described in section 4.2 Constant Voltage Materials and Methods, it was quickly found that the solder-wire-electrode connection was highly volatile when used with the cell culture media. The experiments increased the amount of precipitate formed in the media and on the electrodes, the formation of gas bubbles, as well as causing rapid deterioration of the solder.

A white-grey precipitate formed all over the entire solder connection, which can be seen in Figure 3 A, and in extreme cases, the copper was exposed causing a blue-green precipitate, which can be seen in Figure 3 C. In Figure 3 A and B, the increased buildup on the electrodes can be seen on the platinum closer to the solder presenting as a black buildup. All these issues led to the design of L-shaped electrodes.



Figure 6: Electrode deterioration and precipitate formation

- A) increased precipitate buildup on solder post-stimulation
- B) Deteriorated solder exposing copper wires
- C) Deteriorated lead wire with blue precipitate

3.3.2. L-Shaped Electrodes

The L-shaped electrodes eliminated the extreme precipitate buildup from solder being exposed to the media listed in section 3.3.1. The platinum is still reactive with the media by itself, however, and the brown/grey precipitate can be seen in Figure 3 as texture on the electrode surface.



Figure 7: Precipitate buildup on L-shaped electrodes.

While more structurally stable than the bar-shaped electrodes, the L-shaped electrodes were still difficult to position as they had the tendency to rotate based on the positioning of the long lead wires. To combat this, they were held in place with hot-melt adhesive. Throughout testing the electrodes were still found to move slightly as they could get displaced during the cleaning process.

3.3.3. **Electrode Holder Design**

3D printing allows for rapid prototyping for customized design. The electrode holder lid was created using poly-lactic acid (PLA) which is a layer-by-layer fused deposition method of printing. This process creates microchannels in the manufactured part that causes capillary action to occur upon contact with the fluid culture medium. This draws the medium up the microchannels and the medium distributes throughout the part. This caused issues with maintaining media in the wells as it was drawn up into the manufactured lids. It also created a potential contamination issue for future use with cells. As the lid absorbed liquids quite readily, it would be difficult to keep it free of bacteria if it were constantly being seeded with a medium designed to help bacterial cells grow. This led to the conclusion that the lid holding the electrodes could touch the top of the wells but should not come in contact with the medium.

After an extensive prototyping process, it was found that circles needed to be engraved on the bottom of the electrode holder lid to accommodate the lip on the top of the cell culture wells. This made the lid fit snugly to keep it locked in place while in use, but also easily removable to do maintenance and cleaning between experiments.

3.4. Discussion

3.4.1. Electrode Design

Platinum has been used extensively in ES experiments to create inert electrodes for biological environments, however, they still disassociate in these environments with the introduction of ES [87], [100]. This process is further expedited when other metals are introduced such as through the use of solder. Solder is made from a mixture of metals to achieve proper physical properties for melting while maintaining electrical conductivity.

This mixture of metals when combined with an electrolyte and a driving force of ES causes an increase in both faradaic and non-faradaic reactions in the media, creating potentially toxic pH changes, gas formation and precipitate formation that is detrimental to cell health. Keeping solder out of contact with an electrolyte is beneficial for both the health of the electrolyte and the electrodes as it decelerates the degradation process.

While L-shaped electrodes reduce this issue by holding the solder out of the media, there are still many degrees of freedom for movement that are amplified when the attached lead wire is hundreds of times longer than the electrode itself. To eliminate this issue, the electrode should either be held more snugly in its holder or have a 2nd or 3rd bend creating a “z” shaped electrode. This would allow for more control of how the active sites of the electrode are being held within the media, keeping the placement as parallel as possible in the XY plane and at the same level in the z plane. A more exact electrode placement would allow for more consistent current flow through each well causing more consistent stimulation between each of the experimental wells. The ability to have the electrodes snugly held in their holder without adhesive would also be helpful in the cleaning process. With the electrodes attached to the 3D printed holder, the best way to

clean them is to soak them in acetic acid to try and breakdown the precipitate buildup. However, this does not fully clean them and excessive precipitate often has to be scraped off before the electrodes can be soaked again. This process often results in the electrodes getting bent and misshapen, causing inconsistent placement in future tests. Introducing the electrodes to an alternative cleaning method such as an autoclave may help with the precipitate buildup but would cause damage to the holder as the PLA plastic has a relatively low melting temperature. While they could be detached and reattached between tests, having the electrodes free from the electrode holder would simplify the cleaning process and hopefully decrease the likelihood of damage and excessive deterioration.

3.4.2. **Experimental Design**

As reactions around each electrode are charge-dependent, with differing reactions at the cathode and anode [93] [90], the polarity of each electrode should either be varied during the test, through a biphasic waveform or between tests to ensure electrode wear is occurring consistently. Also, the z-characteristics of the electrodes should be monitored after each test to ensure that the conductive properties of the electrodes have not changed significantly, and to ensure that they do not affect test results.

To get a better understanding of the behaviour around the electrodes, it would be beneficial to introduce a probing array of electrodes at the bottom of each well to measure the field strength throughout the media. It is assumed that there is an even electric field throughout the medium, but it has been shown that the current density drops greatly within a millimetre of the electrode at the electrolyte electrode interface [100]. This

would indicate how much of the stimulating current is getting to the cells that are seeded on the very bottom of each well. If the amount of current getting to the cells is too small, it could be necessary to increase the stimulating current, which would increase the side effects discussed in section 3.1. A balance between cellular stimulation and the potential of toxic side effects would need to be found to get the maximal results out of the cells.

To further the understanding of the current dissipation of the media, it could be characterized and used in a simulation. Simulations have been able to show the drop-off of current density surrounding the electrodes [100], but could potentially differ between medium types as the composition of the electrolyte differs. A set of simulations for each medium type, coupled with experiments using a probing array would give better insight into the consistency of stimulation that the cells in each well are experiencing. As will be further discussed in section 5-Osteoblast-like Cell Testing, some cells naturally respond to the by-products created through ES of media – such as H_2O_2 – and may be the reason cells respond to ES. Being confident in the amount of electrical stimulation the cells are receiving through an experimental setup could help clarify if resulting cellular behaviour is coming from the ES or the ES side effects.

3.5. Conclusion

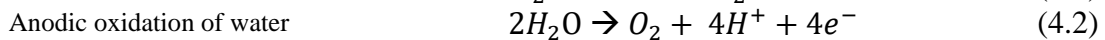
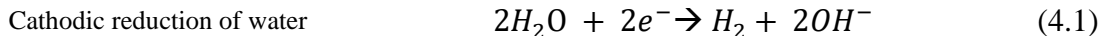
Platinum electrodes are generally inert in biological environments, however, solder used to attach them to leads is not. Solder needs to be kept out of contact with any electrolyte for the health of both components. This decreases the severity of the chemical byproducts created through ES and leads to a better overall environment for cells in culture. The electrodes themselves will still deteriorate slowly over time and this should be monitored

for consistency between experiments. To fully understand what is happening within the media while stimulated, the generated byproducts should be characterized and the electric field within the media should be measured with probing electrodes. Having a better understanding of the behaviour of the media will increase the success of ES of cells as the medium conditions can be kept as optimal as possible to not cause stress or death of the cells.

4. Electrical Stimulation in Media

4.1. Introduction

Pure water is a very poor conductor of electricity, but the addition of a water-soluble electrolyte allows current to flow through the movement of ions. This process works best if the electrolyte ions are not easily oxidized or reduced as the anode and cathode naturally reduce and oxidize species respectively [113]. The electrodes themselves break down and change as they collect or lose electrons. Sodium chloride is a common electrolyte, and when added to water the positively charged sodium is drawn to the cathode and the negatively charged chloride is drawn to the anode, creating chlorine gas [113] This is called electrolysis, as it is using electricity to break down elements. With high enough voltages, the electrolysis of water also occurs following equations (4.1) and (4.2) at the cathode and anode respectively [96].



Ionic current flow and traditional current flow vary in their definition. In general, an electric current is the flow of electric charge, but the particle that carries that charge differs depending on the situation. In standard electric circuits, the current is said to flow from the positive supply to ground following the flow of positive charges. In electrolytic cells, there is movement of both negative and positive ions but the current is defined by the flow of positive charges as in standard circuitry [113]. In these cases, there needs to be an electric source driving the current as the electrodes are generally inert. In galvanic cells, there is movement of both positive and negative ions as well, but the current flow is

measured in the direction of electron movement. This current is driven by potential differences that occur as the electrodes are reacting with the substrate they are submerged in [113].

4.1.1. **Chapter Motivation**

To determine the behaviour of cell culture media with the introduction of ES, many different stimulation shapes and strengths should be used to get a full picture of expected outcomes. It was assumed that some electrochemical reactions may occur, and the size of them would depend on the size of the stimulus. It was also hypothesized that DC stimulation would generate the most of these side effects, and biphasic or AC stimulation, the least.

Experiments were initially done with a constant voltage to try and recreate results from studies that used constant electric fields to stimulate cells. This was a simple setup that allowed for easy exploration of different stimulation shapes and strengths. These experiments were useful in understanding the basic behaviour of media under ES and producing an experimental setup that would generate more consistent results. There is a wide range of experiments done to begin narrowing down the optimal stimulation parameters. As testing went on, it was quickly seen that the constant voltage that was being aimed for was not constant. With further literature review, it was decided that stimulation through a constant current would be more optimal for cells and would allow for more consistent constant stimulation.

Constant current stimulation was done more extensively to try and understand the temporal changes in the media throughout an electrical stimulation experiment. Currents within the range of 100-1000 μA were used to determine the resistance of the media over this range, and also the number of electrochemical reactions that would occur at each current level. These experiments were done to try to find the maximum stimulation strength possible without sacrificing cell health due to excessive pH changes.

4.1.2. **Media Stimulation**

Cell culture media are full of an assortment of ions and molecules, most of which have a charge. While these additives are ideal for cell growth and proliferation, they directly interact with any electrical force within the media by causing faradaic and non-faradaic reactions. Faradaic reactions involve electron transfer between the electrode and electrolyte that causes the reduction or oxidation of chemicals within the electrolyte [92]. A non-faradaic reaction occurs when no electrons are transferred between the electrode and electrolyte, but the reaction presents as a redistribution of charged chemical species in the electrolyte [92].

The applied voltage versus current in the media follows a power curve in general, with the faradaic range being linear [100]. When the electrode voltage is under 1.5 volts there is minimal current in the media, indicating the re-distribution of charges is small, similar to processes that occur during capacitive stimulation [92]. Between 1.5 and 3 V, the current increases non-linearly but there are non-faradaic reactions [92]. More than 3V in the media causes a linear current-voltage relationship and causes faradaic processes to occur and this range should be avoided to avoid excessive electrolysis in the culture

media [92]. The four main reactions that occur with ES in biological media were discussed in section 3.1.1.

Electrolysis of water is a detrimental side effect as it produces gas and causes a local pH change near the electrode [87]. The oxidation of saline creates ClO^- , which is a very strong oxidizing agent and can be physiologically toxic [87]. The dissolution of the Pt electrodes is dangerous as the products are usually toxic and generate powerful oxidizing agents that can be reduced by organic species in the medium. [87], [88]. An example of this is glucose, which can be oxidized into acids or CO_2 that are not necessarily detrimental as long as the products are not toxic [87].

A unidirectional electrical stimulus can cause severe pH shifts, hydrogen peroxide, chlorine gas, radical and reactive oxygen species (ROS) formation [86], [88]. Using a biphasic waveform that alters electrode polarity reduces the production of these products but does not eliminate them as biphasic waveforms allow for charge balances but do not cause electrochemical balance [92].

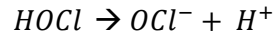
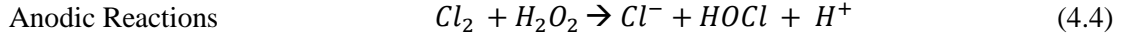
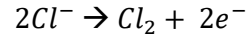
The voltage at the electrode-electrolyte interface will determine which electrochemical reactions occur [113]. A double layer of charged ions forms that acts as a resistor and capacitor in series [92]. The maximal current density occurs at the electrode-electrolyte interface and drops off quickly within 3 mm of the electrode between electrodes and the current density is negligible elsewhere around the electrodes. on the inside and is negligible on the outside. In between the electrodes is where most of the current flow occurs and close to the electrodes the current density is very high and can kill cells [92].

To minimize losses and maximize stimulation, the electrodes can be put closer together and closer to the subject of stimulation [92]. The medium itself usually has an increase in internal resistance over time [114], and a constant current supply is best to maintain slight voltage fluctuations while the resistance changes [89].

In general, electrically stimulated media will have elevated levels of H_2O_2 and metal ions from the decomposition of the electrodes [92]. This can be directly combatted with ascorbic acid and sodium pyruvate, which prevent the media from being oxidized by H_2O_2 by donating an electron [92]. Another way to avoid side effects is to use a stimulator that is isolated from your desired stimulation subject via salt bridges that minimize the faradaic by-products interacting with the cells [91].

4.1.3. **Electrode Polarity**

The polarity of a stimulating electrode will directly affect the type of reactions that occur around it. The cathode is the negatively charged electrode and the anode, the positive. The primary reactions that occur at the specific electrodes can be seen in equations (4.3) - (4.5) [89], [115]. Some of the secondary reactions that occur are not easily reversible, (i.e. cathodic oxygen reduction and anodic electrode corrosion) as they are not inverses of each other [92]. For the most part, these reactions create equal and opposite pH changes resulting in no net change [89].



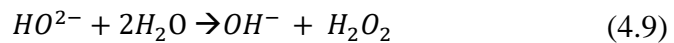
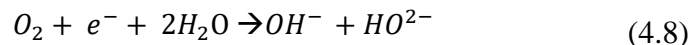
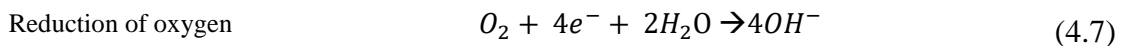
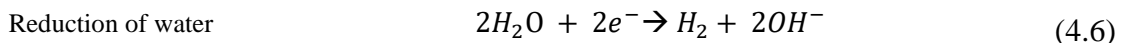
When all combined create:



4.1.3.1. Cathode

At the cathode of stimulation, there are faradaic reactions that reduce species surrounding the electrode, which can change protein conformation through the reduction of disulphide bonds [113]. Oxygen and water get reduced and forms hydroxyl ions, increasing the pH. These reactions can be further broken down into oxygen reduction partial equations that consume oxygen, and generate hydrogen and ROS, including radicals and hydrogen peroxide [90], [93], [113]. These processes can be seen in equations (4.6) - (4.10) [113].

The amount of hydrogen peroxide created from the stimulating cathode is linearly proportional to the amount of time the stimulation occurs [92]. These side effects can be toxic due to an increase in pH from the OH⁻ ions [89]–[91] and if the voltage is too high, an excess of hydrogen gas that forms [90].



4.1.3.2. **Anode**

There is a pH decrease at the anode of ES as H^+ ions and hypochlorous acid are formed [89]. The hypochlorous acid is formed as the ES generates chlorine gas [89]. The anode also reverses some of the cathodic reactions by decomposing H_2O_2 [92].

4.1.4. **Chlorine**

Chlorine is commonly used in liquid form to kill harmful bacteria but is dangerous if generated in a gaseous form. Chloride is an important ion for cellular activity and is present in cell culture media in the form of various salts. While non-toxic in the chloride form, ES in media can cause a significant amount of free chlorine to form from these pre-existing chloride compounds [89]. As chlorine can kill bacteria, its presence in media must be monitored to maintain cell health [89]. At the anode, Cl_2 gas is formed (the full formula can be seen in equation (4.3) and isn't directly harmful in the media, but below pH 7.5 creates hypochlorous acid ($HOCl$) and above creates hypochlorite ion (OCl^-) [89]. As the hypochlorous acid is 100 times more reactive than OCl^- its levels must be carefully monitored to maintain cellular health [89].

4.1.5. **pH**

pH is predominantly driven through 2 ions, H^+ and OH^- . With these ions being charged, the introduction of an electric potential causes relocation. Additionally, ES causes the electrolysis of water causing a cathodic pH increase due to OH^- production and an anodic pH decrease due to chlorine gas production [89]–[91], [93], [96]. The unidirectional stimulus can create severe pH shifts causing a pH gradient to form within the stimulated

electrolyte [88], [89] with current as low as $20\mu\text{A}$ being able to lower medium pH and alter calcium levels [90].

After ES ends, there are usually no significant pH or temperature differences across the wells, with the pH gradient, dissipates after the current is stopped [89], [92]. In general, while acidic and basic elements are generated through ES, the reactions are balanced with no significant pH change overall [92]. However, during stimulation the free chlorine in the media is directly impacted by the local pH changes with free chlorine below pH 7.5 is hypochlorous acid (HOCl) and the hypochlorite ion (OCl^-) above [89]. The hypochlorous acid is much more reactive than OCl^- and trying to minimize this is ideal for cell health [89].

4.1.6. **Signal Shape**

Introducing a unidirectional electric stimulus to an environment naturally causes charged ions to collect at either electrode. These unidirectional stimuli can create severe pH shifts [88], and generally using pulsed stimulation has a lesser response than DC stimulation [92]. Biphasic waveforms allow for charge balances but don't necessarily equate to electrochemical balance as the reactions at each electrode are not direct inverses of each other [88], [92]. To balance charge, there needs to be a controlled current environment and as the reaction impedances are different at each electrode, a true charge balance can only be achieved with a constant current [87].

In the example of hydrogen peroxide, there is a minimum pulse width that generates it but depends directly on both the frequency and voltage of the pulses and if the previous pulse

can discharge before the next one stimulates [92]. In general, an increase in frequency increases the amount of hydrogen peroxide generated in a medium and as an increased voltage attracts more ions, increases the amount of faradaic by-products that are created [92].

4.1.7. **Hydrogen Peroxide**

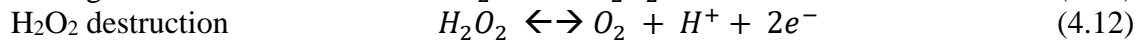
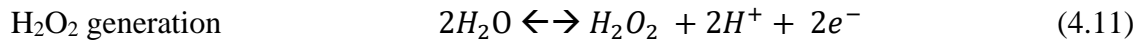
Hydrogen peroxide or H_2O_2 is usually a colourless liquid that is weakly acidic. It is commonly used for bleaching and disinfecting or as an oxidizing agent. H_2O_2 is a common by-product of electrochemical reactions in aqueous solutions [86]. and after an hour of stimulation, there can be significant levels measured in the stimulated electrolyte [86], [92].

The negatively charged cathode converts water and hydroperoxyl radicals into hydroxide and hydrogen peroxide [90], [113] The amount of hydrogen peroxide generated at the cathode is linearly proportional to the amount of time the stimulation occurs and is correlated to the pulse width, frequency, and voltage [92]. In general, an increase in frequency increases the amount of hydrogen peroxide generated in media [92].

Over time the hydrogen peroxide will naturally decompose as it oxidizes other agents in the media, which can create harmful bi-products [92]. If there is enough in the media, the decomposition process can be expedited by introducing a positively charged anode [92]. To minimize the oxidation effects on naturally occurring organic species, ascorbic acid and sodium pyruvate are present in the media to donate electrons to H_2O_2 [92]. The H_2O_2

equilibrium reactions can be seen in equation (4.11) and equation(4.11)

(4.12) respectively [92].



4.2. Constant Voltage Materials and Methods

4.2.1. Voltage Divider Circuit Design

To simultaneously stimulate and monitor the media behaviours, a microcontroller (UNO R3, Sunfounder, Bao'An District, Guangdong Province, China) with a voltage divider was used. The UNO R3 uses the ATMEGA328P chip that powers an Arduino family of microcontrollers and uses the same programming interface. The 5V supply pin from the UNO R3 was used to power the platinum electrodes and a load resistor, which was then connected to the ground pin of the UNO R3. The load resistor was 10 k Ω unless otherwise specified and can be seen in Figure 8. The load resistor served two purposes. First, it allowed for a circuit component of known resistive value to calculate the overall circuit current. Second, R_{Load} could be changed to alter the potential difference across the electrodes through a voltage divider setup. A voltage divider is a circuit that contains two or more resistive elements and divides the input voltage between the resistive elements proportional to the ratio of resistance. It was predicted that the resistance of the media would change over time, and therefore the voltage across the electrodes would change over time, not making this a true “constant” setup. However, for these tests, the changes were predicted to be small enough that the construction of a full constant voltage circuit was not necessary.

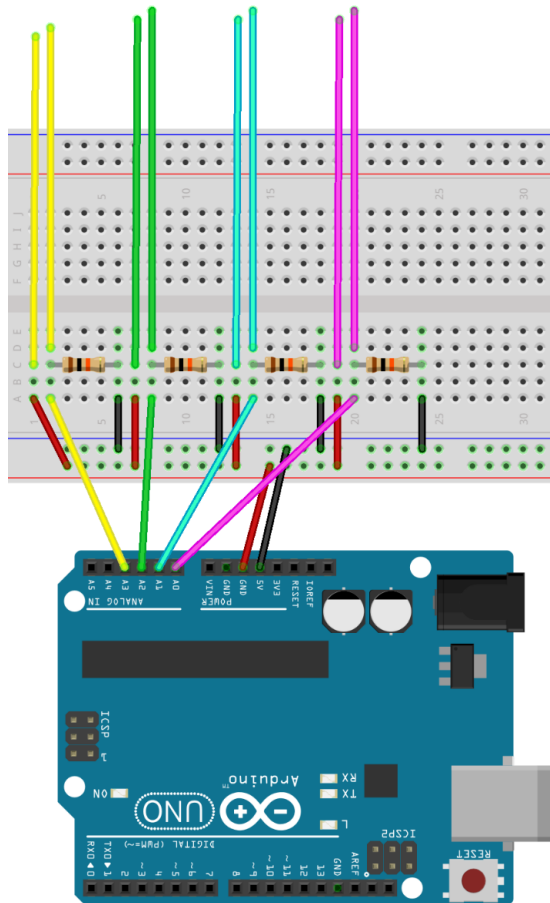


Figure 8: Experimental Circuit Setup

The UNO R3 was programmed to use three of the analog input channels to probe the voltage across the load resistor every 10 minutes for the duration of the test. The six analog to digital converters (ADCs) have a 10-bit resolution that returns integer values ranging from 0 to 1023 corresponding to 0-5 volts. The pins were set to “input” and read using the `analogRead()` function and saved in a temporary storage variable. This was then converted to a voltage value by multiplying the variable by the circuit input voltage (5V) and dividing that value by the 1024 range. This voltage value corresponded to the voltage across the load resistor, which went from the electrodes to ground, so only the voltage at

the top of the resistor needed to be probed. This voltage value could then be used to calculate the voltage across the electrodes and the resistance of the media through equation (4.13), or the rearranged equation (4.14).

$$V_{R_{Load}} = V_{in} \frac{R_{Load}}{R_{Load} + R_{Electrode}} \quad (4.13)$$

$$R_{Electrode} = \frac{R_{Load} \left(\frac{V_{in}}{V_{R_{Load}}} - 1 \right)}{V_{R_{Load}}} \quad (4.14)$$

Through a serial connection with a baud rate of 9600 the voltage and resistance data were used to populate a spreadsheet (Excel, v.2015, Microsoft) through the PLX-DAQ Excel module. This allowed for the resistance to be plotted over time and could be used to calculate other information about the medium. For example, the field strength could be calculated by finding the potential difference across the electrodes and then dividing this value by the 10 mm displacement to get the field strength in V/m or mV/mm. The path of the data can be seen as illustrated in Figure 9.

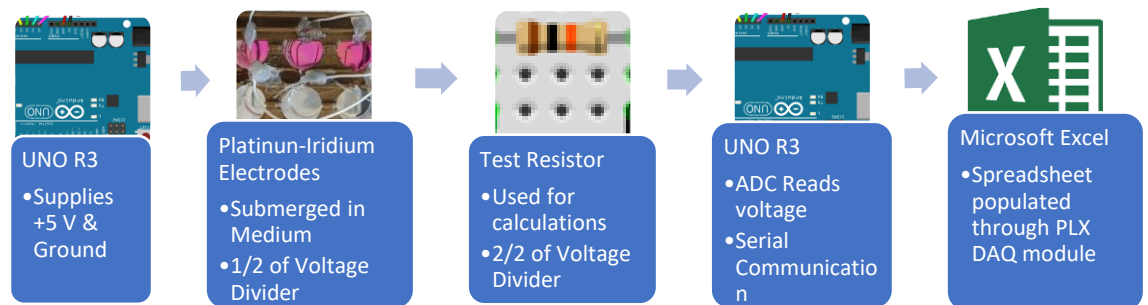


Figure 9: Flowchart of Experimental Setup

4.2.2. Various Constant Voltage Setups

With the limited literature on osteocyte stimulation, papers on the stimulation of other cells along the osteocyte lineage were used as a reference to build a stimulation environment for osteoblast and osteocyte-like cells. The main papers of interest were by Mobini et al [111], [112]. where mesenchymal stem cells (MSCs) were electrically stimulated at 10, 50, 100, and 200 mV/mm for 3, 7, and 10 days. These experiments showed that 200 mV/mm caused cell lysis due to electrochemical reactions in the medium whereas 50 mV/mm and lower had no effect on the cells. It is unknown which electrical factor was causing electrochemical reactions in the medium; the field strength, the voltage, or something else entirely. To investigate this, a set of constant voltage experiments were executed to study the behaviour of the media.

To perform the constant voltage experiments the base voltage divider circuit from Section 4.2.1 was used. Three tests were run: 1) direct current (DC) stimulation, 2) square wave cyclic DC stimulation, and 3) alternating current (AC) stimulation (see sections 4.2.2.1 - 4.2.2.3 for explanation and test setup).

The testing was done with a standard Dulbecco's Modified Eagles Medium (DMEM) (Sigma-Aldrich, St. Louis, MO) as well as McCoy's 5A Modified Medium (Sigma-Aldrich, St. Louis, MO) supplemented with fetal bovine serum (FBS). The testing on McCoy's medium was done to see the effect the electrical stimulation had on the fetal bovine serum as it contains a lot of added proteins. Proteins tend to have a combination of charged sections that could potentially cause extra electrochemical reactions on top of the reactions from the ionic components of the media.

4.2.2.1. **DC Stimulation**

The direct current (DC) stimulation experiments were done using the base voltage divider circuit for six hours at a time. This was done with a range of load resistances to look at the effects of different field strengths on the media. The target field strength of 100vm/mm was used in many tests as this was the most effective field strength found by Mobini et al. [111], [112]. The data from these tests were used as control data to compare with square wave and AC tests to see if there was a significant difference in the media behaviour. The data were taken from the serial communication connection log in the Arduino software and converted into a CSV file to be manipulated in Excel.

4.2.2.2. **DC Square Wave Stimulation**

The base voltage divider circuit was modified to have an input of a pulsed DC signal in the form of a square wave of either 1 Hz or 1/3600 Hz. The UNO R3 5V and ground supply pins cannot be shut off without powering down the device so a different method was needed to accomplish the cyclical power to the electrodes. The UNO R3 analog pins can be used for both inputs to read voltage or outputs to supply 0 or 5V. In the square wave “off” state, the analog pins were set to HIGH making the voltage on both sides of the electrodes 5V, resulting in a potential difference of 0 V. To measure the resistance of the media in the “off” state, this alteration was temporarily disabled, powering the electrodes to measure the resistance, and then was enabled again. The resistance of the media can only be measured when there is an electrical current going through it, which directly contradicts being in an “off” state. However, this entire process took fractions of

a second and has a very low impact on the media responses overall. This process is illustrated in Figure 10.

The data were taken from the serial communication connection log in the Arduino software and converted into a CSV file to be manipulated in Excel.

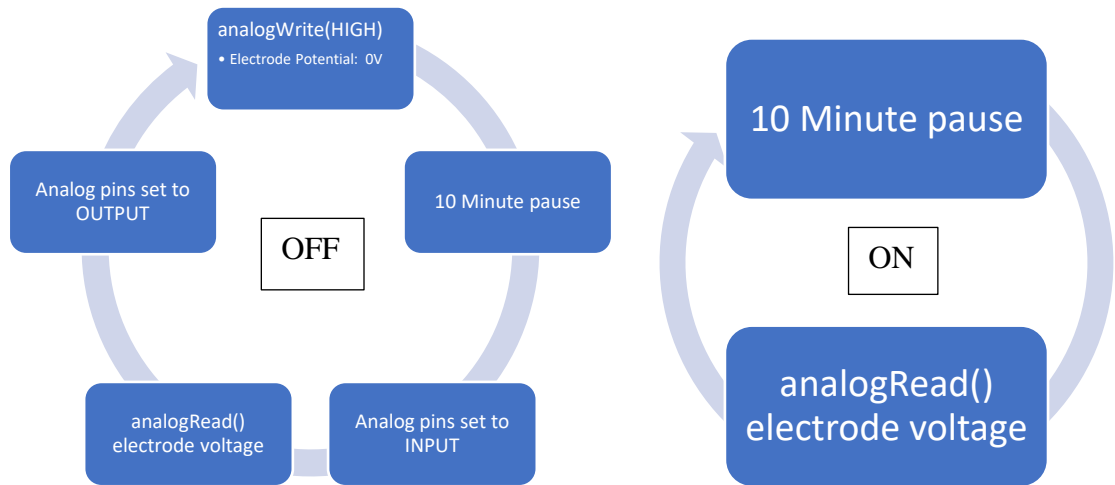


Figure 10: UNO R3 Code Flowchart Off State, On state

4.2.2.3. AC Stimulation

The base voltage divider circuit was powered and monitored with an UNO R3 based circuit with a DC stimulus greater than 0 volts. The UNO R3 microcontroller is not able to handle negative voltages so the production of an AC stimulus that went from -5 to 5 volts was not possible. To correct this issue, the Digilent Analog Discovery USB oscilloscope (National Instruments, Austin, TX) unit was used instead as the power, ground, and measuring device. The Analog Discovery is a USB-powered device that has a collection of electrical functions including the ability to be an oscilloscope, function generator, voltmeter, or data logger. The function generator module can create signals of various shapes, ranging from -5 to +5 volts. This results in an input voltage of 3.535 root

mean square (RMS) or $\sqrt{5}$. The trade-off with this module is that it only has two monitoring channels so only two sets of electrodes could be tested at a time.

The two sets of electrodes were connected to the supply and ground leads from the Analog Discovery. The data logger function was then used to monitor the voltage across the load resistor over time to calculate the media resistance as well as the field strength that was being achieved and was saved as a comma-separated value (CSV) file to be used in Excel to track the media trends throughout the test and to see if any extraordinary changes in the resistance occurred.

4.3. Constant Voltage Results

To find a starting point for the behaviour of the cell culture medium over time, different field strengths and stimulation shapes were used in each well to determine a range that would cause faradaic negative side effects. This was achieved using potentiometers or resistors to alter the load resistance until the desired field strength was achieved in the media. Independent of the field strength, there was a basic trend that each experiment exhibited. The increase in media resistances increased the proportion of the voltage that dropped across the electrodes versus that on the load resistor. This increase in voltage caused an increase in the field strength through the media as the field strength is determined by the voltage over the displacement of the electrodes. As the displacement is not changing, the field strength must increase if the voltage is increasing.

There were varying amounts of side effects in the media depending on the stimulation parameters. There was consistently a white precipitate that formed on the cathode

electrode and in some cases a precipitate formed in the media and settled to the bottom of the container. There was also the formation of bubbles around both electrodes. In cases where the solder was in contact with the culture media, there was an increase in the side effects as well as the formation of blue precipitate on the electrodes. The solder also broke down rapidly with some electrodes detaching during the testing.

4.3.1. AC Stimulation

AC stimulation with a sine wave allows for the electrode polarity to be reversed continuously throughout testing. To see if there were less precipitate and gas formation from changing polarity, a function generator created a 1.21 V sinusoidal waveform. The voltage across the load resistor was measured with an oscilloscope with the measurements taken manually by reading values off the screen every 10 minutes. The inefficiency of this testing method meant it was only used once before a more efficient system was implemented. This method was shown to have fewer negative side effects however they were not eliminated.

With the promising results of altering the electrode polarity to reset the media, another test with a sine wave was performed over a longer period. The change in resistance was very small over time. This setup still did not eliminate precipitate and gas formation.

4.3.2. Square Wave Stimulation

The application of a square wave in hour on and off cycles allowed for DC stimulation to occur but to also have time for the media to recover to try and mitigate the side effects. The curves for the “On” states followed similar behaviour to DC tests with larger changes

in resistance initially, followed by a relatively stable value. The resistance decreased once the stimulation was turned off but dropped more once the stimulation began again and the ions had time to realign with the field. When pulsed off, however, the resistance drops down and remains significantly lower until the field is turned on again.

4.3.3. DC Simulation

4.3.3.1. DMEM Medium

The initial targets for constant voltage DC stimulation were 0.25, 0.5, 0.75, and 1 V/cm.

Using the UNO R3 constant voltage setup with potentiometers as load resistances, the test was run for 200 minutes with measurements taken in 5-minute increments. As the tests went on, the final achieved field strengths were 1.08, 1.02, 1.62 and 0.76 V/cm.

This experiment resulted in minimal precipitate and gas formation indicating that the field strength could be increased for the second set of tests with the desired field strength being 0.25, 0.5, 1 and 2 V/cm. This was achieved by tuning the potentiometers until the desired voltage across the electrodes was achieved. At the end of the 120 minutes, the achieved field strengths increased to 1.5, 1.7, 2.4, and 3.84 V/cm. As this test was not run past the 60-120 minute threshold for plateauing, the resistance of the media did not appear to plateau in the same way as other tests.

With the above tests having negative side effects because of the solder in the medium, the following tests were done with the solder out of the medium with the new L-shaped electrodes discussed in section 3.3.2 L-Shaped Electrodes. All DC tests created small amounts of precipitate in the medium but far less than previous tests with submerged solder. All tests had white buildup on the cathode of the electrode pair. As it was also

found that the resistance of the media plateaued between 60-120 minutes the following series of tests were done for a prolonged period to confirm this.

After speaking with Dr. Sandy Raha's lab where they do stimulation of muscle cells, it was found that the negative side effects we were getting were unique. They never had precipitate or foam around the electrodes, but they consistently ran their tests with larger electrodes submerged 0.5 mm into the medium 20 mm apart horizontally. They used a 1-2 Hz (2ms duty cycle) square biphasic wave signal for an hour at a time. This is used to create a 1.5 V/cm field whereas these experiments have been generating a 3 V/cm field. They also had more additives in the cell culture medium, which may have been the factor that suppressed the negative side effects. To test this, the next set of tests were done using the standard DMEM Medium with the addition of FBS and Pen/Strep antibiotics to try and mimic their conditions.

Similar results to previous DC testing occurred with the introduction of FBS to the media. Plateauing of the resistance in the media occurred at approximately 30 minutes into the testing. However, at the interface between the media and the electrode, a foam was created with an increased amount of precipitate. This foam and precipitate did not fully disappear the next day, indicating a permanent chemical reaction occurred within the media. The increase in the amount of gas creation caused the solder to be submerged in the media causing increased electrochemical reactions.

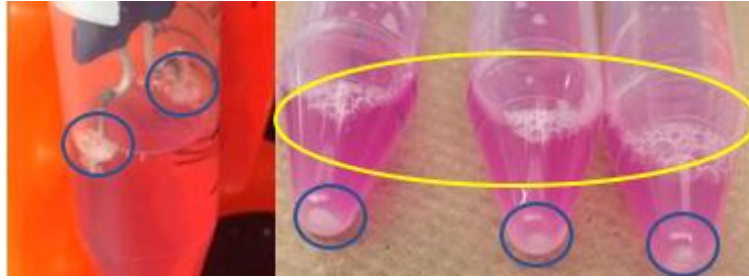


Figure 11: Precipitate (blue) Gas formation (yellow)

Decreasing electrode spacing was done to try and reduce the amount of voltage across the electrodes. This caused an increased amount of foam at the electrode-medium interface which caused interaction between the solder and the medium resulting in inconsistent test results. This also caused chemical reactions between the medium and the solder resulting in a new flakey precipitate and oxidization that caused solder deterioration and medium discolouration. The discolouration in the media worsened with time after the test was complete.

Electrode set zero had the electrode detach very early into the test and graphical representation of the results was not included. The physical results can be seen below.

Electrode set one had an increased level of foam created that caused a blue/green precipitate to form when the solder was interacting with the foam. Additionally, the solder was weakened to the point of detachment after the test. Electrode set two remained intact throughout and post-testing. There was little to no change in the resistance of the media over this test and resulted in significantly more precipitate than the other two tests. This can be seen in Figure 12.



Figure 12 Electrode gas formation 10 min, 210 Minutes, 420 Minutes



Figure 13: Electrode precipitate and gas formation

- A) Early electrode detachment, control test
- B) Oxidization of electrodes resulting in discolouration of medium
- C) Oxidization of electrodes resulting in discolouration – 24 hours later,

4.3.3.2. **McCoy's Medium**

Saos-2 osteoblast-like cells are cultured in McCoy's Medium, which has a differing composition from the DMEM Medium, which could result in different behaviour with the introduction of electrical stimulation. The resistance followed a similar trend to all the previous DMEM tests with an increase in resistance that stabilizes between 60-120 minutes. However, there were a lot more inconsistencies in the trends potentially due to the wear on the electrodes.

4.4. **Constant Voltage Discussion**

4.4.1. **Precipitate Formation**

The application of electrical stimulation in cell culture media causes some of the contents of the media to precipitate out. This can present as gas formation, precipitate on the electrodes, or precipitate that forms and sinks to the bottom of the stimulation container.

The amount of precipitate that forms can be greatly reduced by keeping anything other

than the platinum electrodes out of the media. In the future, both the precipitate from the electrodes and the sedimentary precipitate should be collected and analyzed to get a better understanding of what reactions are occurring in the media. With the number of chemical elements that present as white powders, it is impossible to know what this precipitate is without an analysis, but it is most likely calcium or salt, based on the medium composition.

4.4.2. **Solder**

The presence of solder in media was quickly found to be an issue that was discussed in 3.4.1 Electrode Design. Figure 12 and Figure 13 are examples of increased gas and precipitate formation due to electrochemical reactions between the solder and the media. The solder also directly affected the resistance of the electrodes by breaking down the bond between the leads and the electrodes. An increased amount of gas and precipitate formation may indicate larger pH change as well as ROS and chlorine creation that would be extremely toxic for cells. The presence of different metals in an electrolyte will instantaneously form an electrolytic cell causing the deterioration of one metal and the formation of oxides on the other, impacting its future electrical behaviour and the contents of the media surrounding the electrodes. It is for these reasons that solder should remain out of contact with cell culture media for the health of present cells.

4.4.3. **Stimulation shape**

Biphasic waveforms are generally preferred in tissue stimulation as unidirectional electrical stimuli can cause severe pH shifts, hydrogen peroxide production, chlorine gas and radical formation as well as reactive oxygen species (ROS) [86], [88]. While biphasic

waveforms reduce these unwanted byproducts, it does not eliminate these effects as they allow for charge balances but do not cause electrochemical balance as the reactions at each electrode are not inverses of each other [92].

Using a variety of stimulation shapes and times, we found that the resistance of cell culture media increases with electrical stimulation no matter the shape or time. While direct stimulation causes the most drastic changes and amounts of side effects, the use of AC or square-shaped pulses do not eliminate them. AC waveforms seemed to generate the only visible pH separations within the media indicating that a bi-directional pulse may increase the reactions driving pH changes.

4.4.4. **Field Strength**

While the original plan was to maintain a constant field strength across the electrodes by maintaining a constant voltage, this was found to be difficult to maintain. The resistance of the media increases over time and will eventually settle. While pulsed stimulation through a square or sine wave decreases the resistance change, there is still an increase upon the initial stimulation. A constant voltage could be supplied directly to the electrodes, eliminating the load resistor but this makes monitoring of the media behaviours more difficult. The addition of an external measuring source would involve a second set of electrodes, which would be difficult to place precisely and consistently within the current setup. If a constant voltage is applied to maintain a constant field strength, there would be a corresponding drop in current over time as the resistance increased. This would reduce the amount of ion flow through the media, effectively

reducing the amount of stimulation cells seeded at the bottom of the well are seeing, indicating no stimulation in an electrolyte is ever truly constant.

A better way to maintain a constant stimulation to the cells would potentially be the use of a constant current to try and maintain the ion flow past the cells. This solution will be explored more in sections 4.5 and 4.6.

4.5. Constant Current Materials and Methods

4.5.1. Constant Current Circuit Design

Through a review of published studies, the important factor in bone stimulation appears to be the amount of charge delivered as opposed to the field strength [54]. This more directly relates to stimulation through current rather than voltage [87]. The data from these studies also suggest that the current range the cells should respond to is around 250 μ Amps [91], [116]

A constant current circuit can be advantageous over the simple circuit used in section 4.2.1. as the design isolates the load so that fluctuations in the load resistance do not cause changes in the target current. As the constant voltage tests showed, the resistance of the media increased over time. So, a constant current circuit would be better to maintain the stimulation parameters over time.

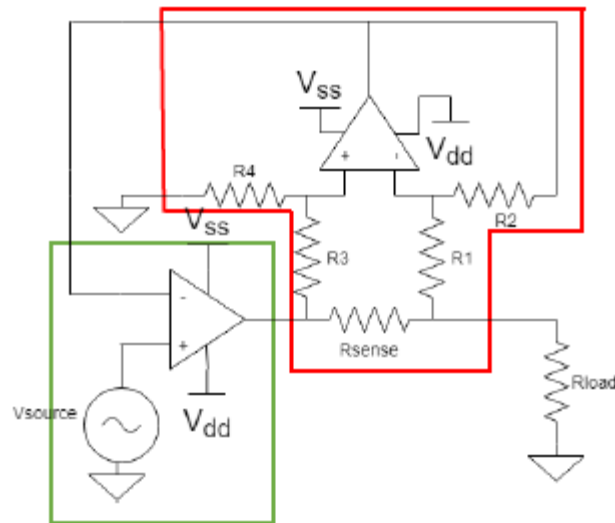


Figure 14: Circuit Schematic [117]

The constant current circuit shown in Figure 14 achieves the isolation of the load using two operation amplifier (OpAmp) stages. The first stage (shown in the red box) is a differential amplifier and the second (in the green box) is a comparator circuit. The comparator takes in the source voltage and outputs a specific voltage to try and maintain the same voltage across both inputs. This causes the output of the difference amplifier to be equal to the source voltage as well. The difference amplifier circuit produces an output voltage based on the difference between the two input voltages. As the output is fixed based on the comparator circuit, the difference between the two inputs must also stay fixed maintaining a set potential difference across R_{Sense} , which then controls the output current through R_{Sense} . As the resistance of the other resistive elements in the circuit would be higher than the resistance of the electrode load, most of this generated current

would go through the load as the path of least resistance. The final output current was then decided based on the equation (4.15).

$$I_{out} = \frac{V_{In}}{R_{Sense} * \frac{R_2}{R_1}} \quad (4.15)$$

The use of a difference amplifier is also able to eliminate signals that are a part of both inputs and only amplifying the difference between the two. This function allows noise from the equipment within the circuit to be eliminated and not influence the output. This is referred to as the common-mode rejection ratio and is a function of the gain of the circuit and the tolerance of the resistors used.

To build the difference amplifier, an integrated circuit (IC; INA106KP, Texas Instruments, Dallas, TX) was used. This IC has two built-in 10 k Ω resistors and two 100 k Ω resistors giving it a gain of 10. The voltage rails were supplied with ± 5 V from a power supply (Anatek Model 24-2D, Anatek, Santa Clara, CA). A schematic of this can be seen in Figure 14.

The comparator circuit was built using an operational amplifier (LT1014CN Quad Precision operational amplifier, Texas Instruments, Dallas, TX). This IC contains four op-amps and only one was used. The voltage rails of this IC were also supplied with ± 5 V from the Anatek power supply with a reference ground. The input voltage to the comparator was a variable 0-5V DC signal from the Digilent Analog Discovery module as described in section 4.2.2.3.

To calculate the current produced by the circuits, equation (4.15) was used. However, upon preliminary testing, it was found that these circuits were not sufficiently accurate to produce currents in the μAmp range and did not have behaviour that followed this equation. The design of this circuit allows for a constant current to be produced no matter the output load, but due to the desired current range, the output resistance, coupled with the R_{sense} both directly affected the output current. The resistance of the media is dependent on the current applied, but the current generated by the circuit depends on the load resistance from the media, generating a mutual relationship. Therefore, to manipulate the circuit, R_{sense} and R_{Load} were changed to achieve the desired current.

Preliminary results were used to calculate an approximate resistance for the media at specific currents using the MATLAB curve fitting toolbox (MathWorks, Natick MA). From this, it was found that there was a power relationship approximately following $2.072 \times 10^6 x^{-0.93}$. This data was used to maximize the UNO R3 voltage resolution for each current level. As the UNO R3 can only measure 0 to 5V, the voltage drops across the electrodes and the R_{Load} cannot be larger than 5V. To get the most accurate readings, the voltage across R_{Load} needs to be maximized while keeping the total voltage less than 5V. To ensure the values do not exceed the maximum, a 15% safety was built in, and the chosen resistor values were selected to be close to these values while using stock resistors. The results of this can be seen in Table 3: Predicted Resistances

However, the instability of the circuit proved to be more difficult to control and the measurement resistor was chosen from three resistors: 2.2k, 1k or 220 Ω depending on which one created the current value closest to the desired value for the test. This was

further tweaked by altering R_{sense} and to finish the tuning process, the input voltage from the Analog Discovery model was modulated between 0-5 V DC until the current output was in the desired range. With the knowledge that the current would decrease as the media resistances increased over time, the initial current output was chosen to be at least $50 \mu\text{A}$ greater than the desired value so it would settle to the desired value over time.

To monitor the current through the electrodes, the analog measurement pins from an UNO R3 microcontroller was used as in section 4.2.1. The output from each constant current circuit was fed through the electrodes submerged in media and then through the known load resistor. The load resistor was then tied to the reference ground of the amplification circuits. The UNO R3 probed the voltages both before and after the electrodes, which allowed for monitoring of the voltage across the electrodes and the voltage across the load resistor. The voltage across the load resistor was then used to calculate the output current. The voltage across the electrodes and the output current was then used to calculate the resistance of the electrodes and culture medium.

4.5.2. **DMEM vs McCoy's Testing**

The testing setup for both the McCoy's medium and DMEM Mediummedium was created as described in section 4.5.1. The L-shaped platinum electrodes were positioned 10 mm apart rotated 180 degrees from each other and adhered to the 3D printed electrode plate. The attached wires were then fed through the channels on the plate to avoid getting tangled and to stabilize them as much as possible. They were then connected to the rest of the circuitry through an additional breadboard.

McCoy's medium or DMEM (2 mL) was put into four wells. Three wells held electrodes and the fourth served as a non-stimulated control. The power supply and input voltage were then turned on and the connection from the UNO R3 to the Excel spreadsheet was initiated. The recorded values were monitored for the first 10 minutes to ensure stability and then left for 6-10 hours. To minimize any effect of capacitive coupling from the long electrode leads or disturbance of the media, the setup was not disturbed during the duration of the experiments. The media were photographed periodically throughout the testing using a set white background to maintain contrast consistency.

Upon the completion of a test, the UNO R3-Excel connection was terminated, and the data saved. The electrode plate was then removed from the cell culture plate and the media were disposed of. The electrodes were then cleaned with a 5% acetic acid solution and rinsed with water.

4.5.3. **Data Analysis**

Using Microsoft Excel (Microsoft Office, Redmond, WA) the data from each test were plotted on a time versus resistance curve to analyze the behaviour of the medium over time. This allowed for an overall visualization of the resistance but also allowed for the detection of outliers or extraordinary events. The resistance of the media is very dependent on its ability to settle, as it was left unsupervised there were times that it was disturbed by other factors in the lab such as power blips and accidental movement of the experimental setup. These events could be seen as changes in the trends in the data and these tests were removed from the data collection completely or the data point was removed leaving the rest of the set intact. In some cases, two of the three wells were

properly stimulated with the third well remaining unstimulated. Due to the regular behaviour of the two stimulated wells, they were left as part of the data set and the unstimulated well was removed.

The constant current tests produced a large set of data including current, resistance, and voltage for both McCoy's and DMEM Medium. Using a Pivot Table in Microsoft Excel, an average resistance and the standard deviation for each current value was calculated.

These data were then plotted with standard deviation error bars in comparative plots.

Plots of current versus resistance, current versus voltage, and voltage versus resistance were created for each medium type and fit with exponential, power, and linear curves. R^2 values were calculated for each curve and the fit of each curve was assessed. The best fit was chosen based on the best R^2 values.

4.6. Constant Current Results

Studies on cell stimulation have generally concluded that electrical charge is the most important factor affecting the cells [54]. This directly correlates to the stimulating current, which is the rate of flow of charges, or Q/t . To test out how current affects the cell culture media, it was determined that the input should be a constant current circuit that can be tuned to various current values in the μA range.

The proposed circuit was designed to isolate the load of the circuit from the current supply to maintain the same constant current despite changes in the load resistance. From the constant voltage experiments in section 4.3, it was determined that the resistance of the media increases over time so isolating these changes from the circuit was very important.

The behaviour of the circuitry was found to be unpredictable and did not follow the ideal equation in section 4.5. To tune the circuit both R_{Sense} and R_{Load} were manipulated considering the predicted media resistances for each current level to try and achieve current values from 100 - 900 μA . As there was not 100% isolation between the two sides of the circuit, the resistance fluctuations did impact the current, decreasing it as time went on. This is listed with each set of data as the average and standard deviation of the achieved current.

The shape of the resistance graphs showed similar trends to the constant voltage experiments from section 4.3. There was an increase in the resistance that plateaued between 100-200 minutes into stimulation. The results differed when looking at the physical side effects in the media. Almost instantly upon the application of current into the media, there was a colour change that occurred around each electrode. The media around the negative electrode became pink, which is a more basic state demonstrated by the phenol red indicator. The media around the positive electrode became yellow, indicating a very acidic environment. This change caused a distinct split in the media that eventually dispersed at around 100-200 minutes of stimulation resulting in a constant colour and pH throughout the media. In some cases, there was a permanent change in the pH of the media as the testing ensued, this was dependent on both the time and strength of the stimulating current. As the pH of the culture media is very dependent on the concentration of CO_2 in the media, it is most often used in a CO_2 and temperature-controlled environment. The pH will change dependent on both temperature and CO_2 and if neither is held constant, the change is even more pronounced. As these experiments

were not done in a controlled CO₂ or temperature environment, a control well was used in most tests to compare the relative pH change from start to finish rather than the absolute pH change. The pH was analyzed solely based on the colour of the indicator as a pH probe would not be precise enough to gather pH changes across the well and would disturb the gradient, altering the differential of the pH between the electrodes. To estimate the pH change in the media, the photographs at various points in the experiment were compared to a known pH scale for the DMEM Medium found at [105]. Due to lighting differences and contrast differences in photos, an estimated visual comparison was made with each photo, rather than attempting to inaccurately calculate quantitative colorimetric values. The decreased amount of phenol red in McCoy's Medium meant that the colour was less vibrant and lighter. The DMEM colour scale had the brightness and contrast adjusted to match McCoy's Medium as accurately as possible.

In addition to pH changes, there was consistently a white precipitate that was built-up on the negative electrode with minimal to no precipitate on the positive electrode. The amount of precipitate depending on both the stimulation time and current strength.

4.6.1. **DMEM Medium**

The DMEM culture medium is very vibrant due to the amount of phenol red it contains. This made the colour changes that occurred very pronounced. Figure 15 A shows a very pronounced pH split that occurred instantaneously with 750 μ A of stimulation. The estimated pH levels at the top and bottom were approximately 8 and 6.9 respectively with the middle being the initial 7.4. The increased gas production can be seen around the negative electrode indicating electrochemical reactions that created the precipitate. Figure

15 B shows the medium at the end of 1060 minutes of stimulation. No stimulation was delivered to the bottom well due to connection issues, which allows for a direct comparison to what the pH should be after the temperature and CO₂ settle in an uncontrolled environment. The top two stimulated wells had the phenol red indicator break down, which is a drastic difference from the basic pH in the control well. The basic pH in the bottom well is at the maximum basic end of the spectrum and the stimulated wells are much lighter in colour. For comparison, Figure 15 C shows the three stimulated wells with the control well below 700 μ A stimulation for 600 minutes. All the wells still have a very basic pH with a slight break down of the indicator in the stimulated wells.



Figure 15: Media pH gradient

- A) Medium colour gradient 750 μ A 0 Minutes
- B) Colour bleaching 400 μ A 1060 minutes
- C) Small colour change 700 μ A 660 minutes

4.6.1.1. **DMEM Stimulation - 100 μ A Range**

In the 100 μ A range, there were very minimal changes in the pH of the media permanently. The pH split created at the start of stimulation was an approximate 7.5/8 split. In this range, there was very minimal precipitate formed on the negative electrode. The resistance of the media started between 15-20 k Ω and settled between 25-30 k Ω at approximately 100 minutes.

Current (μ A)	128.76
STD (μ A)	± 12.75
Voltage	2.911 V
Time	365 mins
R _{Load}	220 Ω
RSense	4.4 k Ω
Max pH	8
Min pH	7.6
Final pH	Slight \downarrow

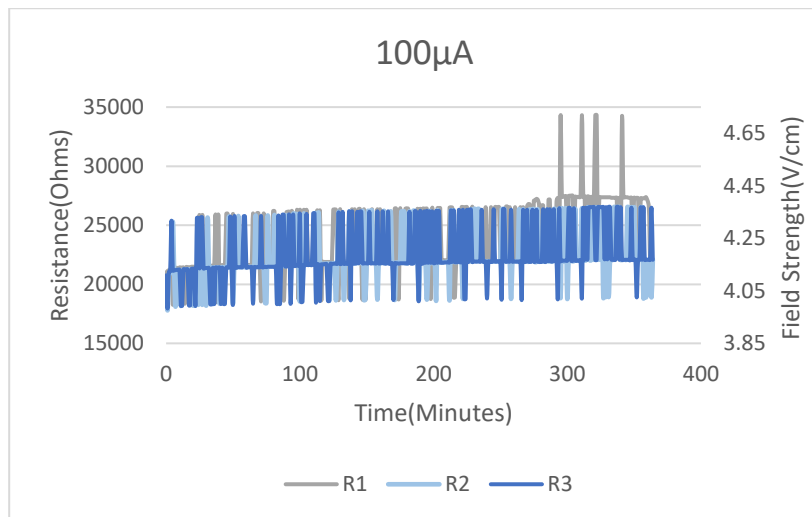


Figure 16: DMEM Medium 100 μ A stimulation 365 minutes

Note inadequacy of UNO resolution resulting in discrete resistance levels.

Current (μA)	106.28
STD (μA)	± 7.94
Voltage	3.11V
Time	648 mins
R_{Load}	2.2 k Ω
R_{Sense}	2.2 k Ω
Max pH	8
Min pH	7.4
Final pH	No Δ

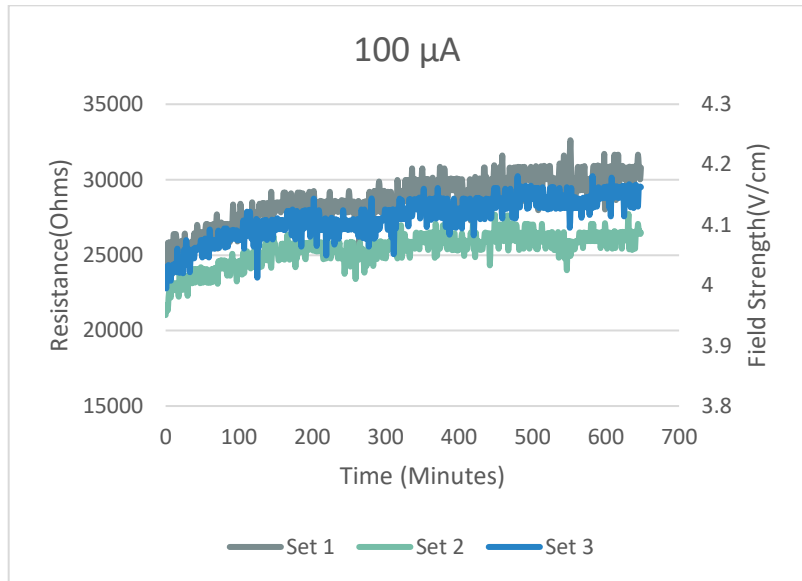


Figure 17: DMEM Medium 100 μA stimulation 648 minutes

Current (μA)	141.23
STD (μA)	± 11.61
Voltage	2.987V
Time	489 mins
R_{Load}	1 k Ω
R_{Sense}	470 Ω
Max pH	7.9
Min pH	7.5
Final pH	No Δ

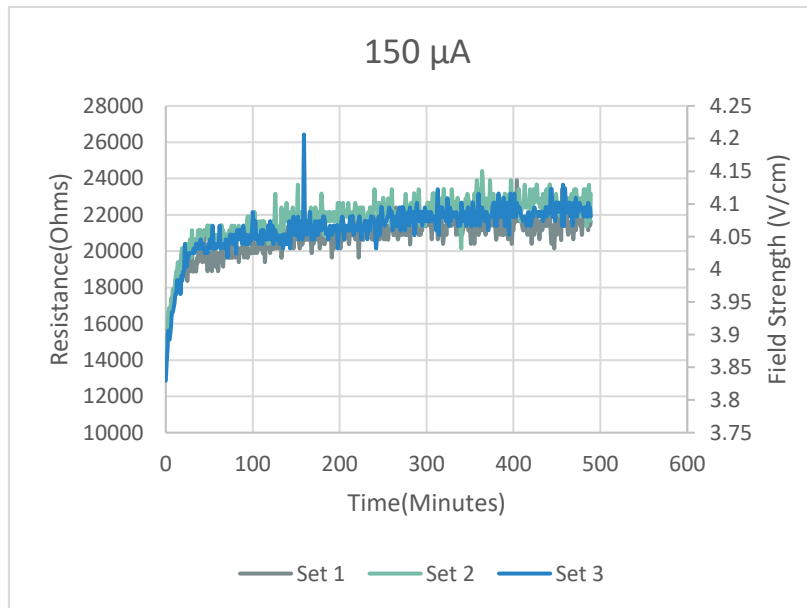


Figure 18: DMEM Medium 150 μA stimulation 489 minutes

4.6.1.2. DMEM Stimulation - 200 μA Range

In the 200 μA range, there were very minimal changes in the pH of the media permanently. The pH split created at the start of stimulation was an approximate 7.3/8

split, slightly larger than the 100 μA range in section 4.6.1.1 DMEM Stimulation - 100 μA Range. In this range, there was very minimal precipitate formed on the negative electrode. The resistance of the media started between 8-12 $\text{k}\Omega$ and settled between 10-20 $\text{k}\Omega$ in the range of 60-100 minutes.

Current (μA)	186.89
STD (μA)	± 21.45
Voltage	3.038 V
Time	728 mins
R_{Load}	220 Ω
R_{Sense}	4.4 $\text{k}\Omega$
Max pH	N/A
Min pH	N/A
Final pH	Slight \downarrow

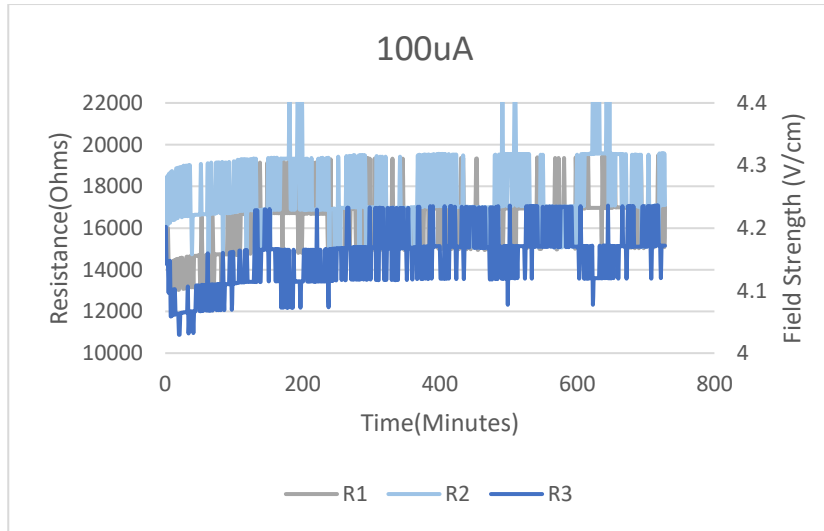


Figure 19: DMEM Medium 200 μA stimulation 728 minutes
Note inadequacy of UNO resolution resulting in discrete resistance levels.

Current (μA)	249.27
STD (μA)	± 15.1
Voltage	2.857V
Time	361 mins
R_{Load}	470 Ω
R_{Sense}	1 $\text{k}\Omega$
Max pH	8
Min pH	7.3
Final pH	No Δ

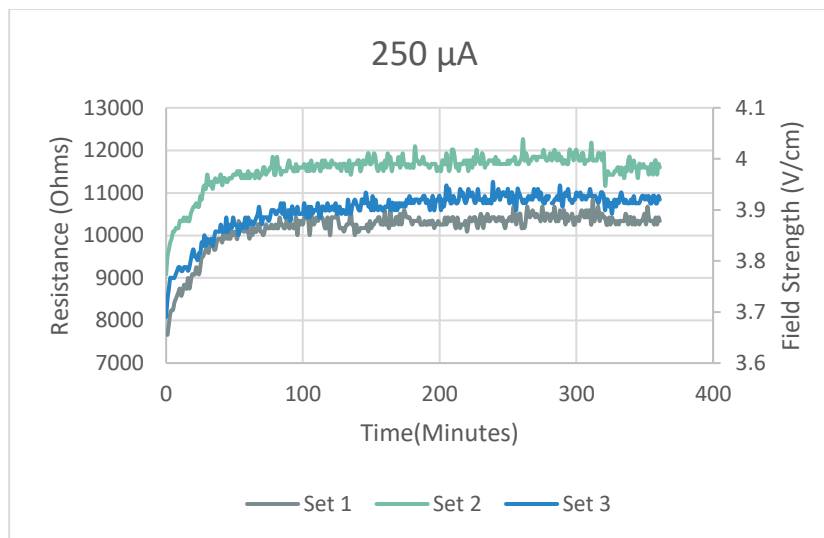


Figure 20: DMEM Medium 250 μA stimulation 361 minutes

4.6.1.3. DMEM Stimulation - 300 μ A Range

In the 300 μ A range, there were very minimal changes in the pH of the media permanently. The pH split created at the start of stimulation was an approximate 7.5/7.8 split, slightly more acidic than the 200 μ A range in section 4.6.1.2 DMEM Stimulation - 200 μ A Range. In this range, there was very minimal precipitate formed on the negative electrode. The resistance of the media started between 8.5-9 k Ω and settled between 9.5-10 k Ω at approximately 150 minutes.

Current (μ A)	334.73 \pm 13.66
Voltage	3.501V
Time	915 mins
R _{Load}	1 k Ω
RSense	220 Ω
Max pH	7.8
Min pH	7.5
Final pH	No Δ

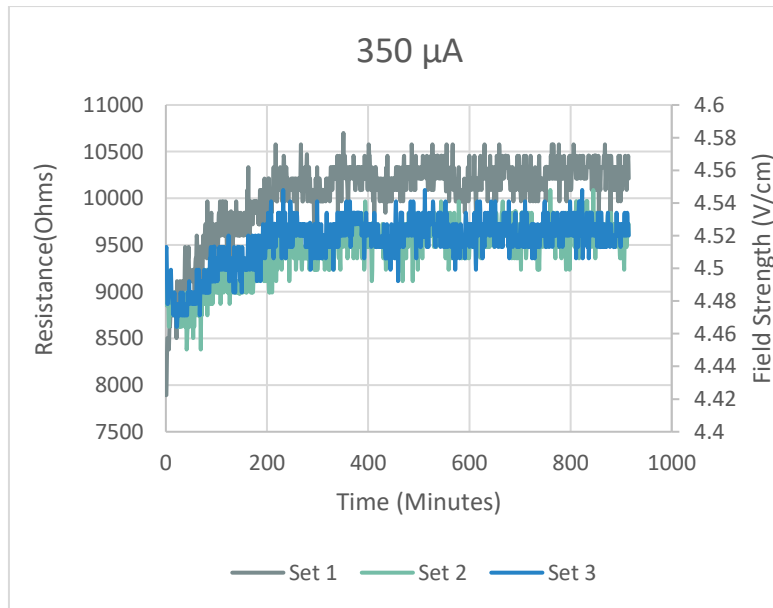


Figure 21: DMEM Medium 350 μ A stimulation 915 minutes
 Note inadequacy of UNO resolution resulting in discrete resistance levels.

4.6.1.4. DMEM Stimulation - 400 μ A Range

In the 400 μ A range, the media was bleached after the 1060-minute testing period due to the pH becoming extremely basic. The pH split created at the start of stimulation was an approximate 7.4/8 split, similar to the 100 μ A range in section 4.6.1.1 DMEM Stimulation - 100 μ A Range. In this range there a sizeable amount of precipitate formed on the negative electrode. The resistance of the media started around 7 k Ω and settled between 8-8.5 k Ω in approximately 150 minutes. The third set of electrodes received no stimulation due to connection errors and was not included in the data set.

Current (μ A)	389.73
STD (μ A)	± 11.56
Voltage	4.033V
Time	1061 mins
R _{Load}	2.2 k Ω
RSense	1 k Ω
Max pH	8
Min pH	7.4
Final pH	Bleached

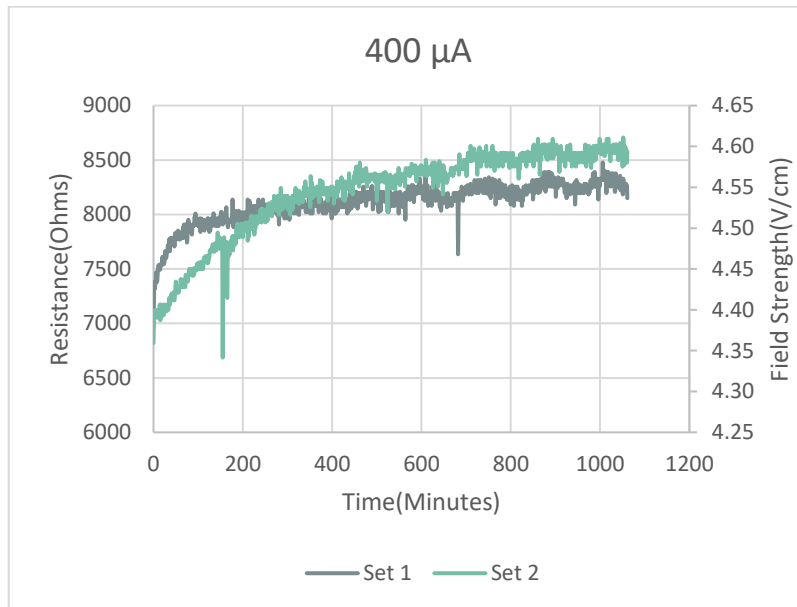


Figure 22: DMEM Medium 400 μ A stimulation 1061 minutes

4.6.1.5. DMEM Stimulation - 500 μ A Range

In the 500 μ A, the media was bleached after the 791-minute testing period due to the pH becoming extremely basic. The pH split created at the start of stimulation was an approximate 7.1/7.9 split, a larger and more acidic range than any previous test. In this range, there was a sizeable precipitate buildup on the negative electrode. The resistance of the media started around 5 k Ω and settled between 6-6.5 k Ω in approximately 100 minutes.

Current (μ A)	520.37
STD (μ A)	± 18.34
Voltage	4.717 V
Time	791 mins
R _{Load}	1 k Ω
R _{Sense}	220 Ω
Max pH	7.9
Min pH	7.1
Final pH	Bleached

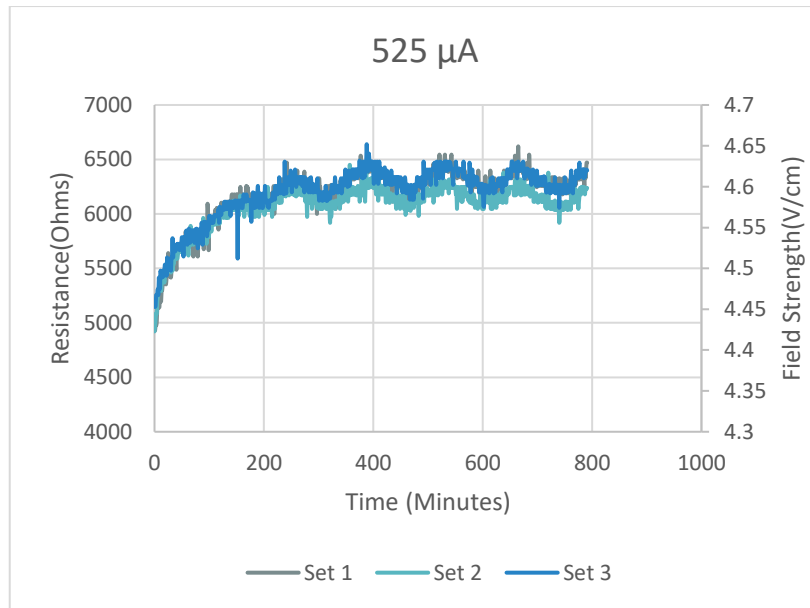


Figure 23: DMEM Medium 525 μ A stimulation 791 minutes

4.6.1.6. DMEM Stimulation - 600 μ A Range

In the 600 μ A range, the media became slightly bleached but much less than in sections 4.6.1.4 DMEM Stimulation - 400 μ A Range and 4.6.1.5 DMEM Stimulation - 500 μ A Range. The pH split created at the start of stimulation was an approximate 7.2/8 split, slightly larger than the 100 μ A range in section 4.6.1.1 DMEM Stimulation - 100 μ A Range. In this range there was some precipitate formation on the negative electrode but less than in sections 4.6.1.4 DMEM Stimulation - 400 μ A Range and 4.6.1.5 DMEM Stimulation - 500 μ A Range. The resistance of the media started between 3.2-4.2 k Ω and settled between 4.6-5.2 k Ω at approximately 100 minutes.

Current (μ A)	612.28
STD (μ A)	± 29.44
Voltage	3.178V
Time	552 mins
R _{Load}	220 Ω
R _{Sense}	1 k Ω
Max pH	8
Min pH	7.2
Final pH	Slight Bleaching

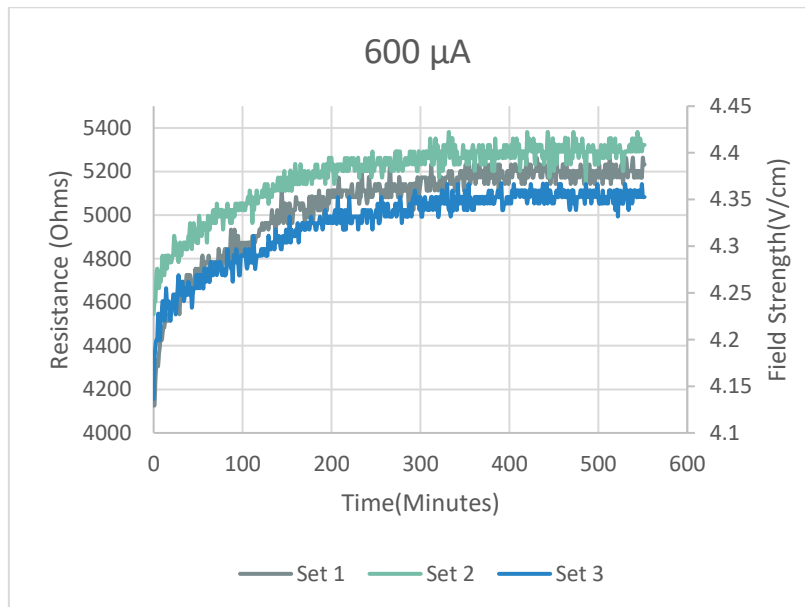


Figure 24: DMEM Medium 600 μ A stimulation 552 minutes

Current (μA)	665.55
STD (μA)	± 28.03
Voltage	3.229V
Time	660
R_{Load}	220 Ω
R_{Sense}	2.2 k Ω
Max pH	7.9
Min pH	7.2
Final pH	Slight Bleaching

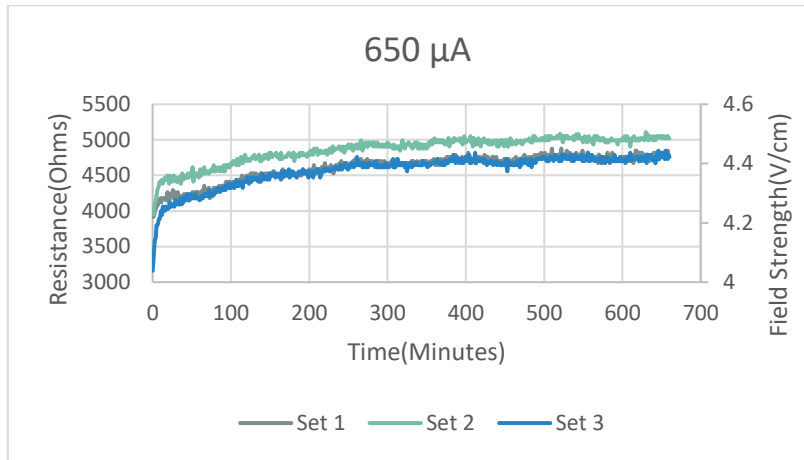


Figure 25: DMEM Medium 650 μA stimulation 660 minutes

4.6.1.7. DMEM Stimulation - 700 μA Range

In the 700 μA range, there were minimal changes in the pH of the media permanently.

The pH split created at the start of stimulation was an approximate 6.9/8 split, the largest difference that was observed. In this range, there was minimal precipitate formed on the negative electrode. The resistance of the media started between 4-5 k Ω and settled at 4.3 k Ω very quickly. This was the first test conducted and the large changes to the media caused the test to be ended instantly as it was an unexpected result.

Current (μA)	771.48
STD (μA)	30.71
Voltage	3.253 V
Time	24 mins
R_{Load}	220 Ω
R_{Sense}	1 k Ω
Max pH	8
Min pH	6.8
Final pH	No Δ

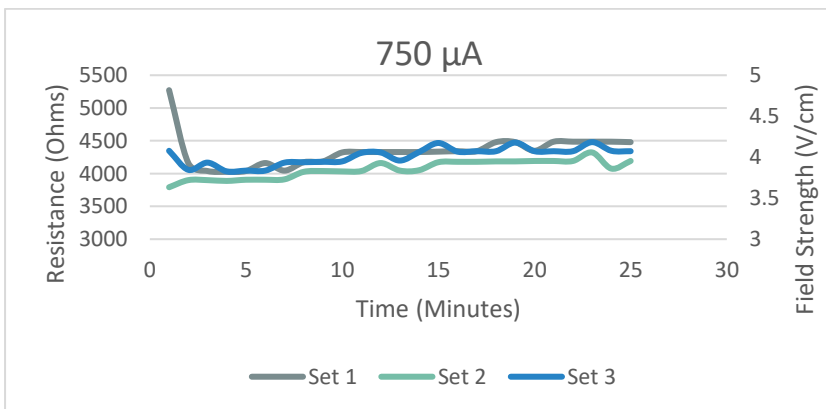


Figure 26: DMEM Medium 750 μA stimulation 24 minutes

4.6.1.8. **DMEM Medium IR Characteristics**

The data from the tests in sections 4.6.1.1-4.6.1.7 were compiled into one large data set. For each achieved current value, the resulting media resistances were averaged, and the standard deviation of these values was used to create error ranges for each value. The values were then plotted as resistance versus current to analyze the IR characteristics of the media. Most resistive elements follow a linear trend with either no change in resistance with current or a linearly proportional change. The DMEM Medium follows a power curve trend with the formula of $2151072.84 x^{-0.94}$ with an r-squared fit value of 99.4%. This can be simplified as $R = 2.15 \times 10^6 I^{-0.94}$. This indicates that there is a steep decrease in media resistances with small changes in stimulation current from 0-500 μA and the relationship flips from 500-1000 μA with large current changes creating small resistance changes. The results of this can be seen in Figure 27.

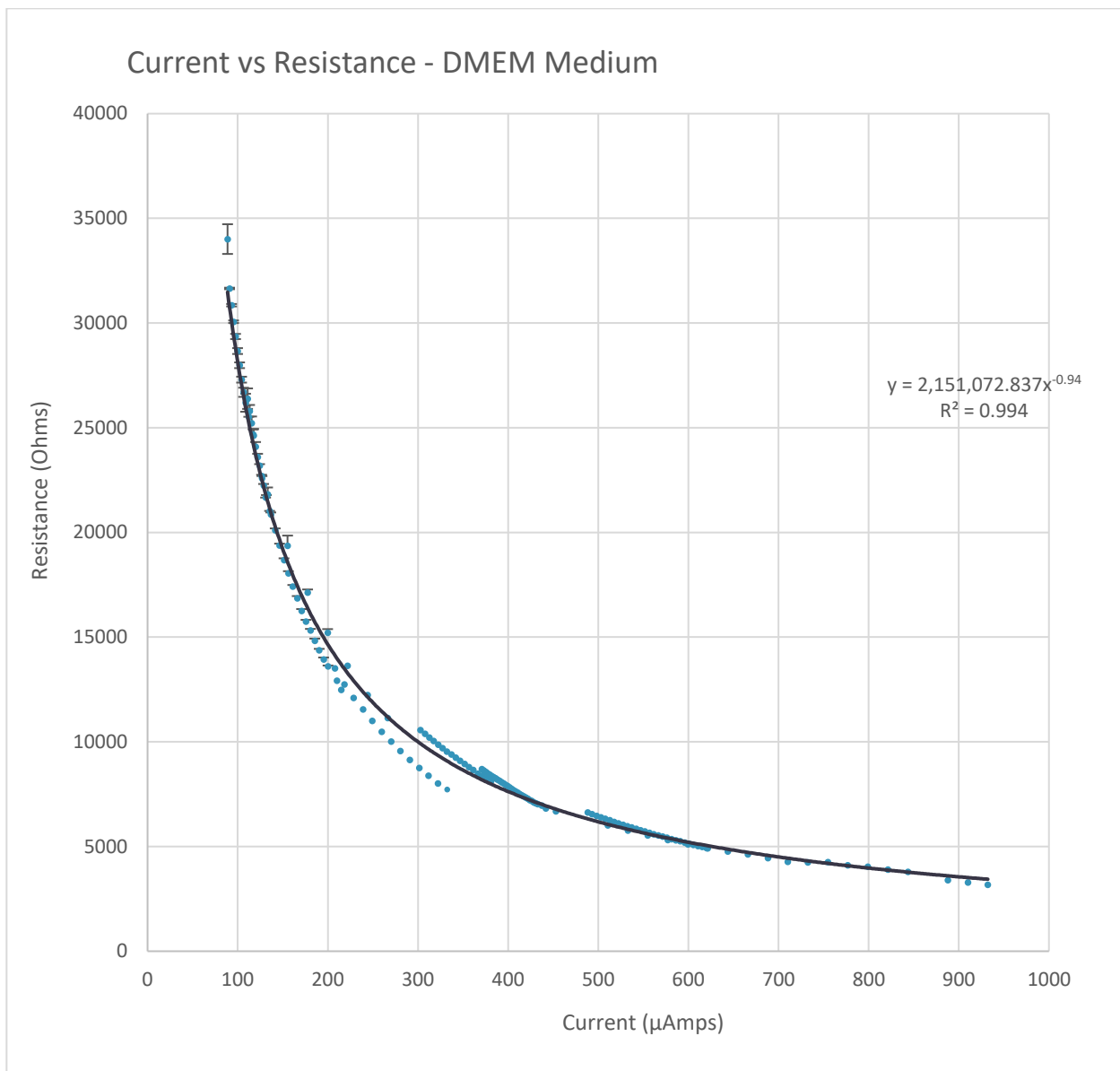


Figure 27: DMEM Medium Current vs Resistance graph

There is a strong power relationship between the current and resistance. Error bars included but are relatively small.

4.6.2. **McCoy's Medium**

McCoy's culture medium is less vibrant than DMEM as it contains less of the phenol red salt. This made the colour changes less pronounced than the same current in DMEM Medium. Figure 28 A shows a very pronounced pH split that occurred instantaneously with 450 μ A of stimulation. The estimated pH levels at the top and bottom were 8 and 6.9 respectively with the middle being the initial 7.4. The increased gas production can be seen around the negative electrode indicating electrochemical reactions that created the precipitate. Figure 28 B shows the medium at the end of 1250 minutes of stimulation. There was a break down of the phenol red indicator in the stimulated wells, which can be seen in comparison to the bottom control well. The basic pH in the bottom well is at the maximum basic end of the spectrum and the stimulated wells are lighter in colour due to indicator break down. For comparison, Figure 28 C shows the three stimulated wells with the control well below with 600 μ A stimulation for 360 minutes. All the wells still have a very basic pH with a slight break down of the indicator in the stimulated wells.



Figure 28: Media colour changes

- A) Medium gradient $450\mu\text{A}$ 10 Minutes
- B) Medium bleaching $450\mu\text{A}$ 1250 Minutes
- C) Minimal colour change $600\mu\text{A}$ 360 Minutes

4.6.2.1. **McCoy’s Medium Stimulation - 100 μ A**

In the 100 μ A range, there were very minimal changes in the pH of the media permanently. The pH split created at the start of stimulation was an approximate 7.5/8 split. In this range, there was very minimal precipitate formed on the negative electrode. The resistance of the media started between 15-18 k Ω and settled between 24-30 k Ω and settled in approximately 100 minutes. These are all similar results to the 100 μ A testing in DMEM Medium in section 4.6.1.1 DMEM Stimulation - 100 μ A Range.

Current (μ A)	112.48
STD (μ A)	± 13.2
Voltage	3.091V
Time	494 mins
R _{Load}	2.2 k Ω
RSense	2.2 k Ω
Max pH	8
Min pH	7.5
Final pH	Slight \downarrow

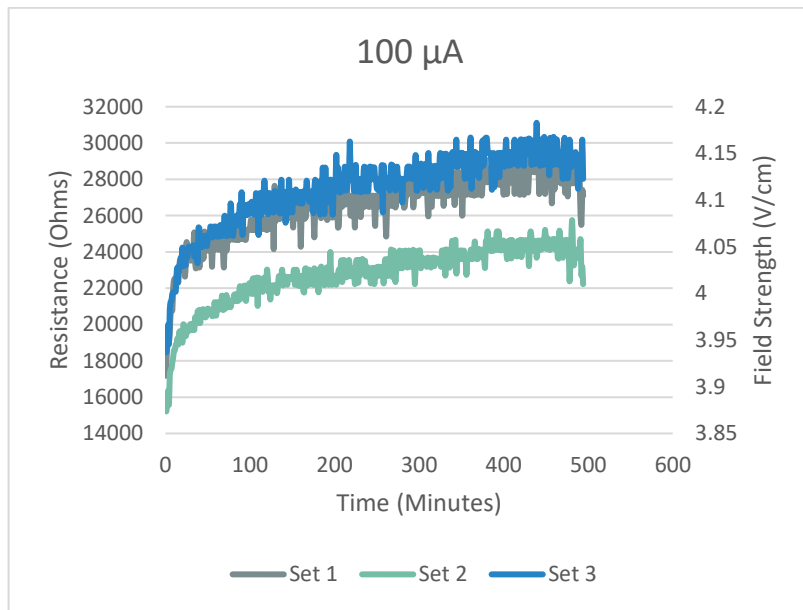


Figure 29: McCoy’s Medium 100 μ A stimulation 494 minutes
 Note inadequacy of UNO resolution resulting in discrete resistance levels.

4.6.2.2. **McCoy's Medium Stimulation - 200 μ A**

In the 200 μ A range there very minimal changes in the pH of the media permanently. The pH split created at the start of stimulation was an approximate 7.2/8 split, slightly larger than the 100 μ A range in section 4.6.2.2 McCoy's Medium Stimulation - 200 μ A. In this range, there was very minimal precipitate formed on the negative electrode. The resistance of the media started between 18-20 k Ω and settled between 25-27 k Ω and settled in approximately 100 minutes. These are all similar results to the 200 μ A testing in DMEM Medium in section 4.6.1.2 DMEM Stimulation - 200 μ A Range.

Current (μ A)	188.99
STD (μ A)	± 15.23
Voltage	3.403V
Time	360 mins
R _{Load}	2.2 k Ω
R _{Sense}	470 Ω
Max pH	8
Min pH	7.2
Final pH	No Δ

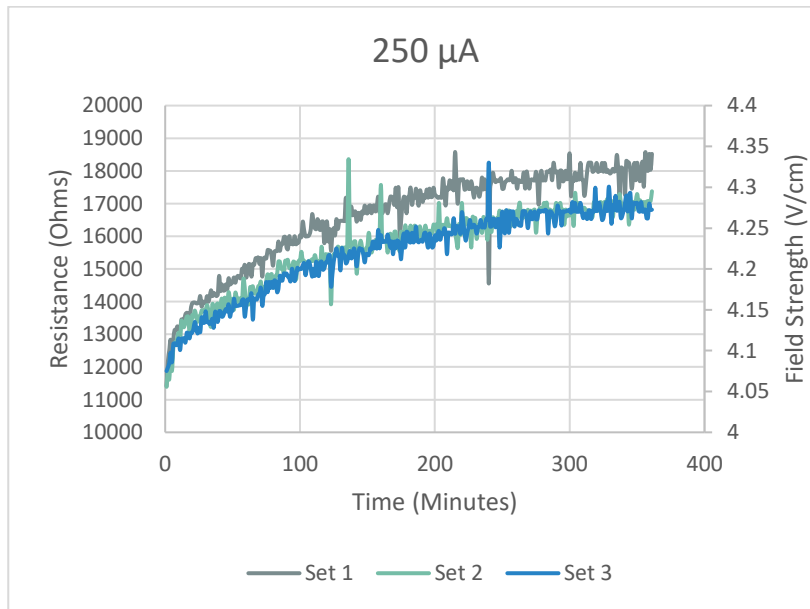


Figure 30: McCoy's Medium 250 μ A stimulation 360 minutes

4.6.2.3. **McCoy’s Medium Stimulation - 300 μ A**

In the 300 μ A range, there were very minimal changes in the pH of the media permanently. The pH split created at the start of stimulation was an approximate 7/8 split, slightly larger than the 200 μ A range in section 4.6.2.2 McCoy’s Medium Stimulation - 200 μ A. In this range, there was some precipitate formation on the negative electrode, but it was very minimal. The resistance of the media started between 7.5-8.5 k Ω and settled between 8.9-9.6 k Ω at approximately 100 minutes.

Current (μ A)	316.81
STD (μ A)	± 15.86
Voltage	3.039V
Time	371 mins
R _{Load}	470 Ω
RSense	2.2 k Ω
Max pH	8
Min pH	7
Final pH	No Δ

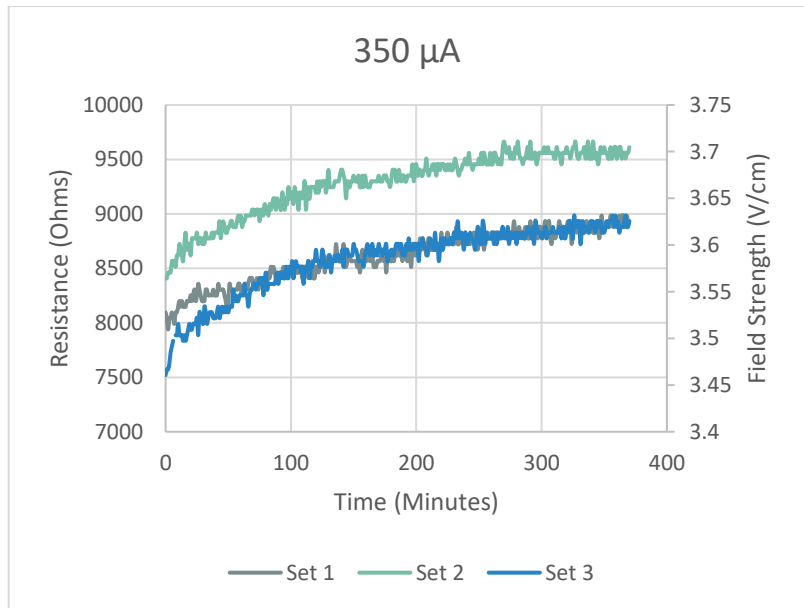


Figure 31: McCoy’s Medium 350 μ A stimulation 371 minutes

4.6.2.4. **McCoy’s Medium Stimulation - 450 μ A**

In the 450 μ A range, the media became permanently bleached due to an extremely basic pH. The pH split created at the start of stimulation was an approximate 6.9/8 split, slightly larger than the 300 μ A range in section 4.6.2.3 McCoy’s Medium Stimulation - 300 μ A.

In this range, there was some precipitate formation on the negative electrode that was minimal but more than in section 4.6.2.3 McCoy’s Medium Stimulation - 300 μ A. The resistance of the media started between 5- 6 k Ω and settled between 7.1-7.5 k Ω at approximately 150 minutes.

Current (μ A)	435.58
STD (μ A)	\pm 20.41
Voltage	3.303
Time	1253 mins
R _{Load}	470 Ω
RSense	1 k Ω
Max pH	8
Min pH	6.9
Final pH	Bleached

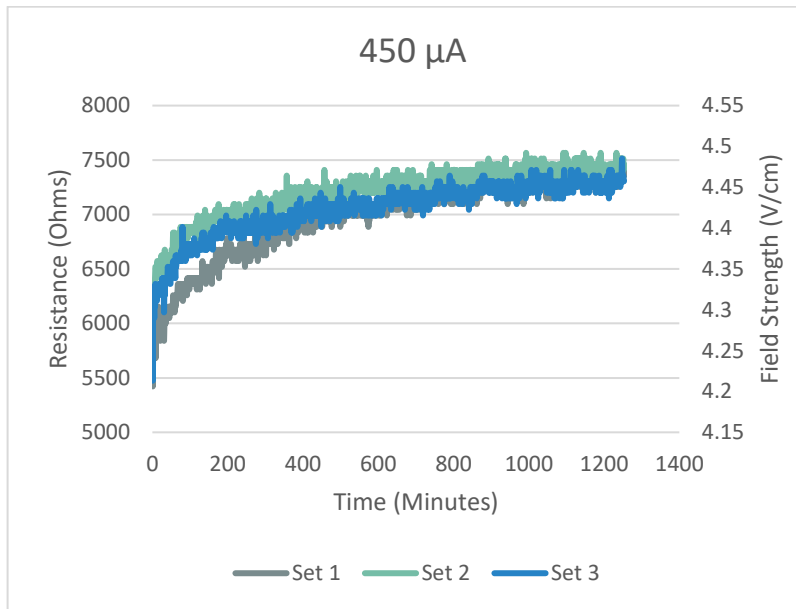


Figure 32: McCoy’s Medium 450 μ A stimulation 1253 minutes

4.6.2.5. **McCoy’s Medium Stimulation - 600 μ A**

In the 600 μ A range, the media has a slight decrease in pH. The pH split created at the start of stimulation was an approximate 7.3/8 split, smaller than the 400 μ A range in section 4.6.2.4 McCoy’s Medium Stimulation - 450 μ A. In this range, there was some precipitate formation on the negative electrode. The resistance of the media started between 4.3 - 4.5 k Ω and settled between 4.6-5.2 k Ω at approximately 80 minutes.

Current (μ A)	606.39
STD (μ A)	± 20.51
Voltage	3.046V
Time	360 mins
R _{Load}	2.2 k Ω
R _{Sense}	2.2 k Ω
Max pH	8
Min pH	7.3
Final pH	Slight \downarrow

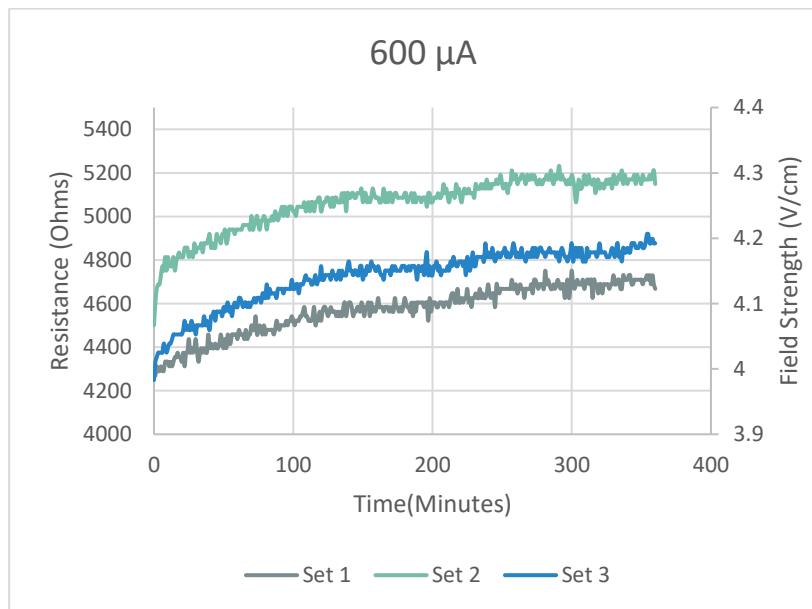


Figure 33: McCoy’s Medium 600 μ A stimulation 360 minutes

4.6.2.6. McCoy’s Medium Stimulation - 800 μ A

In the 800 μ A range, the media has a slight decrease in pH at the end of the test. The pH split created at the start of stimulation was an approximate 7.4/8 split, smaller than the 600 μ A range in section 4.6.2.5 McCoy’s Medium Stimulation - 600 μ A. In this range, there was minimal precipitate formation on the negative electrode. The resistance of the media started between 3.2-4.5 k Ω and settled between 4.4-4.6 k Ω at approximately 50 minutes.

Current (μ A)	783.0
STD (μ A)	± 20.57
Voltage	3.295V
Time	360 mins
R _{Load}	220 Ω
RSense	1 k Ω
Max pH	8
Min pH	7.4
Final pH	Slight \downarrow

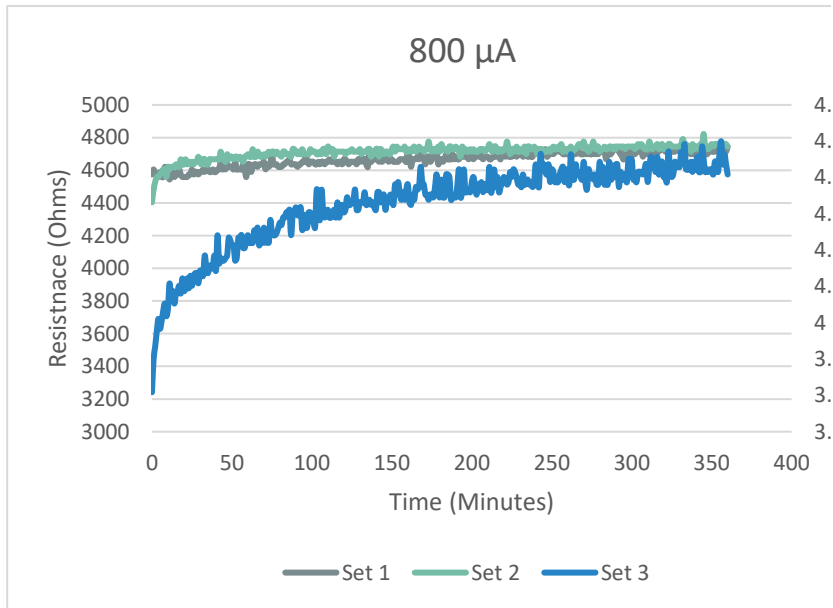


Figure 34: McCoy’s Medium 800 μ A

4.6.2.7. McCoy’s Medium IR Characteristics

The data from the tests in sections 4.6.2.1 - 4.6.2.6 were compiled into one large data set. For each achieved current value, the resulting media resistances were averaged, and the standard deviation of these values was used to create error ranges for each value. The values were then plotted as resistance vs current to analyze the IR characteristics of the media. The McCoy’s Medium follows a power curve trend with the formula of

$2370570.981 x^{-0.96}$ with an R-squared fit value of 99.7%. This can be simplified as $R = 2.37 \times 10^6 I^{-0.96}$ with resistance (R) in ohms and current (I) in μA . This indicates that there is a steep decrease in media resistances with small changes in stimulation current from 0-400 μA and the relationship flips from 400-1000 μA with large current changes creating small resistance changes. This can be seen in Figure 35: McCoy's Medium IR Characteristics.

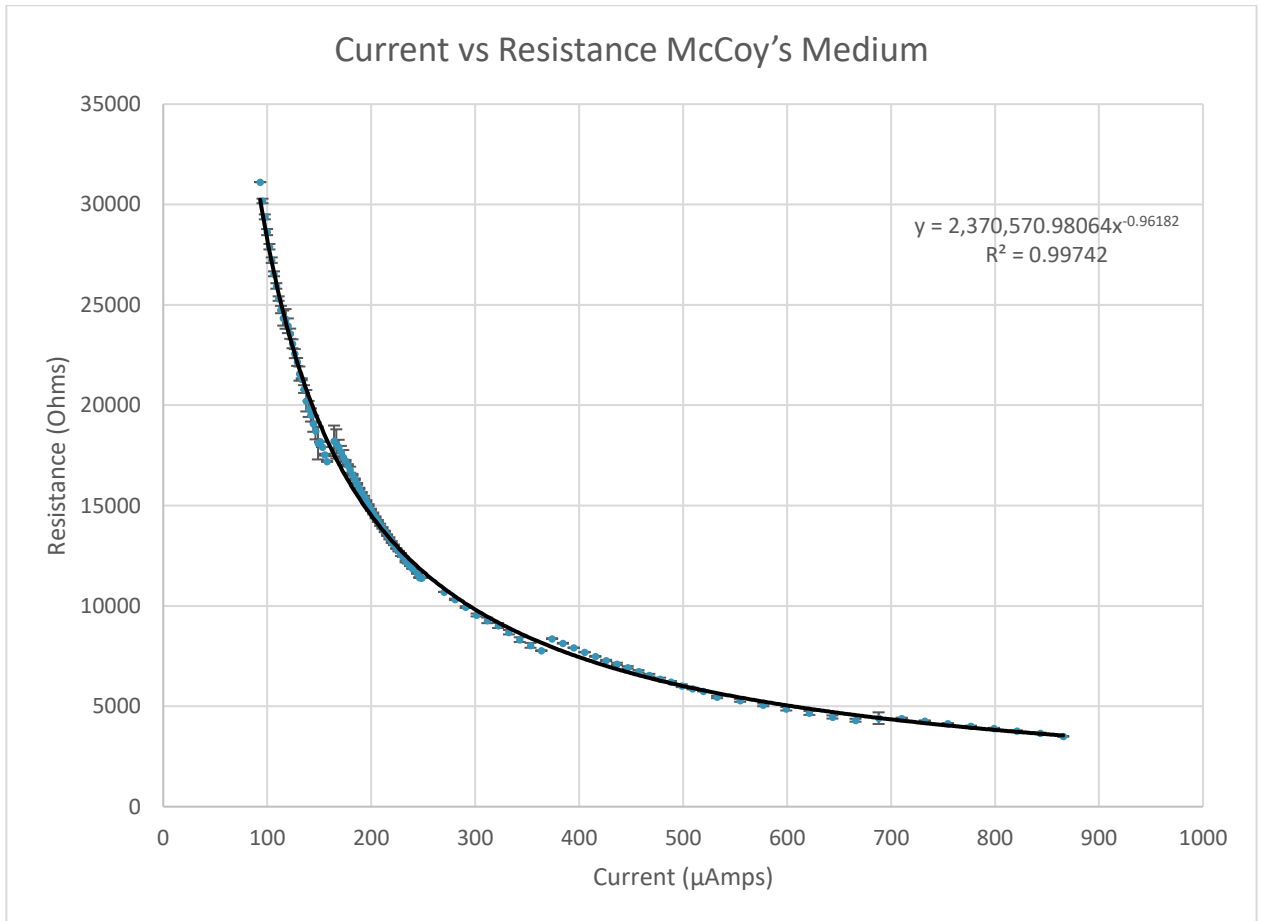


Figure 35: McCoy's Medium IR Characteristics

4.7. Constant Current Discussion

A constant current supply can compensate for small resistance changes by altering the output resistance and should be used in situations where the resistance may change over time [89]. However, the circuitry design has its electrical limits, which were quickly realized during this set of constant current experiments. The load resistance from the media was supposed to be isolated from the input circuitry and not affect the output current. It was realized very quickly that the output current would slowly drop as the output resistance increased, indicating this was not behaving as expected. Secondly, the ideal output current could be determined by equation (4.15). With the R_1/R_2 ratio fixed to 10, the output current should have been a direct relationship between the input voltage and R_{sense} . This assumption was used in a set of preliminary tests and it was found that the output resistance, input voltage, and R_{sense} were all unpredictably affecting the output voltage. To achieve the desired output current for the rest of the tests Table 3: Predicted Resistances was used as a guide to try and maximize the voltage across R_{load} to maximize measurement efficiency. The final method ended up being a tuning process of changing R_{sense} and R_{load} until the achieved current was within $100 \mu A$ of the desired target current and then using the input voltage to complete the tuning process. The circuitry's behaviour was a function of all these factors as well as thermal and equipment noise making the actual equation to calculate the output current difficult to decipher. This may indicate that the selected circuitry was not suitable to generate consistent current.

4.7.1. **Temporal Behaviour**

With the application of electric current to tissue, the medium usually has an increase in internal resistance over time [114]. As the current is applied there is a redistribution of the charged particles presenting as a non-faradaic reaction [92]. The applied voltage versus current in the media follows a power curve in general, with the faradaic range being a linear portion at the tail end [92]. The resistance of the media over time also follows a power relationship generally with the resistance increasing rapidly at the start eventually levelling off. The normalized resistance versus time graphs can be seen in appendix 7.8 and 7.9. The rate of change is consistent across both medium types and the various stimulating currents with the resistance stabilizing between 100 and 200 minutes. However, the increase in resistance is more extreme with the lower stimulating currents. While the shape of the curve is flatter with the higher stimulating current, they are far noisier as the overall resistance is lower, and small changes are greater compared to the mean.

The output voltage of the constant current circuit was not fixed and is a function of the current coming out and R_{load} . Therefore, the voltage is not a controlling factor of the resistance of the media but a result of the resistance through the medium. As the ions are carrying the current through the media, a higher current indicates more ion movement and therefore a lower resistance to flow. The more rapid movement of ions may also indicate why there is less resistance change over time with higher currents, as the ions reach equilibrium states sooner as it is easier to mobilize them.

4.7.2. **pH split**

One of the most prominent effects of ES in media is the distinct colour change. The pH in the media is controlled by a bicarbonate buffer system that is CO₂ and temperature-sensitive [101], [102], [104]. ES in media causes the electrolysis of water causing a cathodic pH increase due to OH⁻ production and an anodic pH decrease due to chlorine gas production [89]–[91], [113]. Hydrogen peroxide is also produced by the cathode and the amount is linearly proportional to the amount of time the stimulation occurs [92]. These side effects can be toxic due to an increase in pH from the OH⁻ ions [89]–[91] and if the voltage is too high, an excess of hydrogen gas that forms [90]. The gas formation at both electrodes can be observed visually by bubbles that form on the electrodes and in extreme cases forms a foam in the media.

The pH gradient between the electrodes forms almost instantaneously with the application of ES and dissipates between 100 and 200 minutes, which corresponds to the plateauing of resistance. The stability of the media resistances corresponds to an equilibrium of the movement of charged ions and chemical reactions. As the pH is charge-dependent with H⁺ and OH⁻ as the driving factors, once these ions in the media reach equilibrium, these measurable factors all do as well.

As the bicarbonate buffer system is temperature and CO₂ sensitive, performing these experiments outside of an incubator adds environmental effects to the changes in media behaviours, specifically the colour. The pH of the media naturally increases as the temperature increases from 4C to 21C and as CO₂ diffuses out of the media. To have more consistent results, experiments with bicarbonate buffered systems should be done in

a temperature and CO₂ controlled environment. However, CO₂ and temperature-controlled environments are associated with cell incubators and typically require tight controls for sterilization. Since there were no cells in culture for these experiments, it was much easier to run the experiments with a non-stimulated control well.

In general, the acidic and basic elements generated through ES are balanced with no significant pH change overall, but extremes can cause permanent pH changes. Both the time of stimulation and the strength of the stimulating current influence the permanent pH change. Both factors affect the amount of faradaic side effects generated and directly impacts the pH, which can cause bleaching of the media. While the by-products of ES were not characterized in these experiments, the presence of a bleach-like scent and the equations listed in 4.1.4 may indicate an excess of chlorine gas production was the factor causing this change.

4.7.3. **Electrodes**

Throughout testing, there was a consistent precipitate that formed on the platinum electrodes presenting as a thin white film. This precipitate formed predominantly on the cathode and the amount was dependent on the current and voltage. Higher currents and voltages caused more precipitate to collect on the electrodes. This precipitate has been collected but was not analyzed. With the amount of chemical elements that present as white powders in their solid form, it is impossible to determine this precipitate is without chemical analysis, but it is most likely calcium or salt based on the media composition.

As testing progressed, the data appeared to get noisier and the electrodes were more difficult to clean and appeared less shiny. This may be evidence of electrode dissolution. To maintain electrode integrity throughout testing, the Z-characteristics of the electrodes should be monitored before each test and compared to a baseline. This could be an indicator for when electrodes need to be replaced after too much deterioration occurs, to ensure consistent stimulation is delivered and excessive platinum ions are not being expelled into the medium. This is also an important consideration for interpreting published experimental data with platinum electrodes. It is not clear from the published studies if any precautions were taken to guard against the decline of charge stimulus over time.

4.7.4. **IR Relationship**

Electronic circuit elements can fall into either the ohmic or non-ohmic category. An ohmic element has consistent resistance no matter the applied voltage or current, whereas the resistance of a non-ohmic element can vary. A capacitor or diode are examples of non-ohmic elements as they behave differently depending on the applied current shape or voltage, respectively. A resistor is an example of an ohmic element, that has the same resistance no matter the current or voltage. The way to analyze this is to look at a voltage versus current curve, with the slope being the resistance. If there is a linear trend the element can be considered ohmic, otherwise it is non-ohmic.

In the case of cell culture media, the current versus voltage and resistance versus voltage graphs appeared to have no relationship, which indicates a decisively non-ohmic behaviour. However, the resistance versus current graph shows a strong relationship

following a power trend with the resistance in ohms being approximately four times the inverse of the current in amps. This relationship indicates that the voltage does not directly impact the behaviour of the medium, but the current does.

A similar study by Srirussamee using constant field strengths in culture media found that applied voltage versus current in the media follows a power curve in general, with the faradaic range being linear [92]. When the electrode voltage was less than 1.5 volts there was minimal current in the media, indicating the re-distribution of charges is small, similar to processes that occur during capacitive stimulation [92]. As all current ranges used in the constant current experiments caused immediate pH changes and the electrode voltage was above 1.5 V, this range was not examined. Between 1.5 and 3 V, they found that the current increases non-linearly but there are electrochemical reactions [92]. A large portion of our constant current experiments existed in the high end of this range, breaching on the next range. This non-linear current change with voltage indicates non-ohmic behaviour. More than 3 V in the media caused a linear current-voltage relationship causing faradaic processes to occur and they found this range should be avoided to avoid excessive electrolysis in the culture media [92]. As a lot of our experimental values were in this range, there was likely a lot of faradaic reactions occurring due to electrolysis. This relationship however was not found to be linear. This could potentially be due to the amount of electrolysis occurring in the media, changing the conformation and amounts of charged species and therefore their contribution to the current and resistance in the media.

4.7.5. **Circuitry Limitations**

This lack of voltage related relationships could be due to the constant current supply itself. The circuitry was designed to maintain a constant output current despite changes in R_{Load} . However, the output current was directly affected by R_{Load} and increased over time and did not follow the behaviour indicated by the design equations. This unpredictable behaviour could have led to a larger source of error in the applied voltage, distorting the relationship.

Error in the calculations may also come from the resolution of the UNO R3 system. The ADC has a resolution of 1024 bits over a 5V range, giving it the ability to detect changes as small as 4.882 mV. However, a 4.882 mV difference with the minimum measurement resistance measured of 220 Ohms could produce errors in the current measurement as great as 25 μ Amps. Additionally, Figure 16 and Figure 19 are examples of the measurement range not being accurate enough and the values only spanning over five bits, creating discrete resistance levels rather than a smooth curve. This was mitigated in subsequent tests by maximizing the measurement resistance as much as possible, to get the largest voltage range for measurement. This resulted in less information lost as the voltage divided by a larger resistance, would have each bit represent a smaller current range. Using an ADC with more bits or resolution could eliminate this issue.

4.8. **Conclusion**

The two goals in this chapter both shared the idea of constant stimulation. However, many complications prevented anything from being truly constant. Cell culture media contain an abundance of charged particles that are mobilized upon the initiation of ES.

The ES also causes faradaic reactions changing the properties of the media over time. While the faradaic and non-faradaic reactions reach equilibrium, there is a change in the electrical properties of the media. The magnitude of these changes can depend on environmental factors such as CO₂ concentration and temperature, or electrical factors such as the strength of the stimulation or positioning of the electrodes. To definitively identify the amount of stimulation that is occurring in media, measurements should be taken at various points between the electrodes to identify spatial behaviours in addition to the temporal that have been explored here. To help with this, the sources of error should also be minimized by better controlling the parameter that is to be held constant. This may involve the use of external measuring systems and a more robust electrical supply circuitry. This may help better define if there is a voltage relationship that is being masked by inconsistencies in the current data. Finally, the by-products that are generated through ES should be characterized to see if there is a difference in products in a voltage-driven situation versus a current-driven one.

5. Osteoblast-like Cell Testing

5.1. Intro

5.1.1. Chapter Motivation

While a lot of studies have been done on ES of cells in culture, few report electrochemical reactions and byproducts that we found in sections 3.3, 4.3, and 4.6. The amount of precipitate can be controlled by how much stimulation is delivered but as the byproducts were not characterized in sections 3.3, 4.3, and 4.6 it is unknown what effect these molecules would have on cells. The purpose of this chapter was to look at the effects of ES on cells in culture and if it caused increased or decreased cellular activity. This could also present as increased or decreased cellular proliferation or apoptosis.

As the cell line used is osteoblast-like, this was also an opportunity to see if direct electrical stimulation through a constant voltage setup designed for MSCs, would illicit a migration response from the cells. It is possible that osteoblast-like tumour cells, do not behave the same as osteoblasts that are *in situ* when electrically stimulated.

5.1.1. Cell Electrical Stimulation

When bone is mechanically deformed, stress generated potentials form as fluid flows through the canaliculi and lacuna, directly around osteocytes [2], [13], [38], [42], [43]. This results in bone cells in the area being directly exposed to these electrical signals. The bioelectric activity of bone tissue has led to many studies recreating this behaviour using electrical stimulation *in vitro*. A summary of studies can be seen in **Table 5**: Reviewed studies on *in vitro* stimulation of cells. An important finding from these studies is that the magnitude of bone formation is driven by the recruitment of more cells, not by altering the behaviour of the cells [35]. Bone cells have a refractory period for stimulation and

some frequencies work better than others for getting a maximal stimulation response [30]. The amount of bone formation is related to the current density and charge [54] with the amount of charge delivered being the most important factor [31]. This would indicate that a DC stimulation would provide the largest response from the cells.

Osteocytes communicate through gap junctions, which can be directly regulated by electric fields increasing communication factor production [60], [78]. Interestingly, the protein CX43 creates gap junctions and is produced in lower volumes with the application of PEMFs but is increased with shear stress [78]. This indicates that the PEMFs do not cause increased connectivity between cells but may increase the amount of communication between already connected cells. PEMFs also inhibit cellular apoptosis and increase the length of the cellular dendrites, which are responsible for sensing the electrical environment around them [79].

More osteogenesis occurs at the cathode when electrically stimulating bone [2], [34], [48]–[54] and a lot of this can be explained when looking at the migration of osteoblasts under electrical stimulation. Osteoblasts have been shown to move towards the stimulating cathode [14], [27], [51], [57]. This is carried out through the growth of lamellipodia on the cathodic side of the cell [13], [27].

5.2. Materials and Methods

The results from the constant voltage testing in section 4.3 Constant Voltage Results allowed for insight into the basic behaviour of the culture media with the introduction of electricity. With this information and the data from the studies from Mobini and

colleagues [111], [112], the next logical step was to try to recreate the experiment by Mobini et al. with Saos-2 osteoblast-like cells. While the goal was to stimulate osteocyte-like cells, the availability of the Saos-2 cells, as well as studies on their behaviour under electrical stimulation [64] made them a good first step before moving onto osteocyte-like cells.

To avoid the negative side effects stemming from the solder-medium interactions, the L-shaped second-generation electrodes (described in section 3.3.2 L-Shaped Electrodes) were used to stimulate the cells. This was done to minimize the faradaic side effects in the media and to decrease the likelihood of cell death due to contamination of the media. The 3D printed electrode holder (mentioned in section 3.3.3 Electrode Holder Design) was introduced for these tests to maintain consistent electrode spacing in each well. The electrode holder was fit for a 24 well plate with three sets of electrodes adhered to spots corresponding to adjacent wells. The fourth well in the row was used as a control well for visual inspection of changes as well as a control well for use with a plate reader.

Saos-2 cells were grown in a cell culturing flask in McCoy's 5A Modified Medium with FBS and penicillin/streptomycin and then transferred into six wells of the 24 well plate. This allowed for three stimulated wells and three unstimulated wells to have replicates to compare against. The cells were left overnight in a 37°C incubator with 5% CO₂ concentration.

Before testing each day, the cell culturing medium was exchanged to replenish the nutrients and remove the cellular waste from the previous day. The three stimulated wells

were then subjected to an electric field with a strength of 100 mV/mm, which was deemed most effective by Mobini et al [111]. This was applied for 30 min and was repeated for four days. This was done through the experimental setup as described in section 4.2.2.3 AC Stimulation but supplied with 0.8 V DC rather than AC. This alteration was done to make it easier to supply the exact required voltage across the electrodes to achieve a 100 mV/mm field strength. The Analog Discovery module supply lead can be varied between -5 and 5V in mV increments whereas the UNO R3 can only be 0 or 5 V. The voltage across two of the stimulated wells was monitored through the two analog discovery measurement channels, with the assumption that the third well would follow the same trends. The cells were all imaged daily with an inverted brightfield microscope (IX51S1F-3, Olympus Life Sciences, Tokyo, Japan). They were then returned to the incubator until the following day.

The cells were imaged daily. On the fourth day, the cell metabolism was analyzed using the alamarBlue assay (Sigma-Aldrich, St. Louis, MO). AlamarBlue changes colour when in the presence of cellular respiration. The byproducts of respiration cause the blue dye in the assay to turn pink. The fluorescence of the media was read with a Tecan M1000 plate reader using an excitation wavelength of 540 nm and an emission wavelength of 560 nm (Tecan, Männedorf, Switzerland). Each well was normalized to a true negative control well with no cells. Nine reads were taken in each well and the values were normalized depending on the location. To assess if the electrical stimulation caused an increase in cell number or metabolism, the fluorescence of the media for electrically stimulated cells was

then compared to control wells with the unstimulated cells through a one-tailed t-test with a significance of 0.05.

5.3. Results

The SaOs-2 osteoblast-like cells were stimulated for 30 minutes a day for four days. Bright-field microscopy imaging was performed each day post-stimulation except for the final day where a viability assay was done instead. The images show no visible difference between the cells on each day. There was no difference in the number of dead cells in each well and the growth pattern of the cells was not changed. The cells naturally created a large grouping in the middle of the well and around the edges and this was intact with both the stimulated and control wells. This can be seen in Figure 36.

The constant voltage setup was used and the voltage across the electrodes was measured during stimulation. The small voltage measurements across the load resistor caused an excessive error in the readings and the resistance and current in the circuit could not be calculated reliably, but the field strength measurements can be seen in Appendix 7.5.

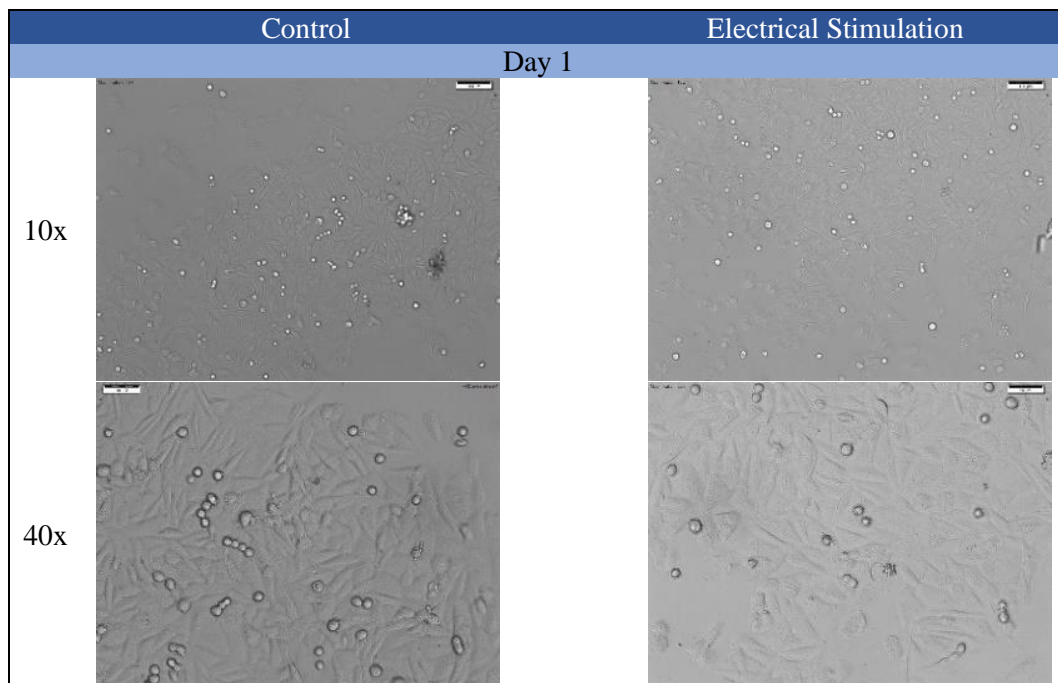


Figure 36: Saos-2 cells 1-day stimulation

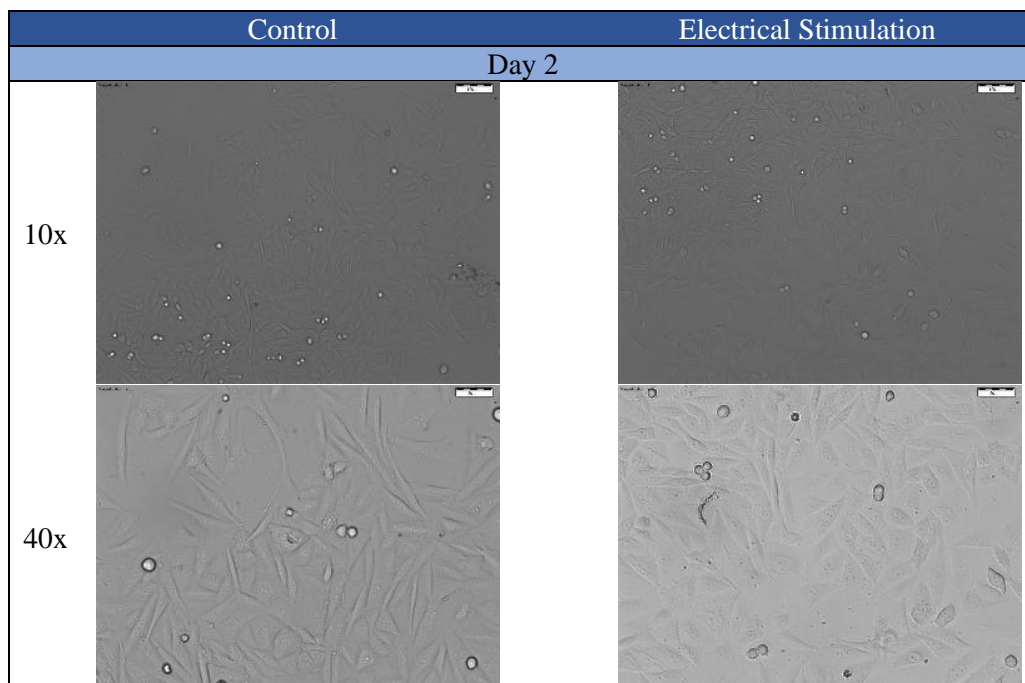


Figure 37: Saos-2 cells, 2 days stimulation

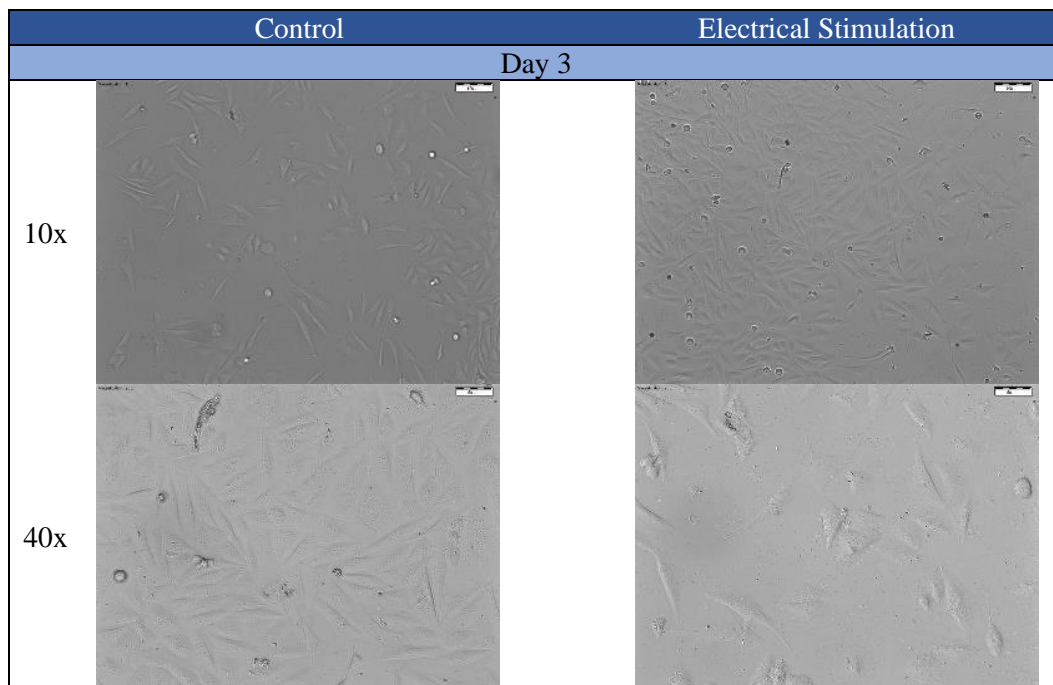


Figure 38: Saos-2 cells, 3 days of stimulation

The alamarBlue viability assay was performed and read with a plate reader that analyzed the fluorescence of the redox reaction of the indicator when excited by 540 nm green light. The reader sampled values from nine locations in each cell well and took the average and standard deviation of these values, this can be seen in Figure 39. The full set of values can be seen in Appendix 7.7.

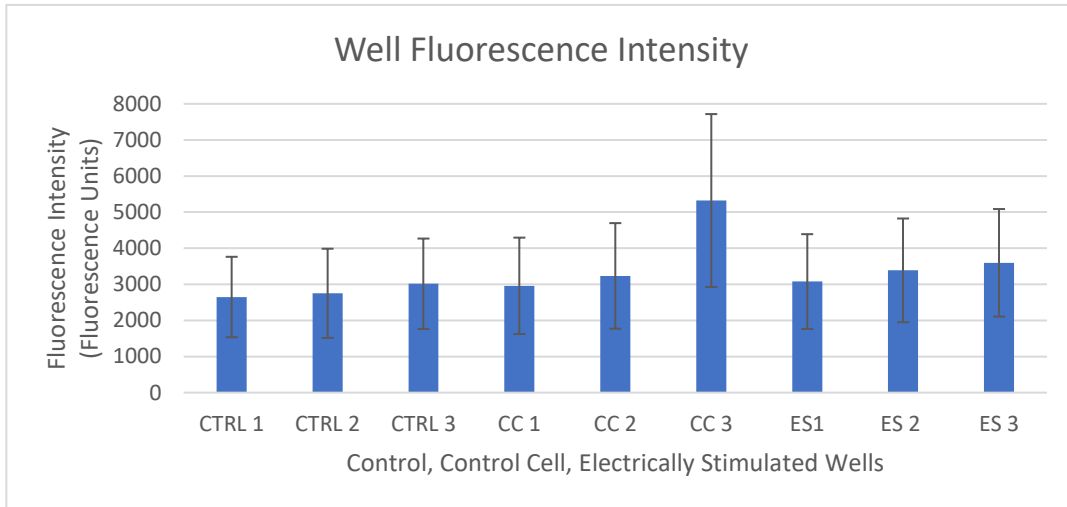


Figure 39: Fluorescence readings from TECAN plate reader

Further analysis indicated that the nine locations in the well had differing mean values for fluorescence values, potentially due to the shape of the culture dish. The averages for each location can be seen in Table 1. To eliminate the effect of location on each reading, the means were subtracted from each reading in that location. The corrected fluorescence values for each well can be seen in Appendix 7.7.

Table 1: Average Fluorescence Values for nine reading locations within the circular well

4417	3425	1431
1996	4338	5485
4207	3237	1455

The normalized values were then analyzed with t-tests comparing the means for each set of wells: 1) control wells versus just the viability agents and no cells (CTRL), 2) the control wells with unstimulated cells and viability agents (CC), and 3) the electrically stimulated cells with viability agents (ES). The t-tests were done assuming unequal variances and with one tail to see if the fluorescence increased with the addition of cells, or in the case of the final test, the addition of electrical stimulation. The t-test results can be seen in Table 2. There was a significant increase in the fluorescence between the control wells and the wells containing cells ($p = 0.0019$, 0.0269 for CC and ES, respectively) indicating the assay was working properly. However, there was no significant effect of the stimulation ($p=0.077$). This indicates that the metabolic activity of the control cells and the electrically stimulated cells were statistically the same.

Table 2: T-Tests

t-Test: Two-Sample Assuming Unequal Variances

	CTRL	CC	CTRL	ES	CC	ES
Mean	-67.0101	919.8081	-67.0101	450.9596	919.8081	450.9596
Variance	1195454	2330707	1195454	1096927	2330707	1096927
Observations	33	33	33	33	33	33
Hypothesized Mean Difference	0		0		0	
df	58		64		57	
t Stat	-3.01886		-1.96525		1.454763	
P(T<=t) one-tail	0.001883		0.026864		0.07561	
t Critical one-tail	1.671553		1.669013		1.672029	

5.4. Discussion

The ES methods used in this experiment were adapted from Mobini et al [111], which involved stimulated MSCs. Their work indicated that 1 hour a day of <100 mV/mm (1V/cm) stimulation does not affect the MSCs whereas >200 mV/mm (2 V/cm) has negative side effects such as cellular apoptosis. They found that ~ 100 mV/mm (1 V/cm) had positive effects on the cells, including increased proliferation. This is the field strength that was used to stimulate the Saos-2 osteoblast-like cells as a starting point. The Mobini experiment stimulates for 1 hour a day for 7 days, however, to save time on a preliminary test this was shortened to 30 minutes/day for 4 days.

With this experimentation using osteoblast-like cells, there was no significant difference between the stimulated and non-stimulated cells ($p=0.077$) using the 100 mV/mm, 30 minutes / 4-day stimulation parameters. There are many aspects of this experimental setup that could be altered to try and get more conclusive results. The simplest approach would be increasing the number of days that the cells are stimulated. The study of BM-MSCs that we based out stimulation parameters on saw significant results after 7 days [111]. The addition of the three extra days could be the difference between significant and nonsignificant results. Basing experimental protocol for osteoblast-like cells off one made for BM-MSCs may also be problematic, as in general as these are two very different cell types. The 100 mV/mm stimulation strength may be enough for BM-MSCs but the sensitivity of the Saos-2 cells could be completely different. This requires a more thorough investigation into what electrical stimulation strengths affect the cells. Additionally, Saos-2 cells are osteoblast-like and are derived from osteosarcoma.

Osteoblast cells vs osteoblast-like cells do not display identical behaviours; it is very possible that the electrical sensitivity of these cell types differ and the future use of harvested osteoblast cells may be more beneficial in an electrical stimulation study. To get a more robust understanding of the cell's sensitivity it may be necessary to stimulate the cells to the level of apoptosis and then decrease the stimulation from that level until the health is not negatively impacted.

As the main result of osteoblast-like stimulation is migration the best way to track the osteoblast activity with ES would be to use gridded coverslips and single-cell tracking to look at their migration. This is a more exhaustive method involving microscopy over the stimulation time in locations both around the electrodes and the centre of the stimulation area rather than just after stimulation. This again may be behaviour displayed by osteoblasts but not osteoblast-like cells so this would be a consideration for future studies using these cells.

5.4.1. **Field Strength Uniformity**

One of the large unknowns of this experimental setup is the field strength throughout the well. The overall estimation of the field strength is coming from the voltage across the electrodes divided by the electrode spacing. This is using the assumption that the field strength is uniform across the media. The liquid medium is not spatially or temporally consistent as seen in section 4 Electrical Stimulation in Media. To know what level of stimulation the cells are seeing, a next step should be the development of a measurement array of electrodes for the bottom of the well to measure the field uniformity between the

electrodes as well as at differing depths within the well. This will provide more insight into the uniformity of the stimulation environment but also a definitive answer as to what levels of stimulation that the cells can respond to.

5.4.2. **Constant Current vs Constant Voltage**

As the resistance of the stimulated media increases over time, the only way to maintain a steady amount of charge to the cells is through the use of a constant current supply. Using a constant current to stimulate the cells rather than a constant voltage, may result in a different outcome for the cells. This setup also runs the risk of delivering a signal too different from the endogenous signal by being a constant flow of charge past the cells rather than a varying one. There is also the risk of increased reactions and charge buildup around the electrodes that may be detrimental to cellular health.

5.4.3. **Statistical Significance**

While the results from this experiment indicate no significant difference between stimulated and control wells, the p-value of 0.0756 is very close to the 0.05 level needed to be significantly different. With the variance present in this data, to achieve a statistical significance with a power of 80, approximately 100 replicates would be needed to achieve statistical significance. There is not enough data to make a strong conclusion about the behaviour of the cells using this experimental setup.

5.5. **Conclusion**

These experiments were based on the principle that the response of osteoblasts to direct electrical stimulation could be inferred from the response of BM-MSCs, and so the experimental setup from other studies could be used as a starting point. With the differing

sensitivity of cells from different lineages and for different purposes, there is likely a different response to ES. Based on studies that use mechanical stimulation it has been seen that pre-osteoblasts can respond to pulsed ultrasound, whereas mature osteoblasts and osteocytes do not [118]. However, all three cell types respond to fluid flow as they are sensitive to the type of stimulation they receive [119], [120]. This indicates that the behaviour of one cell type does not necessarily correlate to the same behaviour in others. While this experimental setup was effective for BM-MSCs, it did not produce notable results with osteoblast-like cells. Even if there were detectable effects of ES on osteoblast-like cells, there could be completely different results with other osteoblast-like cells from different sources, and almost definitely with osteocyte and osteocyte-like cells.

6. Conclusion

There is an abundance of evidence supporting the hypothesis that bone tissue is electrically active. This can be extended to the hypothesis that bone cells are electrically sensitive and can sense the electrical charges in their environment. To study this, it is easiest to have bone cells in culture which introduces cell culture media to the experimental setup. Direct ES with metallic electrodes within the media causes ion movement, which causes both the desirable ES and also unplanned faradaic by-products. While not necessarily detrimental to cell health, it is important to try and minimize these reactions to maintain culture conditions as close to ideal as possible, specifically the pH. Direct ES of culture media causes pH changes dependent on electrode polarity, and the changes can be amplified based on time or ES strength. The medium around the cathode becomes basic and acidic around the anode. This gradient disperses over time usually resulting in no net change in the pH of the media. The resistance of the media also increases over time and plateaus when the pH gradient disperses. This usually occurs between 100 and 200 minutes. Some precipitates and gasses form on and around the electrodes, no matter the stimulation time or strength. The by-products can be reduced through the use of long L-shaped electrodes to keep any material other than platinum out of the media. The pH changes specifically could also be lessened through an incubator as this would maintain the proper temperature and CO₂ concentration for the media to maintain its buffer system properly.

Interestingly, there is a strong relationship between the electrical stimulation current and resistance of the media. These variables are related by a power trend. No relationship was found between the electrode voltage and resistance or electrode voltage and stimulating current. To investigate a relationship between these factors, a different testing setup may be beneficial.

Using the stimulation parameters from Mobini et al [111] we saw no significant difference between stimulated and non-stimulated Saos-2 osteoblast-like cells. This could have been for a multitude of reasons. The field strength across the electrodes was duplicated, however, the voltage was not; and as no information was listed about the current [111], it is unknown how similar this parameter was as well. Secondly, the published setup was used with MSCs and the sensitivities of the different cell types could be vastly different. Especially with Saos-2 cells being “osteoblast-like” and a cancerous lineage, there is no guarantee that they have the same electrical sensitivity that the normal healthy cells have. These experiments should have been repeated multiple times with varying stimulation times and strengths to draw a stronger conclusion on whether or not the cells were being affected.

6.1. Future steps

As the electrodes collect precipitate over time, it is imperative to adequately clean them between tests so that the precipitates are not changing the electrical properties of the electrodes over time. To verify this, the resistance of the electrodes should be checked between tests to ensure that they have not degraded too much over time. If AC tests are to be used it may also be important to analyze the z-characteristics over time. Looking at the

AC behaviour of the media is of interest as it may have capacitive properties that could increase or decrease the number of reactions that are occurring. This may decrease the pH gradient that occurs across a well but may increase the number of faradaic by-products as they would occur at both electrodes rather than just one.

It is assumed that the field strength throughout the media will be consistent but based on basic electromagnetic principles, this should not be the case. The field strength throughout the media most likely varies with depth and with distance from the electrodes. Simulations could be done to try to predict the behaviour, however, a real-time measurement would be more accurate. The use of a measurement array of electrodes at the bottom of each well will give insight into the amount of ES cells in the bottom of a well would see, and could also measure how the field changes from anode to cathode. The more information that can be gathered about the media's behaviour decreases the number of unknowns to try and comprehend.

A big issue with this experimental setup was the inability to truly achieve any constant stimulation parameter. While all experimental setups maintained the voltage or current within a small range, there was still a change over time as the resistance changed. A perfect constant current supply would keep the current constant while the media resistances increased, causing an increase in voltage across the electrodes. A perfect constant voltage circuit would decrease current as resistance increased to maintain voltage. While both of these would maintain a constant variable, there is no way to keep both constant when the resistance of the culture media will always increase over time as reactions occur and ions settle into equilibrium. Even experimental setups that use

constant stimulation capacitively or inductively are not achieving a “constant” stimulus as there will inevitably be an equilibrium reached when the ions begin to move. The movement of the ions will likely cause faradaic reactions as well, causing the same issues that direct stimulation does.

More accurate results can also be gathered through the use of a better analog to digital converter. The UNO system has a resolution of approximately 5 mV, which can introduce large relative errors to current calculations dependent on load resistance. While 5 mV over a large resistance creates a small error in a current calculation, the smaller the resistance gets, the more impactful this error becomes. The best way to mitigate this is to have the measurement occur over the largest resistance possible, but this also has limitations as the UNO can only handle voltages between 0 and 5 V.

Finally, studies have indicated that the amount of bone formation is related to the current density and charge [54]. This means that the amount of charge delivered is the most important factor [31]. A constant current setup is delivering a more constant stream of ions and therefore more charge than a constant voltage setup. This setup should be used to stimulate cells to get optimal results.

References

- [1] E. Fukada and I. Yasuda, “On the piezoelectric effect of bone,” *J. Phys. Soc. Japan*, vol. 12, no. 10, pp. 1158–1162, Oct. 1957, doi: 10.1143/JPSJ.12.1158.
- [2] C. Andrew and C. A. L. Bassett, “Electrical Effects in Bone,” *Sci. Am.*, vol. Vol. 213, no. 4, pp. 18–25, 1965, doi: 10.1038/scientificamerican1004-76.
- [3] C. A. L. Bassett and R. O. Becker, “Generation of electric potentials by bone in response to mechanical stress.,” *Science*, vol. 137, no. 3535, pp. 1063–4, Sep. 1962.
- [4] A. A. Marino and R. O. Becker, “Piezoelectric Effect and Growth Control in Bone,” *Nature*, vol. 228, no. 5270, pp. 473–474, Oct. 1970, doi: 10.1038/228473a0.
- [5] C. T. Brighton *et al.*, “Fracture healing in the rabbit fibula when subjected to various capacitively coupled electrical fields,” *J. Orthop. Res.*, vol. 3, no. 3, pp. 331–340, 1985, doi: 10.1002/jor.1100030310.
- [6] W. J. Kane, “Direct current electrical bone growth stimulation for spinal fusion,” *Spine (Phila. Pa. 1976)*, vol. 13, no. 3, pp. 363–365, doi: 10.1097/00007632-198803000-00026.
- [7] S. Akhter *et al.*, “Efficacy of Electrical Stimulation for Spinal Fusion: A Systematic Review and Meta-Analysis of Randomized Controlled Trials,” *Sci. Rep.*, vol. 10, pp. 1–12, 2020, doi: 10.1038/s41598-020-61266-x.
- [8] D. Fredericks, “Effects of Pulsed Electromagnetic Fields on Bone Healing in a Rabbit Tibial Osteotomy Model,” *J. Orthop. Trauma*, vol. 14, no. 2, pp. 93–100, 1999.
- [9] C. Saltzman, A. Lightfoot, and A. Amendola, “PEMF as treatment for delayed healing of foot and ankle arthrodesis,” *Foot ankle Int.*, vol. 25, no. 11, pp. 771–3, 2004, doi: 10.1177/107110070402501102.
- [10] P.-H. G. Chao, R. Roy, R. L. Mauck, W. Liu, W. B. Valhmu, and C. T. Hung, “Chondrocyte Translocation Response to Direct Current Electric Fields,” *J. Biomech. Eng.*, vol. 122, no. 3, p. 261, Jun. 2000, doi: 10.1115/1.429661.
- [11] C. P. Huang, X. M. Chen, and Z. Q. Chen, “Osteocyte: The impresario in the electrical stimulation for bone fracture healing,” *Med. Hypotheses*, vol. 70, no. 2, pp. 287–290, Jan. 2008, doi: 10.1016/j.mehy.2007.05.044.
- [12] B. M. Isaacson and R. D. Bloebaum, “Bone bioelectricity: What have we learned in the past 160 years?,” *J. Biomed. Mater. Res. Part A*, vol. 95A, no. 4, pp. 1270–1279, Dec. 2010, doi: 10.1002/jbm.a.32905.
- [13] R. L. Duncan and C. H. Turner, “Mechanotransduction and the functional response of bone to mechanical strain,” *Calcif. Tissue Int.*, vol. 57, no. 5, pp. 344–358, Nov. 1995, doi: 10.1007/BF00302070.
- [14] M. E. Mycielska and M. B. A. Djamgoz, “Cellular mechanisms of direct-current electric field effects: galvanotaxis and metastatic disease.,” *J. Cell Sci.*, vol. 117, no. Pt 9, pp. 1631–9, Apr. 2004, doi: 10.1242/jcs.01125.
- [15] Y. Nabil, S. Abdalfattah, and M. Lotfy, “A clinical study on the effect of electric stimulation on segment transfer distraction osteogenesis for mandibular reconstruction,” *Egypt. J. Oral Maxillofac. Surg.*, vol. 5, pp. 10–15, 2014, doi: 10.1097/01.OMX.0000438070.85123.a8.
- [16] M. W. Otter, K. J. Mcleod, and C. T. Rubin, “Effects of Electromagnetic Fields in Experimental Fracture Repair,” *Clin. Orthop. Relat. Res.*, no. 355, pp. 90–104, 1998.
- [17] N. Inoue, I. Ohnishi, D. Chen, L. W. Deitz, J. D. Schwardt, and E. Y. S. Chao, “Effect of pulsed electromagnetic fields (PEMF) on late-phase osteotomy gap healing in a canine tibial model,” *J. Orthop. Res.*, vol. 20, pp. 1106–1114, 2002.
- [18] C. R. Hassler, E. F. Rybicki, R. B. Diegle, and C. L. Clark, “Studies of Enhanced Bone

- Healing via Electrical Stimuli,” *Clin. Orthop. Relat. Res.*, vol. 124, pp. 9–19, 1977.
- [19] A. P. R. Lirani-Galvão, C. T. Bergamaschi, O. L. Silva, and M. Lazaretti-Castro, “Electrical field stimulation improves bone mineral density in ovariectomized rats,” *Brazilian J. Med. Biol. Res.*, vol. 39, no. 11, pp. 1501–1505, Nov. 2006, doi: 10.1590/S0100-879X2006001100014.
- [20] C. Sert, D. Mustafa, M. Z. Düz, F. Akşen, and A. Kaya, “The preventive effect on bone loss of 50-Hz, 1-mT electromagnetic field in ovariectomized rats.,” *J. Bone Miner. Metab.*, vol. 20, no. 6, pp. 345–9, 2002, doi: 10.1007/s007740200050.
- [21] P. Eser, E. D. De Bruin, I. Telley, H. E. Lechner, and H. Knecht, “Effect of electrical stimulation-induced cycling on bone mineral density in spinal cord-injured patients,” *Eur. J. Clin. Invest.*, vol. 33, pp. 412–419, 2003.
- [22] K. S. Eyres, M. Saleh, and J. A. Kanis, “Effect of Pulsed Electromagnetic Fields on Bone Formation and Bone Loss During Limb Lengthening,” *Bone*, vol. 18, no. 6, pp. 505–509, 1996.
- [23] K. Chang and W. H.-S. S. Chang, “Pulsed electromagnetic fields prevent osteoporosis in an ovariectomized female rat model: A prostaglandin E₂-associated process,” *Bioelectromagnetics*, vol. 24, no. 3, pp. 189–198, 2003, doi: 10.1002/bem.10078.
- [24] C. T. Brighton, M. J. Katz, S. R. Goll, C. E. Nichols, and S. R. Pollack, “Prevention and treatment of sciatic denervation disuse osteoporosis in the rat tibia with capacitively coupled electrical stimulation,” *Bone*, vol. 6, no. 2, pp. 87–97, 1985, doi: 10.1016/8756-3282(85)90312-6.
- [25] K. J. Mcleod and C. T. Rubin, “The Effect of Low-Frequency Electrical Fields on Osteogenesis,” *J. Bone Jt. Surg.*, vol. 8, pp. 920–929, 1992.
- [26] C. T. Rubin, K. J. Mcleod, and L. E. Lanyon, “Prevention of Osteoporosis by Pulsed Electromagnetic Fields,” *J. Bone Jt. Surg.*, vol. 71, no. 3, 1989.
- [27] J. Ferrier, S. M. Ross, J. Kanehisa, and J. E. Aubin, “Osteoclasts and Osteoblasts Migrate in Opposite Directions in Response to a Constant Electrical Field,” 1986.
- [28] R. Korenstein, D. Somjen, H. Fischler, and I. Binderman, “Capacitative pulsed electric stimulation of bone cells. Induction of cyclic-AMP changes and DNA synthesis,” *Biochim. Biophys. Acta - Mol. Cell Res.*, vol. 803, no. 4, pp. 302–307, Apr. 1984, doi: 10.1016/0167-4889(84)90121-6.
- [29] M. Noda and A. Sato, “Appearance of osteoclasts and osteoblasts in electrically stimulated bones cultured on chorioallantoic membranes,” *Clin. Orthop. Relat. Res.*, vol. NO. 193, no. 193, pp. 288–298, Mar. 1985, doi: 10.1097/00003086-198503000-00039.
- [30] C. T. Brighton, E. Okereke, S. R. Pollack, and C. C. Clark, “In vitro bone-cell response to a capacitively coupled electrical field. The role of field strength, pulse pattern, and duty cycle.,” *Clin. Orthop. Relat. Res.*, no. 285, pp. 255–62, 1992.
- [31] A. A. Marino, “Direct Current and Bone Growth,” *Mod. Bioelectr.*, pp. 657–709, 1988.
- [32] A. C. Ahn and A. J. Grodzinsky, “Relevance of collagen piezoelectricity to ‘Wolff’s Law’: A critical review,” *Med. Eng. Phys.*, vol. 31, no. 7, pp. 733–741, 2009, doi: 10.1016/j.medengphy.2009.02.006.
- [33] A. Rubinacci and L. Tessari, “Calcified Tissue International A Correlation Analysis Between Bone Formation Rate and Bioelectric Potentials in Rabbit Tibia,” 1983.
- [34] R. W. Treharne, C. T. T. Brighton, E. Korostoff, and S. R. R. Pollack, “An in vitro study of electrical osteogenesis using direct and pulsating currents,” *Clin. Orthop. Relat. Res.*, vol. No. 145, no. 145, pp. 300–306, 1979, doi: 10.1097/00003086-197911000-00047.
- [35] K. J. Lewis *et al.*, “Osteocyte calcium signals encode strain magnitude and loading frequency in vivo.,” *Proc. Natl. Acad. Sci. U. S. A.*, vol. 114, no. 44, pp. 11775–11780,

- Oct. 2017, doi: 10.1073/pnas.1707863114.
- [36] M. A. Qadan *et al.*, “Variation in primary and culture-expanded cells derived from connective tissue progenitors in human bone marrow space, bone trabecular surface and adipose tissue,” *Cytotherapy*, vol. 20, no. 3, pp. 343–360, Mar. 2018, doi: 10.1016/j.jcyt.2017.11.013.
- [37] A. L. Boskey, “Bone composition: relationship to bone fragility and antiosteoporotic drug effects.,” *Bonekey Rep.*, vol. 2, p. 447, 2013, doi: 10.1038/bonekey.2013.181.
- [38] J. C. Anderson and C. Eriksson, “Piezoelectric Properties of Dry and Wet Bone,” *Nature*, vol. 227, no. 5257, pp. 491–492, Aug. 1970, doi: 10.1038/227491a0.
- [39] J. C. Anderson and C. Eriksson, “Electrical Properties of Wet Collagen,” *Nature*, vol. 218, no. 5137, pp. 166–168, Apr. 1968, doi: 10.1038/218166a0.
- [40] G. B. Reinisch and A. S. Nowick, “Piezoelectric properties of bone as functions of moisture content,” *Nature*, vol. 253, no. 5493, pp. 626–627, Feb. 1975, doi: 10.1038/253626a0.
- [41] N. J. Konikoff and H. Jo, “Origin of the Osseous Bioelectric Potentials: A Review,” 1975.
- [42] C. T. Hung, F. D. Allen, S. R. Pollack, and C. T. Brighton, “What is the role of the convective current density in the real-time calcium response of cultured bone cells to fluid flow?,” *J. Biomech.*, vol. 29, no. 11, pp. 1403–1409, Nov. 1996, doi: 10.1016/0021-9290(96)84535-0.
- [43] R. A. Salzman, S. R. Pollack, A. F. T. Mak, and N. Petrov, “Electromechanical potentials in cortical bone—I. A continuum approach,” *J. Biomech.*, vol. 20, no. 3, pp. 261–270, Jan. 1987, doi: 10.1016/0021-9290(87)90293-4.
- [44] S. Singh and S. Saha, “Electrical properties of bone. A review,” *Clinical Orthopaedics and Related Research*, vol. NO. 186, no. 186, pp. 249–271, 1984.
- [45] T. Albrektsson, “Osteoinduction, osteoconduction and osseointegration,” *Eur. Spine J.*, vol. 10, no. 2, p. 96, 2001, doi: 10.1007/s005860100282.
- [46] R. O. Becker, “The Bioelectric Factors in Amphibian-Limb Regeneration : JBJS,” *JBJS*, vol. 43, no. 5, pp. 643–656, 1961.
- [47] A. Rubinacci *et al.*, “Osteocyte-Bone Lining Cell System at the Origin of Steady Ionic Current in Damaged Amphibian Bone,” *Calcif. Tissue Int.*, vol. 63, no. 4, pp. 331–339, Oct. 1998, doi: 10.1007/s002239900536.
- [48] C. Andrew, L. Bassett, R. J. Pawluk, and A. A. Pilla, “Augmentation of Bone Repair by Inductively Coupled Electromagnetic Fields,” *Science (80-.)*, vol. 184, no. 4136, pp. 575–577, 1974, doi: 10.1126/science.184.4136.575.
- [49] A. I. Anisimov, “Action of direct current on bone tissue,” *Bull. Exp. Biol. Med.*, vol. 78, no. 3, pp. 1069–1071, Sep. 1974, doi: 10.1007/BF00796671.
- [50] C. T. Brighton and R. M. Hunt, “Ultrastructure of electrically induced osteogenesis in the rabbit medullary canal,” *J. Orthop. Res.*, vol. 4, no. 1, pp. 27–36, 1986, doi: 10.1002/jor.1100040104.
- [51] H. S. Shandler, S. Weinstein, and L. E. Nathan, “Facilitated healing of osseous lesions in the canine mandible after electrical stimulation.,” *J. Oral Surg.*, vol. 37, no. 11, pp. 787–92, Nov. 1979.
- [52] Z. B. Friedenberg *et al.*, “Bone reaction to varying amounts of direct current,” *Surg. Gynecol. Obstet.*, vol. 131, no. 5, pp. 894–899, Nov. 1970, doi: 10.1097/00006534-197107000-00060.
- [53] L. A. Norton and R. R. Moore, “Bone Growth in Organ Culture Modified by an Electric Field,” *J. Dent. Res.*, vol. 51, no. 5, pp. 1492–1499, Sep. 1972, doi: 10.1177/00220345720510054101.
- [54] C. T. T. Brighton *et al.*, “Electrically induced osteogenesis: relationship between charge,

- current density, and the amount of bone formed: introduction of a new cathode concept.,” *Clin. Orthop. Relat. Res.*, vol. No. 161, no. 161, pp. 122–132, 1981, doi: 10.1097/00003086-198111000-00015.
- [55] A. Rubinacci and L. Tessari, “A correlation analysis between bone formation rate and bioelectric potentials in rabbit tibia,” *Calcif. Tissue Int.*, vol. 35, no. 1, pp. 728–731, Dec. 1983, doi: 10.1007/BF02405114.
- [56] G. V. B. Cochran, “Experimental methods for stimulation of bone healing by means of electrical energy.,” *Bull. N. Y. Acad. Med.*, vol. 48, no. 7, pp. 899–911, Aug. 1972.
- [57] C. A. L. Bassett, R. J. Pawluk, and R. O. Becker, “Effects of Electric Currents on Bone In Vivo,” *Nature*, vol. 204, no. 4959, pp. 652–654, Nov. 1964, doi: 10.1038/204652a0.
- [58] W. S. Jee and W. Yao, “Overview: animal models of osteopenia and osteoporosis.,” *J. Musculoskelet. Neuronal Interact.*, vol. 1, no. 3, pp. 193–207, 2001.
- [59] A. P. R. Lirani-Galvão *et al.*, “Low-Intensity Electrical Stimulation Counteracts the Effects of Ovariectomy on Bone Tissue of Rats: Effects on Bone Microarchitecture, Viability of Osteocytes, and Nitric Oxide Expression,” *Calcif. Tissue Int.*, vol. 84, no. 6, pp. 502–509, Jun. 2009, doi: 10.1007/s00223-009-9227-9.
- [60] R. K. Aaron, B. D. Boyan, D. M. Ciombor, Z. Schwartz, and B. J. Simon, “Stimulation of growth factor synthesis by electric and electromagnetic fields.,” *Clin. Orthop. Relat. Res.*, no. 419, pp. 30–7, 2004.
- [61] C. H. Lohmann *et al.*, “Pulsed electromagnetic field stimulation of MG63 osteoblast-like cells affects differentiation and local factor production,” *J. Orthop. Res.*, vol. 18, no. 4, pp. 637–646, Jul. 2000, doi: 10.1002/jor.1100180417.
- [62] G. S. Stein and J. B. Lian, “Molecular mechanisms mediating proliferation/differentiation interrelationships during progressive development of the osteoblast phenotype,” *Endocr. Rev.*, vol. 14, no. 4, pp. 424–442, 1993, doi: 10.1210/edrv-14-4-424.
- [63] R. A. Hopper *et al.*, “Osteoblasts stimulated with pulsed electromagnetic fields increase HUVEC proliferation via a VEGF-A independent mechanism,” *Bioelectromagnetics*, vol. 30, no. 3, pp. 189–197, Apr. 2009, doi: 10.1002/bem.20459.
- [64] M. Griffin, A. Sebastian, J. Colthurst, and A. Bayat, “Enhancement of Differentiation and Mineralisation of Osteoblast-like Cells by Degenerate Electrical Waveform in an In Vitro Electrical Stimulation Model Compared to Capacitive Coupling,” *PLoS One*, vol. 8, no. 9, p. e72978, 2013, doi: 10.1371/journal.pone.0072978.
- [65] M. Hartig, U. Joos, and H. P. Wiesmann, “Capacitively coupled electric fields accelerate proliferation of osteoblast-like primary cells and increase bone extracellular matrix formation in vitro,” *Eur. Biophys. J.*, vol. 29, no. 7, pp. 499–506, 2000, doi: 10.1007/s002490000100.
- [66] T. Bodamyali *et al.*, “Pulsed electromagnetic fields simultaneously induce osteogenesis and upregulate transcription of bone morphogenetic proteins 2 and 4 in rat osteoblasts in vitro,” *Biochem. Biophys. Res. Commun.*, vol. 250, no. 2, pp. 458–461, 1998, doi: 10.1006/bbrc.1998.9243.
- [67] B. Bragdon, O. Moseychuk, S. Saldanha, D. King, J. Julian, and A. Nohe, “Bone Morphogenetic Proteins: A critical review,” *Cell. Signal.*, vol. 23, no. 4, pp. 609–620, 2011, doi: 10.1016/j.cellsig.2010.10.003.
- [68] H. P. Gerber, T. H. Vu, A. M. Ryan, J. Kowalski, Z. Werb, and N. Ferrara, “VEGF couples hypertrophic cartilage remodeling, ossification and angiogenesis during endochondral bone formation,” *Nat. Med.*, vol. 5, no. 6, pp. 623–628, 1999, doi: 10.1038/9467.
- [69] H. Peng *et al.*, “Synergistic enhancement of bone formation and healing by stem cell-

- expressed VEGF and bone morphogenetic protein-4,” *J. Clin. Invest.*, vol. 110, no. 6, pp. 751–759, 2002, doi: 10.1172/JCI200215153.
- [70] L. D. Yakar S, Rosen CJ, Beamer WG, Ackert-Bicknell CL, Wu Y, Liu JL, Ooi GT, Setser J, Frystyk J, Boisclair YR, “Circulating levels of LGF-1 directly regulate bone growth and density,” *J. Clin. Invest.*, vol. 110, no. 6, pp. 771–781, 2002, doi: 10.1172/JCI200215463.
- [71] W. Hong-Shong Chang, L.-T. Chen, J.-S. Sun, and F.-H. Lin, “Effect of Pulse-Burst Electromagnetic Field Stimulation on Osteoblast Cell Activities,” *Bioelectromagnetics*, vol. 25, pp. 457–465, 2004, doi: 10.1002/bem.20016.
- [72] S. Matsunaga, “Histological and histochemical investigations of constant direct current stimulated intramedullary callus.,” *Nihon Seikeigeka Gakkai Zasshi*, vol. 60, no. 12, pp. 1293–303, Dec. 1986.
- [73] C. T. Brighton, W. Wang, R. Seldes, G. Zhang, and S. R. Pollack, “Signal Transduction in Electrically Stimulated Bone Cells,” *J. bone Jt. surgery. Am. Vol.*, vol. 83, no. 10, pp. 1514–1523, 2001.
- [74] E. M. Aarden *et al.*, “Adhesive properties of isolated chick osteocytes in vitro,” *Bone*, vol. 18, no. 4, pp. 305–313, Apr. 1996, doi: 10.1016/8756-3282(96)00010-5.
- [75] C. Palumbo, “A three-dimensional ultrastructural study of osteoid-osteocytes in the tibia of chick embryos,” *Cell Tissue Res.*, vol. 246, no. 1, pp. 125–131, Oct. 1986, doi: 10.1007/BF00219008.
- [76] E. H. Burger and J. Klein-Nulend, “Mechanotransduction in bone -role of the lacuno-canalicular network,” *FASEB J.*, vol. 13, no. 9001, pp. S101–S112, May 1999, doi: 10.1096/fasebj.13.9001.s101.
- [77] M. L. Knothe Tate, “The osteocyte,” *Int. J. Biochem. Cell Biol.*, vol. 36, no. 1, 2003.
- [78] C. H. Lohmann *et al.*, “Pulsed electromagnetic fields affect phenotype and connexin 43 protein expression in MLO-Y4 osteocyte-like cells and ROS 17/2.8 osteoblast-like cells,” *J. Orthop. Res.*, vol. 21, no. 2, pp. 326–334, Mar. 2003, doi: 10.1016/S0736-0266(02)00137-7.
- [79] P. Wang *et al.*, “Pulsed electromagnetic fields regulate osteocyte apoptosis, RANKL/OPG expression, and its control of osteoclastogenesis depending on the presence of primary cilia,” *J. Cell. Physiol.*, vol. 234, no. 7, pp. 10588–10601, 2019, doi: 10.1002/jcp.27734.
- [80] K. Tanaka *et al.*, “Time-lapse microcinematography of osteocytes.,” *Miner. Electrolyte Metab.*, vol. 21, no. 1–3, pp. 189–92, 1995.
- [81] I. Kramer *et al.*, “Osteocyte Wnt/ -Catenin Signaling Is Required for Normal Bone Homeostasis,” *Mol. Cell. Biol.*, vol. 30, no. 12, pp. 3071–3085, 2010, doi: 10.1128/MCB.01428-09.
- [82] A. L. J. J. Bronckers *et al.*, “DNA fragmentation during bone formation in neonatal rodents assessed by transferase-mediated end labelling,” *J. Bone Miner. Res.*, vol. 11, no. 9, pp. 1281–1291, Dec. 1996, doi: 10.1002/jbmr.5650110913.
- [83] K. Chang, W. H. S. Chang, S. Huang, S. Huang, and C. Shih, “Pulsed electromagnetic fields stimulation affects osteoclast formation by modulation of osteoprotegerin, RANK ligand and macrophage colony-stimulating factor,” *J. Orthop. Res.*, vol. 23, no. 6, pp. 1308–1314, Nov. 2005, doi: 10.1016/j.orthres.2005.03.012.
- [84] K. Chang, W. H. S. Chang, M. T. Tsai, and C. Shih, “Pulsed electromagnetic fields accelerate apoptotic rate in osteoclasts,” *Connect. Tissue Res.*, vol. 47, no. 4, pp. 222–228, Jul. 2006, doi: 10.1080/03008200600858783.
- [85] J. Rubin, K. J. McLeod, L. Titus, M. S. Nanes, B. D. Catherwood, and C. T. Rubin, “Formation of osteoclast-like cells is suppressed by low frequency, low intensity electric fields,” *J. Orthop. Res.*, vol. 14, no. 1, pp. 7–15, Jan. 1996, doi: 10.1002/jor.1100140104.

- [86] T. J. Dauben, J. Ziebart, T. Bender, S. Zaatreh, B. Kreikemeyer, and R. Bader, “A Novel in Vitro System for Comparative Analyses of Bone Cells and Bacteria under Electrical Stimulation,” *Biomed Res. Int.*, vol. 2016, 2016, doi: 10.1155/2016/5178640.
- [87] S. B. Brummer and M. J. Turner, “Electrical stimulation of the nervous system: The principle of safe charge injection with noble metal electrodes,” *Bioelectrochemistry Bioenerg.*, vol. 2, no. 1, pp. 13–25, 1975, doi: 10.1016/0302-4598(75)80002-X.
- [88] S. B. Brummer, L. S. Robblee, and F. T. Hambrecht, “Criteria for Selecting Electrodes for Electrical Stimulation: Theoretical and Practical Considerations,” *Ann. N. Y. Acad. Sci.*, vol. 405, no. 1, pp. 159–171, Jun. 1983, doi: 10.1111/j.1749-6632.1983.tb31628.x.
- [89] E. L. Sandvik, B. R. McLeod, A. E. Parker, and P. S. Stewart, “Direct Electric Current Treatment under Physiologic Saline Conditions Kills *Staphylococcus epidermidis* Biofilms via Electrolytic Generation of Hypochlorous Acid,” *PLoS One*, vol. 8, no. 2, Feb. 2013, doi: 10.1371/journal.pone.0055118.
- [90] C. T. Brighton, S. Adler, J. Black, N. Itada, and Z. B. Friedenberg, “Cathodic oxygen consumption and electrically induced osteogenesis,” *CLIN. ORTHOP.*, vol. No. 107, pp. 277–282, 1975, doi: 10.1097/00003086-197503000-00033.
- [91] Q. Wang *et al.*, “Osteogenesis of electrically stimulated bone cells mediated in part by calcium ions,” *Clin. Orthop. Relat. Res.*, no. 348, pp. 259–268, 1998, doi: 10.1097/00003086-199803000-00037.
- [92] D. R. Merrill, M. Bikson, and J. G. R. Jefferys, “Electrical stimulation of excitable tissue: Design of efficacious and safe protocols,” *Journal of Neuroscience Methods*, vol. 141, no. 2, pp. 171–198, 15-Feb-2005, doi: 10.1016/j.jneumeth.2004.10.020.
- [93] T. Bodamyali, J. M. Kanczler, B. Simon, D. R. Blake, and C. R. Stevens, “Effect of faradic products on direct current-stimulated calvarial organ culture calcium levels,” *Biochem. Biophys. Res. Commun.*, vol. 264, no. 3, pp. 657–661, Nov. 1999, doi: 10.1006/bbrc.1999.1355.
- [94] K. Srirussamee, S. Mobini, N. J. Cassidy, and S. H. Cartmell, “Direct electrical stimulation enhances osteogenesis by inducing Bmp2 and Spp1 expressions from macrophages and preosteoblasts,” 2019, doi: 10.1002/bit.27142.
- [95] M. Cho, T. K. Hunt, and M. Z. Hussain, “Hydrogen peroxide stimulates macrophage vascular endothelial growth factor release,” *Am. J. Physiol. - Hear. Circ. Physiol.*, vol. 280, no. 5 49-5, May 2001, doi: 10.1152/ajpheart.2001.280.5.h2357.
- [96] M. T. Ehrensberger *et al.*, “Cathodic Voltage-Controlled Electrical Stimulation of Titanium Implants as Treatment for Methicillin-Resistant *Staphylococcus Aureus* Periprosthetic Infections,” *Biomaterials*, vol. 41, pp. 97–105, Feb. 2014, doi: 10.1016/j.biomaterials.2014.11.013.
- [97] M. R. Asadi and G. Torkaman, “Bacterial Inhibition by Electrical Stimulation,” *Adv. Wound Care*, vol. 3, no. 2, pp. 91–97, Feb. 2014, doi: 10.1089/wound.2012.0410.
- [98] K. K. Kaysinger and W. K. Ramp, “Extracellular pH modulates the activity of cultured human osteoblasts,” *J. Cell. Biochem.*, vol. 68, no. 1, pp. 83–89, 1998, doi: 10.1002/(SICI)1097-4644(19980101)68:1<83::AID-JCB8>3.0.CO;2-S.
- [99] D. A. Bushinsky, “Metabolic alkalosis decreases bone calcium efflux by suppressing osteoclasts and stimulating osteoblasts,” *Am. J. Physiol.*, vol. 271, no. 1 PART 2, 1996, doi: 10.1152/ajprenal.1996.271.1.f216.
- [100] K. Srirussamee, “Direct Electrical Stimulation Approaches for Bone Repair and Regeneration,” Manchester, United Kingdom, 2019.
- [101] M. Arora, “Cell Culture Media: A Review,” *Mater. Methods*, vol. 3, Mar. 2013, doi: 10.13070/mm.en.3.175.

- [102] L. Kent, “Cell Culture Basics: Stem Cell Media – The ‘What’ and ‘Why’ - Cell Culture Dish - Cell Culture Dish,” 2016. [Online]. Available: <https://cellculturedish.com/cell-culture-basics-stem-cell-media-the-what-and-why/>. [Accessed: 14-May-2020].
- [103] P. Held, “Using Phenol Red to Assess pH in Tissue Culture Media,” *BioTek Live Cell Imaging*, 2018.
- [104] “The pH of culture media | CellCulture.” [Online]. Available: http://cellculture.altervista.org/the-ph-of-culture-media/?doing_wp_cron=1570260623.5416550636291503906250. [Accessed: 14-May-2020].
- [105] M. Schwalbe, “Phenol red pH 6,0 - 8,0.jpg.” [Online]. Available: https://commons.wikipedia.org/wiki/User_talk:Max_schwalbe#File:Phenol_red_pH_6,0_-_8,0.jpg. [Accessed: 27-Jul-2020].
- [106] S. Aldrich, “Dulbecco ’ s Modified Eagle ’ s Medium (DMEM).” [Online]. Available: <https://www.sigmaaldrich.com/content/dam/sigma-aldrich/docs/Sigma/Formulation/d5030for.pdf>.
- [107] S. Aldrich, “McCoy’s 5A Modified Medium.” [Online]. Available: <https://www.sigmaaldrich.com/content/dam/sigma-aldrich/docs/Sigma/Formulation/m4892for.pdf>.
- [108] C. Sekirnjak, P. Hottowy, A. Sher, W. Dabrowski, A. M. Litke, and E. J. Chichilnisky, “Electrical stimulation of mammalian retinal ganglion cells with multielectrode arrays,” *J. Neurophysiol.*, vol. 95, no. 6, pp. 3311–3327, Jun. 2006, doi: 10.1152/jn.01168.2005.
- [109] “Lead-Free Solder - an overview | ScienceDirect Topics.” [Online]. Available: <https://www.sciencedirect.com/topics/materials-science/lead-free-solder>. [Accessed: 17-Jul-2020].
- [110] Z. Qi *et al.*, “Combined treatment with electrical stimulation and insulin-like growth factor-1 promotes bone regeneration in vitro,” *PLoS One*, vol. 13, no. 5, May 2018, doi: 10.1371/journal.pone.0197006.
- [111] S. Mobini, L. Leppik, V. Thottakkattumana Parameswaran, and J. H. Barker, “In vitro effect of direct current electrical stimulation on rat mesenchymal stem cells,” *PeerJ*, vol. 5, p. e2821, 2017, doi: 10.7717/peerj.2821.
- [112] S. Mobini, L. Leppik, and J. H. Barker, “Direct current electrical stimulation chamber for treating cells in vitro,” *Biotechniques*, vol. 60, no. 2, pp. 95–8, Feb. 2016, doi: 10.2144/000114382.
- [113] “Electrolytic Cells.” [Online]. Available: <https://chemed.chem.purdue.edu/genchem/topicreview/bp/ch20/faraday.php>. [Accessed: 19-Aug-2020].
- [114] Z. B. Friedenberg, L. M. Zemsky, R. P. Pollis, and C. T. Brighton, “The response of non traumatized bone to direct current,” *J. Bone Jt. Surg. - Ser. A*, vol. 56, no. 5, pp. 1023–1030, 1974, doi: 10.2106/00004623-197456050-00013.
- [115] D. C. Fredericks *et al.*, “Effects of direct current electrical stimulation on gene expression of osteopromotive factors in a posterolateral spinal fusion model,” *Spine (Phila. Pa. 1976)*, vol. 32, no. 2, pp. 174–181, Jan. 2007, doi: 10.1097/01.brs.0000251363.77027.49.
- [116] J. Zhang, M. Li, E. T. Kang, and K. G. Neoh, “Electrical stimulation of adipose-derived mesenchymal stem cells in conductive scaffolds and the roles of voltage-gated ion channels,” *Acta Biomater.*, vol. 32, pp. 46–56, Mar. 2016, doi: 10.1016/j.actbio.2015.12.024.
- [117] A. Jhirad, “The Effects of Electrical Stimulation on Loss of Bone Mass in The Ovariectomized Rat,” McMaster University, 2018.

- [118] L. F. Bonewald, “Osteocytes: A proposed multifunctional bone cell,” *J. Musculoskelet. Neuronal Interact.*, vol. 2, no. 3, pp. 239–241, 2002.
- [119] N. E. Ajubi, J. Klein-Nulend, P. J. Nijweide, T. Vrijheid-Lammers, M. J. Alblas, and E. H. Burger, “Pulsating Fluid Flow Increases Prostaglandin Production by Cultured Chicken Osteocytes—A Cytoskeleton-Dependent Process,” *Biochem. Biophys. Res. Commun.*, vol. 225, no. 1, pp. 62–68, Aug. 1996, doi: 10.1006/bbrc.1996.1131.
- [120] J. Klein-Nulend, C. M. Semeins, N. E. Ajubi, P. J. Nijweide, and E. H. Burger, “Pulsating Fluid Flow Increases Nitric Oxide (NO) Synthesis by Osteocytes but Not Periosteal Fibroblasts - Correlation with Prostaglandin Upregulation,” *Biochem. Biophys. Res. Commun.*, vol. 217, no. 2, pp. 640–648, Dec. 1995, doi: 10.1006/bbrc.1995.2822.
- [121] J. S. Mendonça, L. M. G. Neves, M. A. M. Esquisatto, F. A. S. Mendonça, and G. M. T. Santos, “Comparative study of the application of microcurrent and AsGa 904 nm laser radiation in the process of repair after calvaria bone excision in rats,” *Laser Phys.*, vol. 23, no. 3, 2013, doi: 10.1088/1054-660X/23/3/035605.
- [122] C. Masureik and C. Eriksson, “Preliminary clinical evaluation of the effect of small electrical currents on the healing of jaw fractures,” *Clin. Orthop. Relat. Res.*, vol. No.124, no. 124, pp. 84–91, May 1977, doi: 10.1097/00003086-197705000-00012.
- [123] J. H. Fonseca *et al.*, “Electrical stimulation: Complementary therapy to improve the performance of grafts in bone defects?,” *J. Biomed. Mater. Res. Part B Appl. Biomater.*, vol. 107, no. 4, pp. 924–932, May 2019, doi: 10.1002/jbm.b.34187.
- [124] J. C. France, T. L. Norman, R. D. Santrock, B. McGrath, and B. J. Simon, “The efficacy of direct current stimulation for lumbar intertransverse process fusions in an animal model,” *Spine (Phila. Pa. 1976)*, vol. 26, no. 9, pp. 1002–1007, 2001, doi: 10.1097/00007632-200105010-00003.
- [125] C. T. Brighton, J. Black, Z. B. Friedenberg, J. L. Esterhai, L. J. Day, and J. F. Connolly, “A multicenter study of the treatment of non-union with constant direct current,” *J. Bone Jt. Surg. - Ser. A*, vol. 63, no. 1, pp. 2–13, 1981, doi: 10.2106/00004623-198163010-00002.
- [126] Z. Wang, C. C. Clark, and C. T. Brighton, “Up-regulation of bone morphogenetic proteins in cultured murine bone cells with use of specific electric fields,” *J. Bone Jt. Surg. - Ser. A*, vol. 88, no. 5, pp. 1053–1065, 2006, doi: 10.2106/JBJS.E.00443.
- [127] M. Eischen-Loges, K. M. C. Oliveira, M. B. Bhavsar, J. H. Barker, and L. Leppik, “Pretreating mesenchymal stem cells with electrical stimulation causes sustained long-lasting pro-osteogenic effects,” *PeerJ*, vol. 2018, no. 6, 2018, doi: 10.7717/peerj.4959.
- [128] B. Hiemer *et al.*, “Effect of electric stimulation on human chondrocytes and mesenchymal stem cells under normoxia and hypoxia,” *Mol. Med. Rep.*, vol. 18, no. 2, pp. 2133–2141, Aug. 2018, doi: 10.3892/mmr.2018.9174.

7. Appendices

7.1. Media Composition

Media Composition			
	DMEM - Low glucose	McCoy's	% difference
Appearance (Turbidity)	Clear	Clear	
pH	7.0/7.6	7-7.6	
Osmolality	308 - 340 mOs/kg	274 - 302 mOs/kg	
Endotoxin Level	<= 1 EU/ml	< 1.0 EU/ml	
Glucose	0.9 - 1.1 g/l	2.7 - 3.3 g/l	
L-glutamine		0.21 g/L	
phenol red		0.011g/L	
NaHCO ₃		2.2g/L	
Glucose		3.0 g/L	
Inorganic Salts			
CaCl ₂	0.2	0.1324324	41%
MgSO ₄	0.09767	0.09766876	0%
KCl	0.4	0.4	0%
NaHCO ₃	3.7	2.2	51%
NaCl	6.4	6.46	1%
NaH ₂ PO ₄	0.109	0.504	129%
Fe(NO ₃) ₃ • 9H ₂ O	0.0001		100%
Amino Acids			
L-Alanine		0.01336	100%
L-Arginine • HCl	0.084	0.04214	66%
L-Asparagine • H ₂ O		0.04503	100%
L-Aspartic Acid		0.01997	100%
L -Cystine • 2HCl	0.0626		100%
L-Cysteine		0.02424	100%
L-Glutamic Acid		0.02207	100%
L-Glutamine	0.584	0.21915	91%
Glycine	0.03	0.00751	120%
L-Histidine • HCl • H ₂ O	0.042	0.02096	67%
Hydroxy-L-proline		0.01967	100%
L-Isoleucine	0.105	0.03936	91%
L-Leucine	0.105	0.03936	91%
L-Lysine • HCl	0.146	0.03654	120%

L-Methionine	0.03	0.01492	67%
L-Phenylalanine	0.066	0.01652	120%
L-Proline		0.01727	100%
L-Serine	0.042	0.02628	46%
L-Threonine	0.095	0.01787	137%
L-Tryptophan	0.016	0.00306	136%
L-Tyrosine • 2Na • 2H ₂ O	0.10379	0.0261	120%
L-Valine	0.094	0.01757	137%
Vitamins			
Ascorbic Acid		0.0005625	100%
p-Amino Benzoic Acid		0.001	100%
D-Biotin		0.0002	100%
Choline Chloride	0.004	0.005	22%
Folic Acid	0.004	0.01	86%
myo-Inositol	0.0072	0.036	133%
Niacinamide	0.004	0.0005	156%
Nicotinic Acid		0.0005	100%
D-Pantothenic Acid • ½Ca	0.004	0.0002	181%
Pyridoxal • HCl		0.0005	100%
Pyridoxine • HCl	0.00404	0.0005	156%
Riboflavin	0.0004	0.0002	67%
Thiamine • HCl		0.0002	100%
Vitamin B-12		0.002	100%
Other			
Peptone		0.6	100%
D-Glucose	1	3	100%
Glutathione (reduced)		0.0005	100%
Phenol Red • Na	0.0159	0.011	36%
Pyruvic Acid Na	0.11		100%

7.2. Constant Voltage Experiments

7.2.1. DC Stimulation

Input Signal	5V DC
Current	9.5 μ A
System	UNO R3
Time	200 mins
Increments	5 mins
R _{Load}	Variable

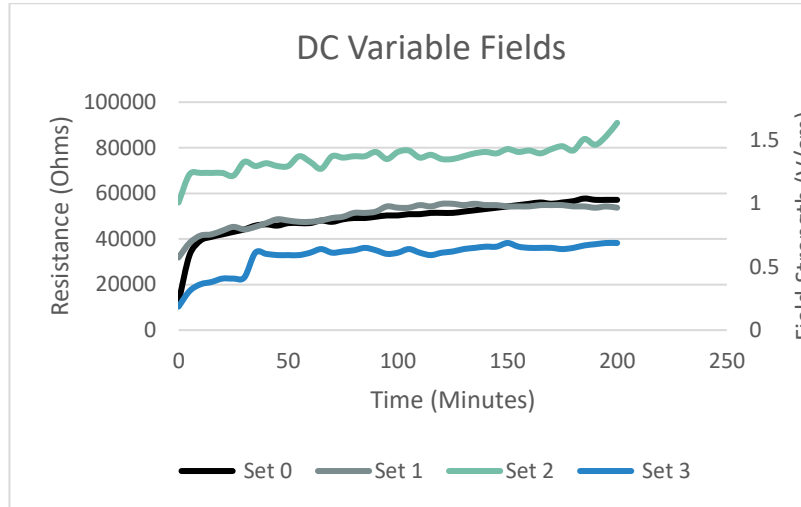


Figure 40: Preliminary Variable Field Test

Four different field strengths were created by using four different load resistances. Due to the large range of measured resistance values, the smaller fluctuations within the data are less prominent and the curves appear smoother.

Input Signal	5V DC
Current	11 μ A
System	UNO R3
Time	120 mins
Increments	5 mins
R _{Load}	91k Ω 28.6 k Ω 25k Ω 45.6k Ω

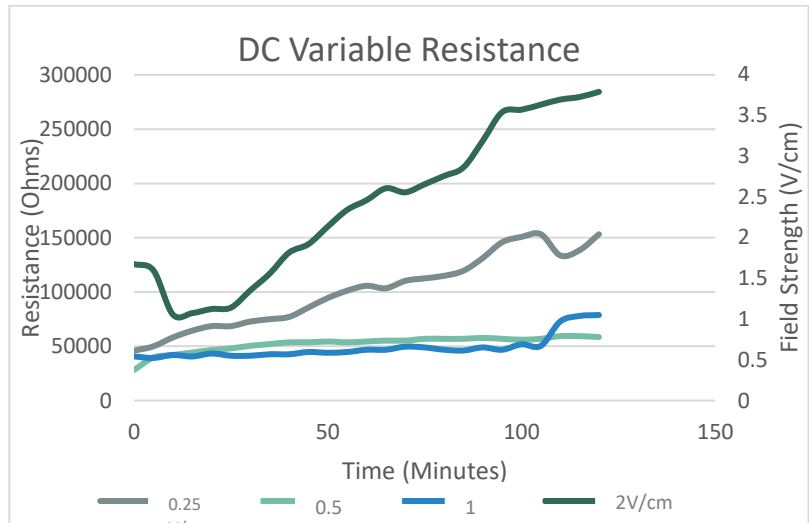


Figure 41: Variable Field Strengths: 0.25, 0.5, 1, 2V/cm for 120 minutes

Input Signal	5V DC
Current	180 μ A
System	UNO R3
Time	420 mins
Increments	10 mins
R _{Load}	10 k Ω

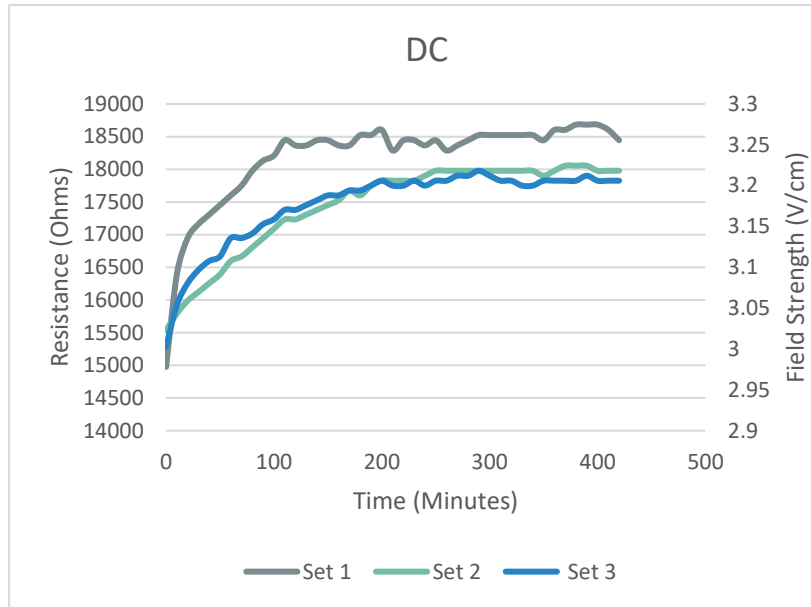


Figure 42: DC Extended Time Test

Input Signal	5V DC
Current	180 μ A
System	UNO R3
Time	420 mins
Increments	10 mins
R _{Load}	10 k Ω

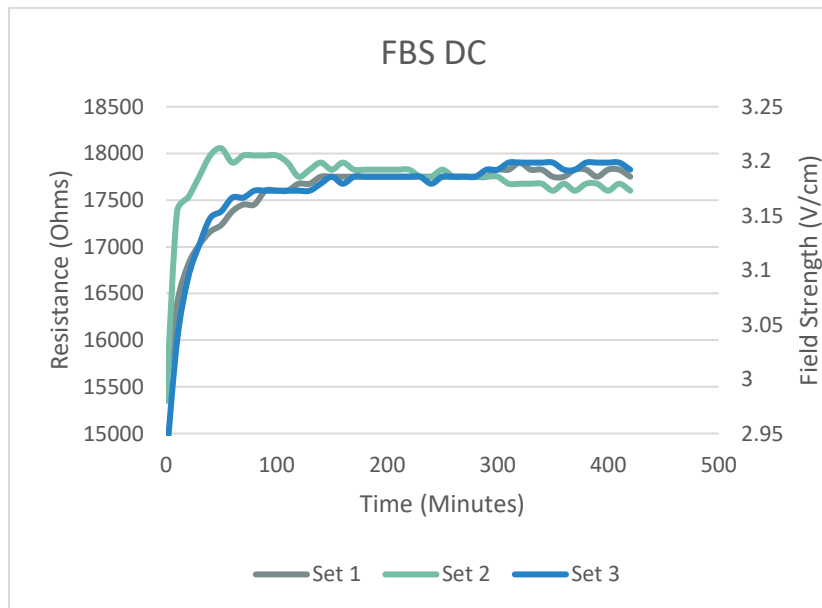


Figure 43: DC Test with the introduction of FBS

Input Signal	5V DC
Current	385 μ A
System	UNO R3
Time	420 mins
Increments	10 mins
R _{Load}	1 k Ω

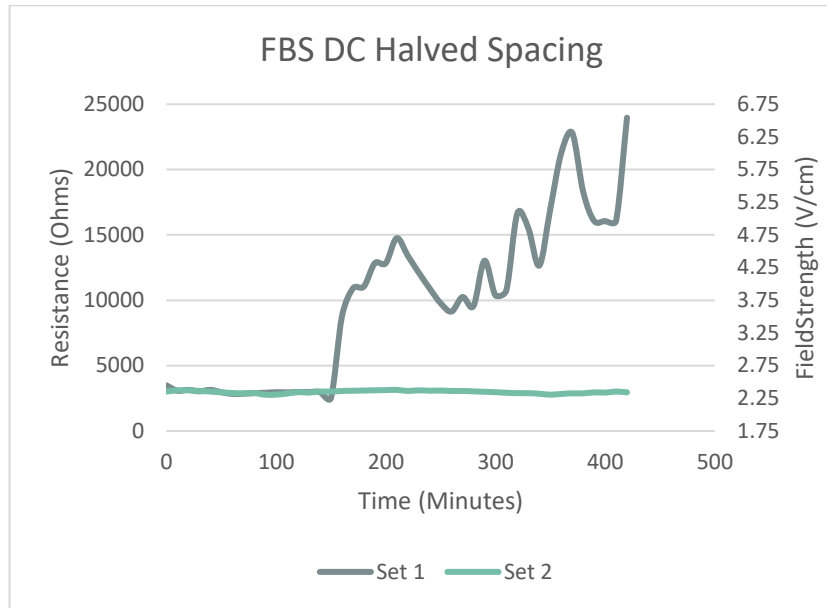


Figure 44: DC Test with the introduction of FBS, reduced spacing to increase the field strength

7.2.2. AC Stimulation

Input Signal	1.212 V Sine
Current	50 μ A
System	Oscilloscope + Function Generator
Time	80 mins
Increments	10 mins
R _{Load}	10 k Ω

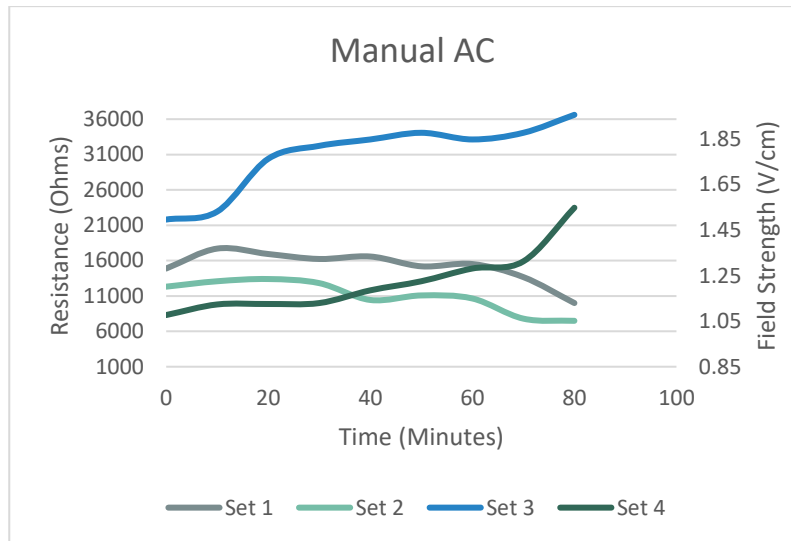


Figure 45: Manual measurements AC Test

Input Signal	5V Sine 3.54V RMS
Current	160 μ A
System	Analog Discovery
Time	168 mins
Increments	0.5 mins
R _{Load}	1 k Ω

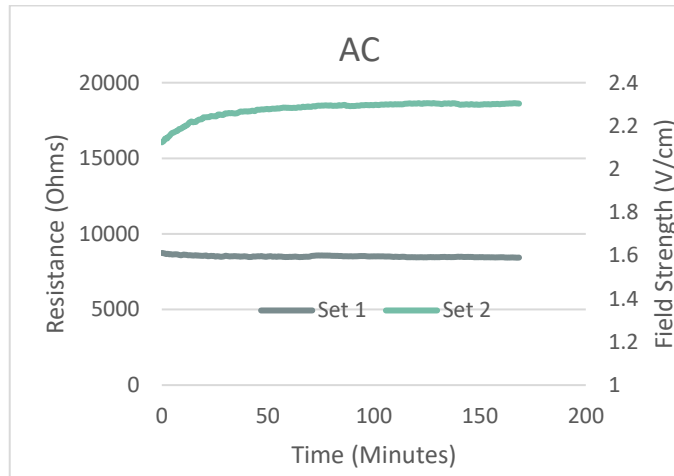


Figure 46: AC Test

7.2.3. Square Wave

Input Signal	2V Square Wave 1Hz
Current	18 μ A
System	Analog Discovery
Time	300 mins
Increments	10 mins
R _{Load}	100 Ω

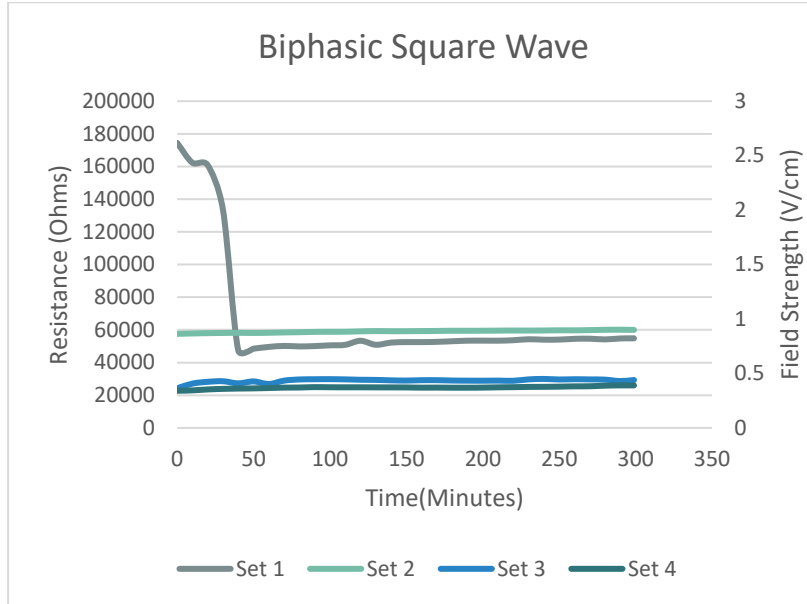


Figure 47: Biphasic Square Wave Test

Input Signal	5V DC
Current	115 μ A
System	UNO R3
Time	470 mins
Increments	10 mins
R _{Load}	10 k Ω

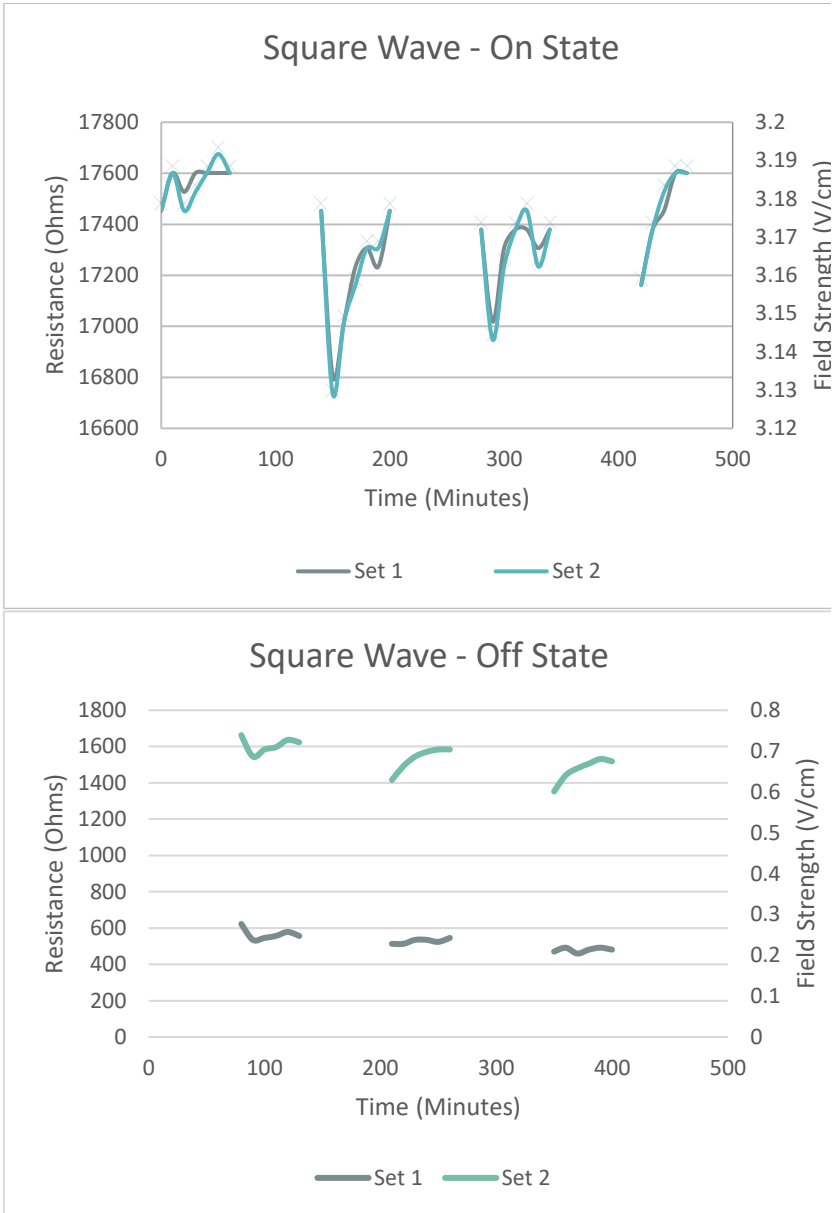


Figure 48: Square Wave Test

7.2.4. **McCoy's Medium**

Input Signal	5V DC
Current	7.5 μ A
System	UNO R3
Time	240 mins
Increments	5 mins
R _{Load}	1 k Ω

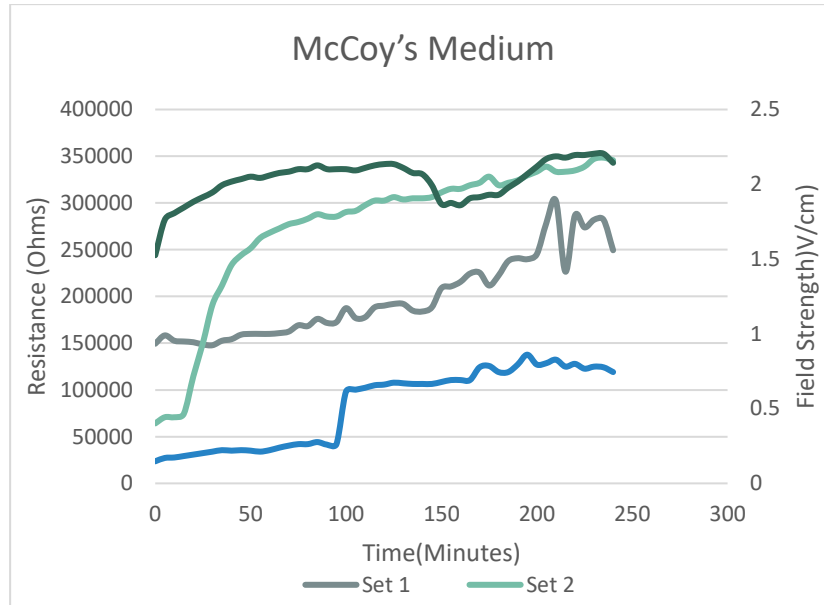


Figure 49: McCoy's Medium Test

Input Signal	5V DC
Current	236 μ A
System	UNO R3
Time	195 mins
Increments	5 mins
R _{Load}	10 k Ω

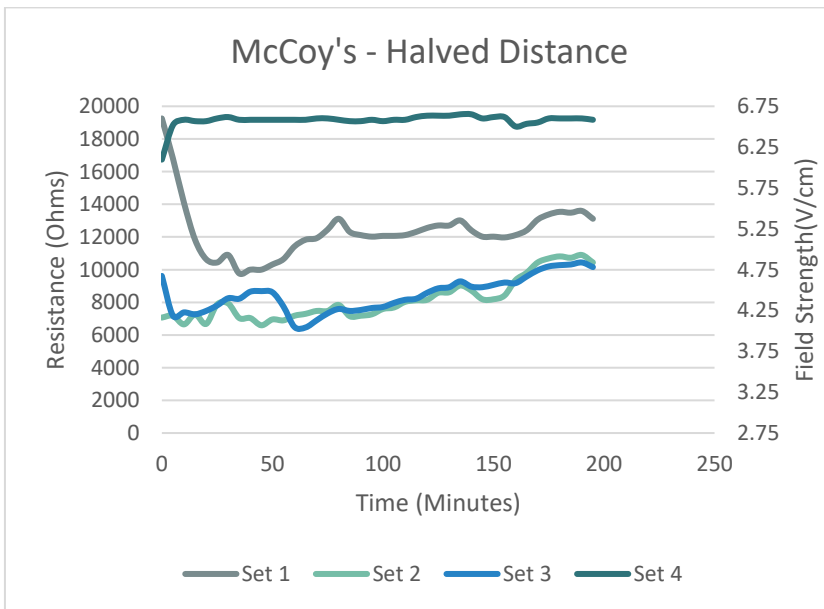


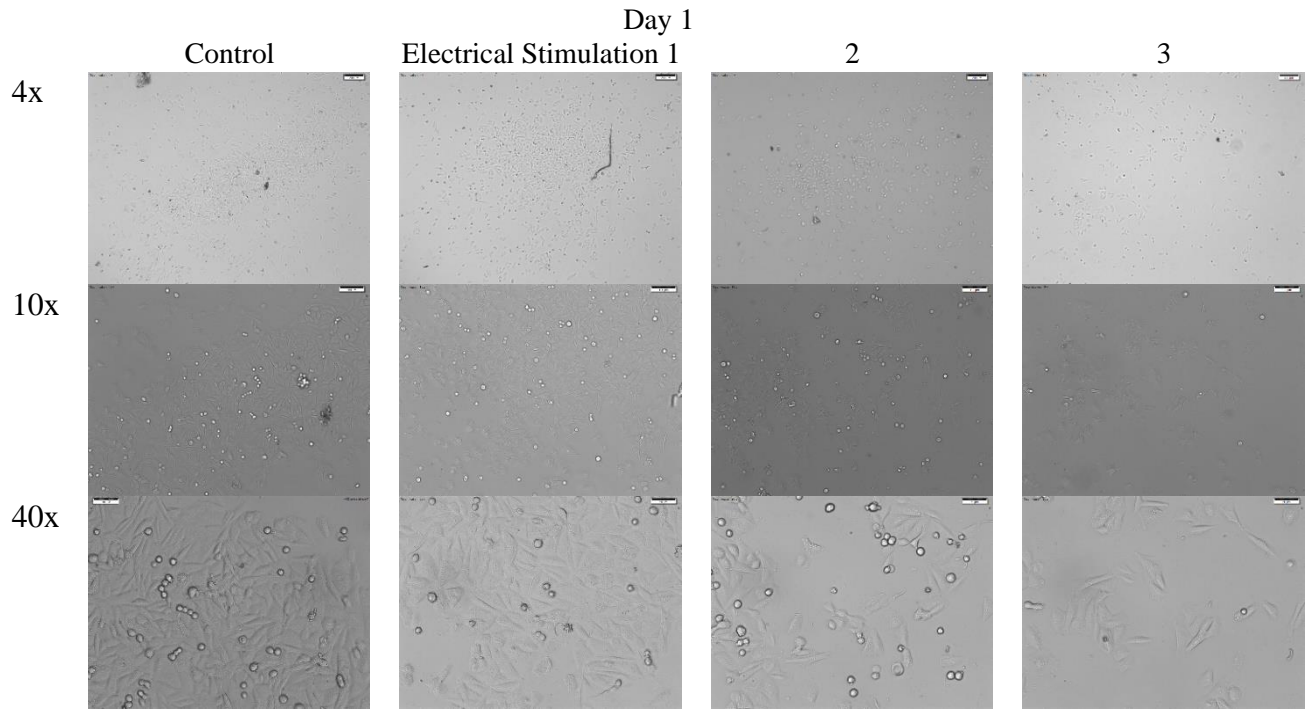
Figure 50: McCoy's Medium Testing Halved Spacing

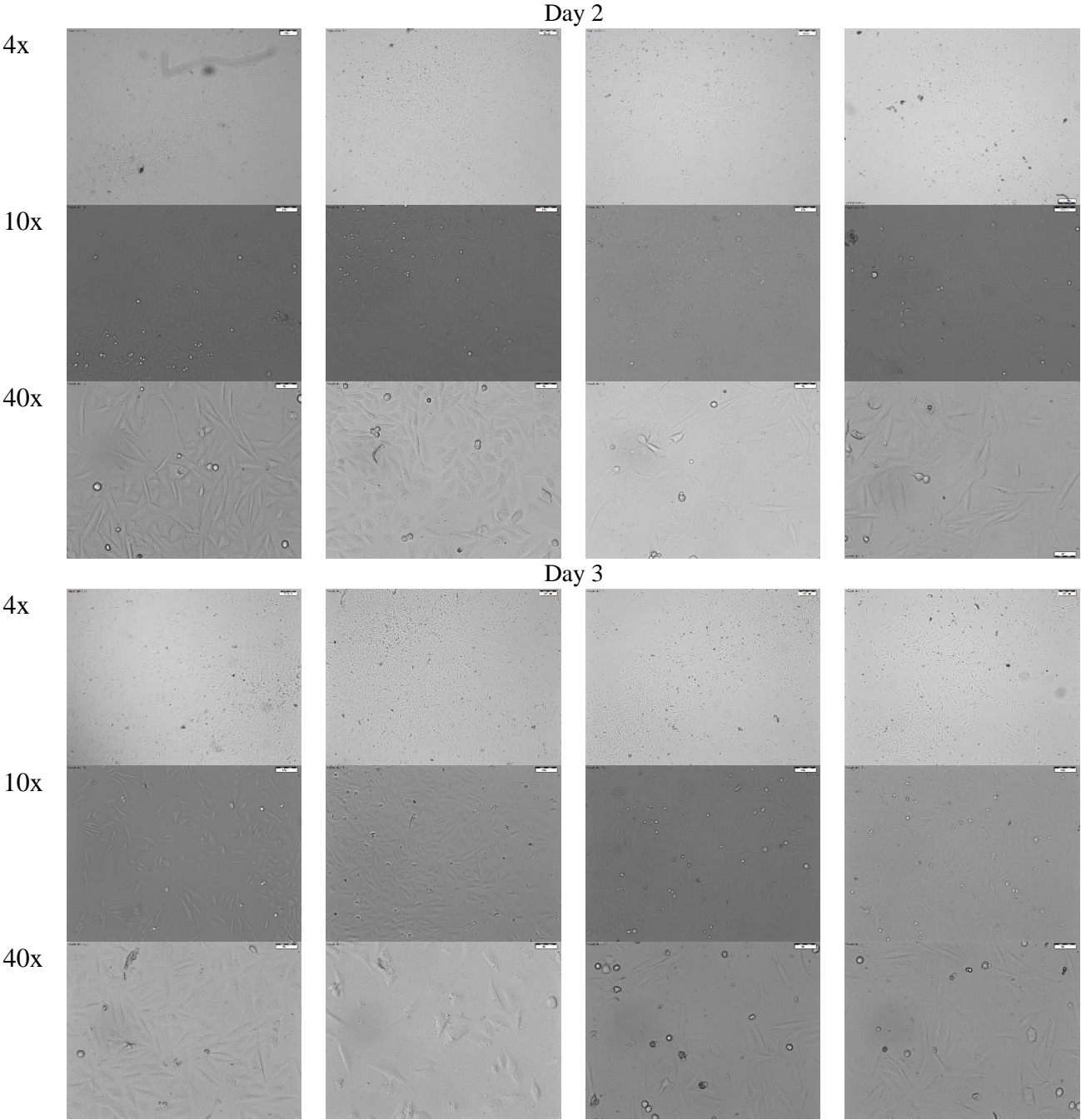
7.3. Predicted Resistances

Table 3: Predicted Resistances

mA	μ A	Predicted Resistance (k Ω)	Predicted Voltage(V)	Max allowed Resistance (k Ω)	Resistance with 15% Safety (k Ω)
0.100	100	28.90	2.89	21.09	16.76
0.150	150	19.84	2.98	13.49	10.51
0.200	200	15.20	3.04	9.80	7.53
0.250	250	12.35	3.09	7.65	5.79
0.300	300	10.43	3.13	6.23	4.67
0.350	350	9.04	3.17	5.24	3.89
0.400	400	7.99	3.20	4.51	3.31
0.450	450	7.16	3.22	3.95	2.88
0.500	500	6.49	3.25	3.51	2.53
0.550	550	5.95	3.27	3.15	2.25
0.600	600	5.48	3.29	2.85	2.03
0.650	650	5.09	3.31	2.60	1.84
0.700	700	4.75	3.33	2.39	1.68
0.750	750	4.46	3.34	2.21	1.54
0.800	800	4.20	3.36	2.05	1.42
1.000	1000	3.41	3.41	1.59	1.07

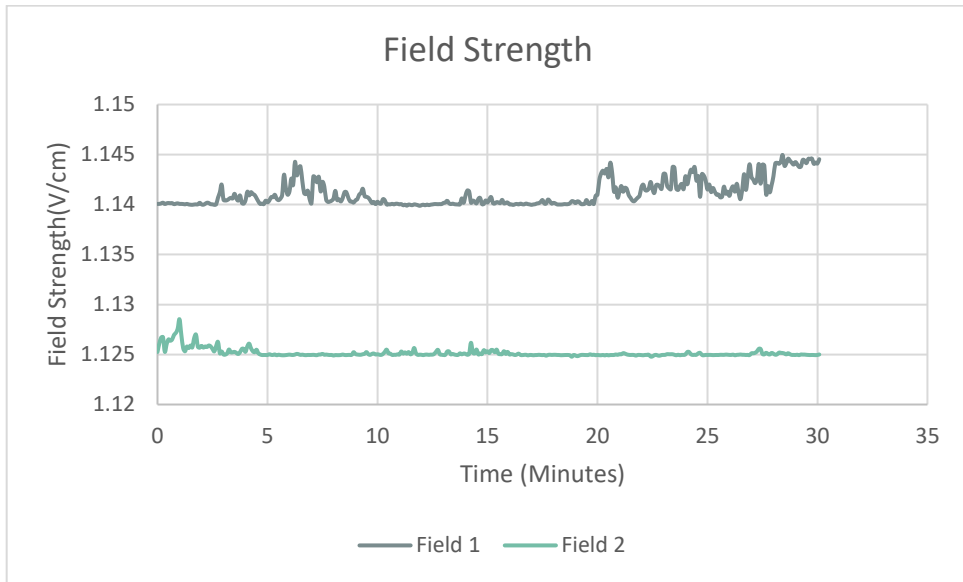
7.4. Cell Microscopy Images



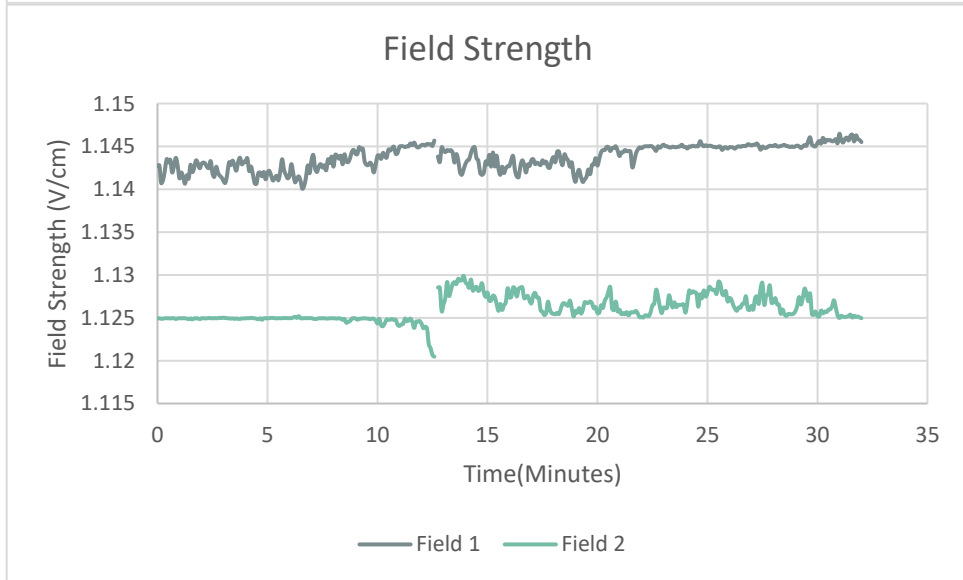


7.5. Cell Stimulation Resistance Graphs (Well 1 and 2)

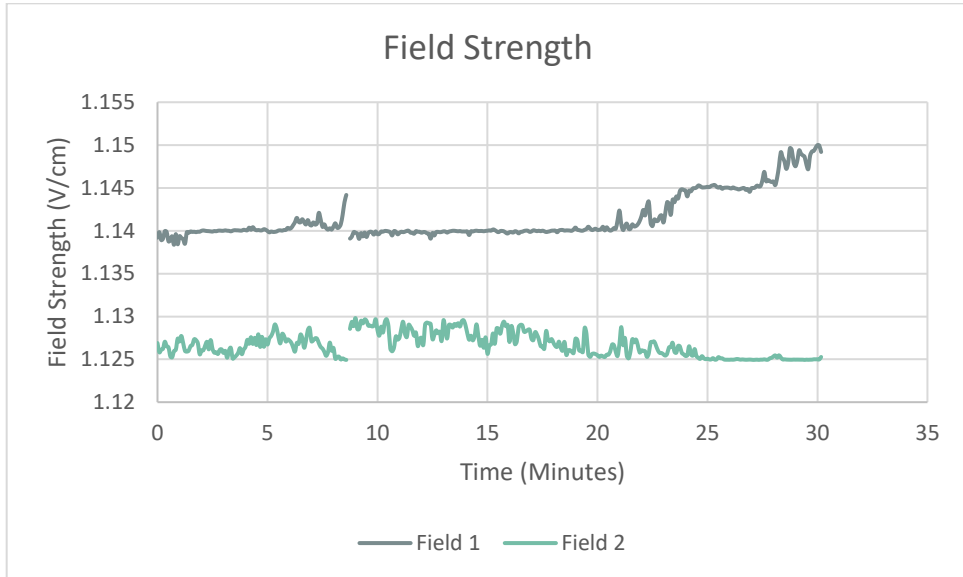
Day1



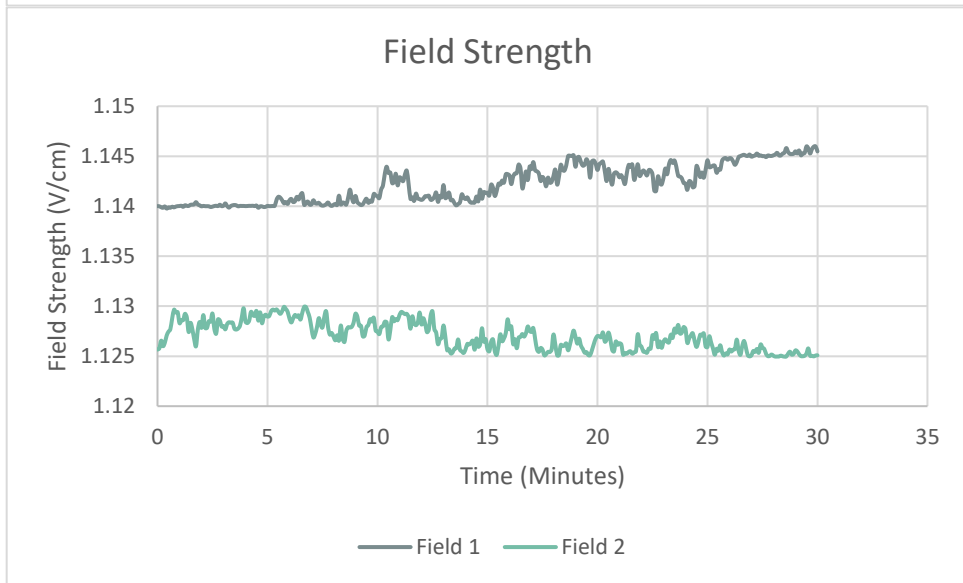
Day 2



Day 3



Day 4



Input Signal	0.8V DC
System	UNO R3
Time	30 mins
Increments	0.5 mins
R _{Load}	1 kΩ

7.6. TECAN Plate Reader Settings

Mode	Fluorescence Top Reading
Excitation Wavelength	540 nm
Emission Wavelength	580 nm
Excitation Bandwidth	5 nm
Emission Bandwidth	5 nm
Gain	217 Calculated From A6 (100%)
Number of Flashes	50
Flash Frequency	400 Hz
Integration Time	20 μ s
Lag Time	0 μ s
Settle Time	10 ms
Z-Position (Manual)	20000 μ m
Part of Plate	A4-A6; B5-D6

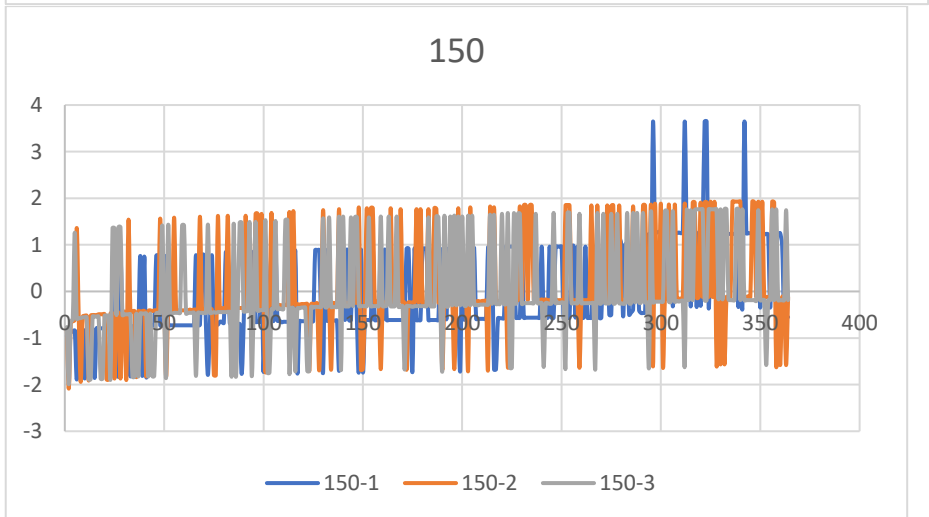
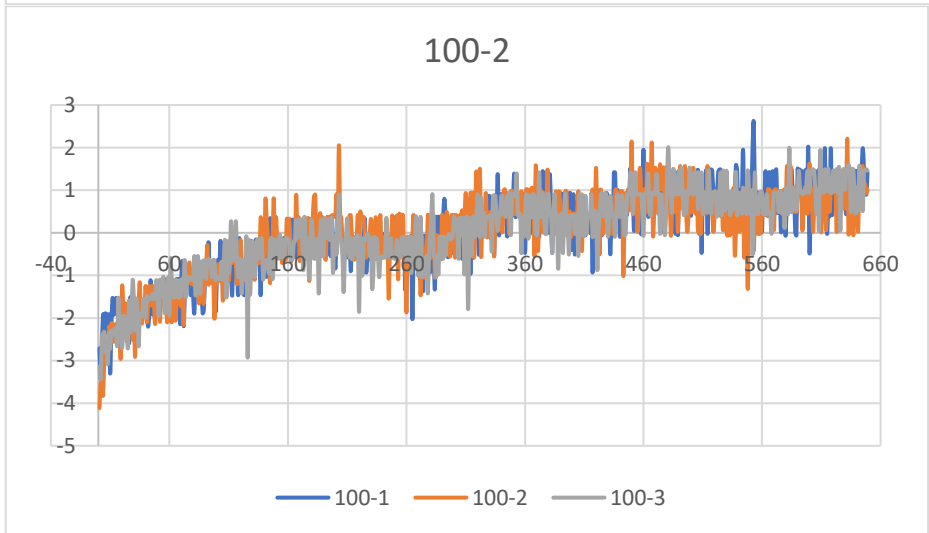
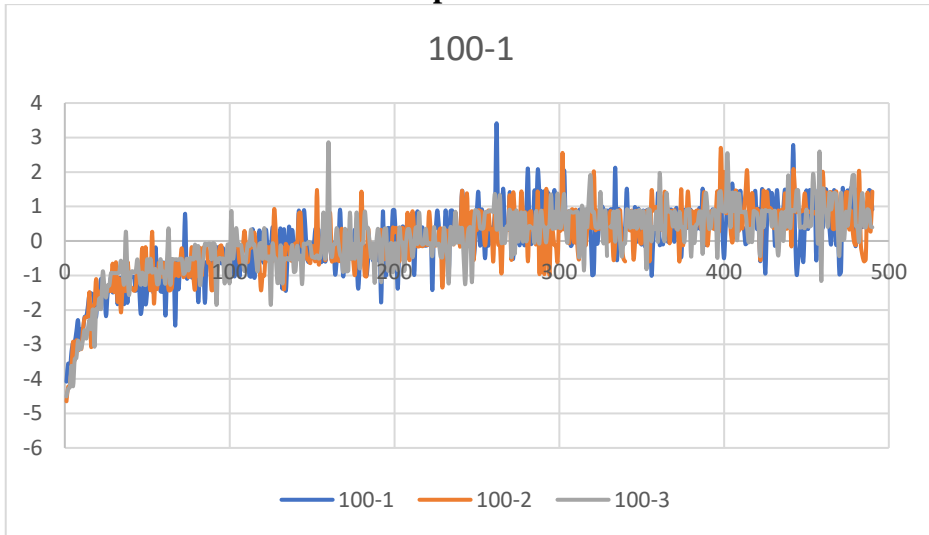
7.7. Alamar Blue Assay Results

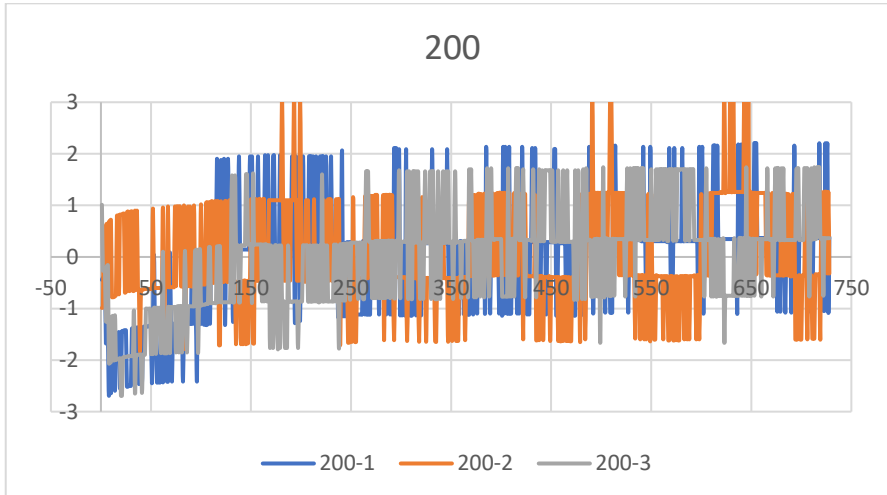
Well		Mean	StDev	0;2	1;2	2;2	2;1	1;1	0;1	0;0	1;0	2;0
CTRL	A4	2649	1114	3516	2986	895	1457	3301	4031	3537	2669	1450
CTRL	A5	2751	1236	3554	2670	1124	1551	3599	4603	3663	2823	1168
CTRL	A6	3016	1252	3883	2855	1236	2107	3910	4887	3910	2975	1382
CC	B5	2959	1335	3751	3131	1243	1486	3939	4929	3884	2979	1286
CC	C5	3233	1463	4364	3384	1375	1650	4281	5374	4144	3117	1404
CC	D5	5322	2394	7265	5725	2761	2732	6783	9286	6164	5025	2157
ES1	B6	3077	1313	3988	2984	1304	2084	3979	5149	3872	3011	1323
Es2	C6	3387	1437	4537	3541	1433	2297	4411	5475	4252	3144	1396
ES3	D6	3597	1489	4894	3545	1507	2601	4836	5632	4438	3390	1530

Normalized based on the position of the measurement

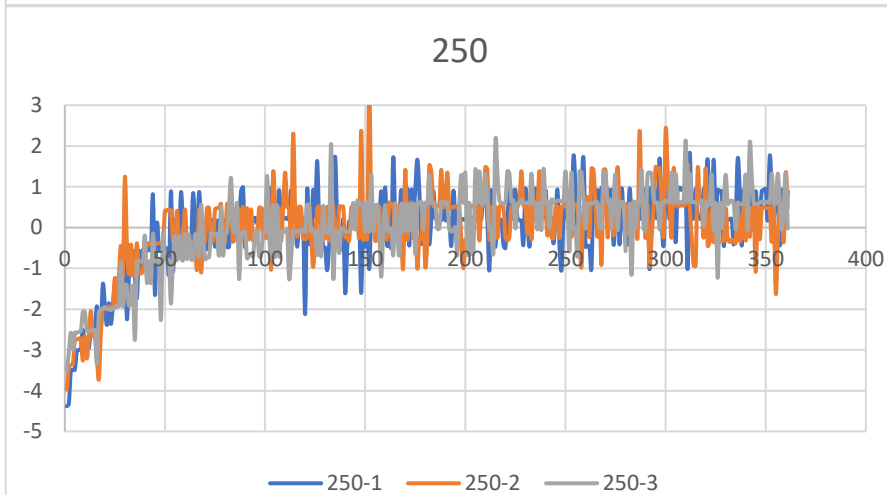
Well		Mean	StDev	0;2	1;2	2;2	2;1	1;1	0;1	0;0	1;0	2;0
CTRL	A4	-683.16	409.6021	-900.889	-438.556	-535.889	-539.111	-1036.67	-1454.11	-670.111	-568	-5.11111
CTRL	A5	-581.716	233.0043	-862.889	-754.556	-306.889	-445.111	-738.667	-882.111	-544.111	-414	-287.111
CTRL	A6	-316.16	240.5701	-533.889	-569.556	-194.889	110.8889	-427.667	-598.111	-297.111	-262	-73.1111
CC	B5	-373.605	171.985	-665.889	-293.556	-187.889	-510.111	-398.667	-556.111	-323.111	-258	-169.111
CC	C5	-99.716	96.45011	-52.8889	-40.5556	-55.8889	-346.111	-56.6667	-111.111	-63.1111	-120	-51.1111
CC	D5	1989.728	1001.796	2848.111	2300.444	1330.111	735.8889	2445.333	3800.889	1956.889	1788	701.8889
ES1	B6	-255.16	172.6049	-428.889	-440.556	-126.889	87.88889	-358.667	-336.111	-335.111	-226	-132.111
Es2	C6	55.06173	117.7267	120.1111	116.4444	2.111111	300.8889	73.33333	-10.1111	44.88889	-93	-59.1111
ES3	D6	264.7284	204.736	477.1111	120.4444	76.11111	604.8889	498.3333	146.8889	230.8889	153	74.88889

7.8. Normalized DMEM Graphs

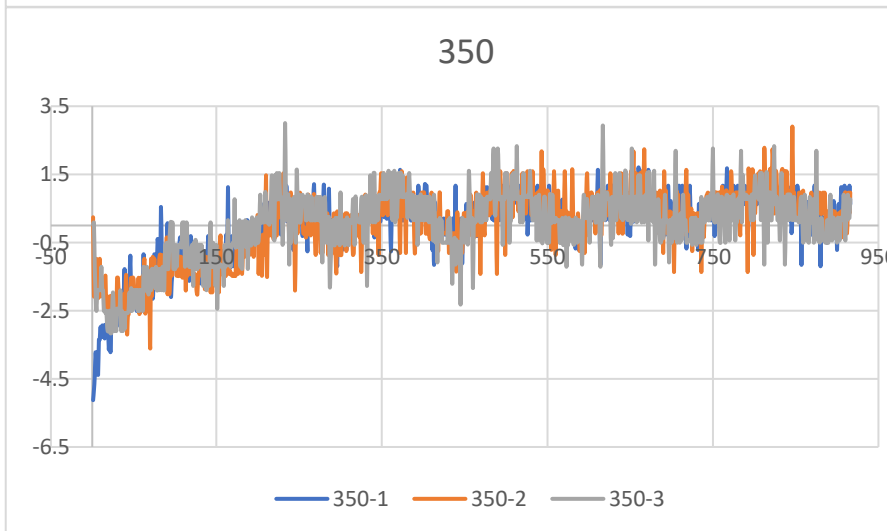




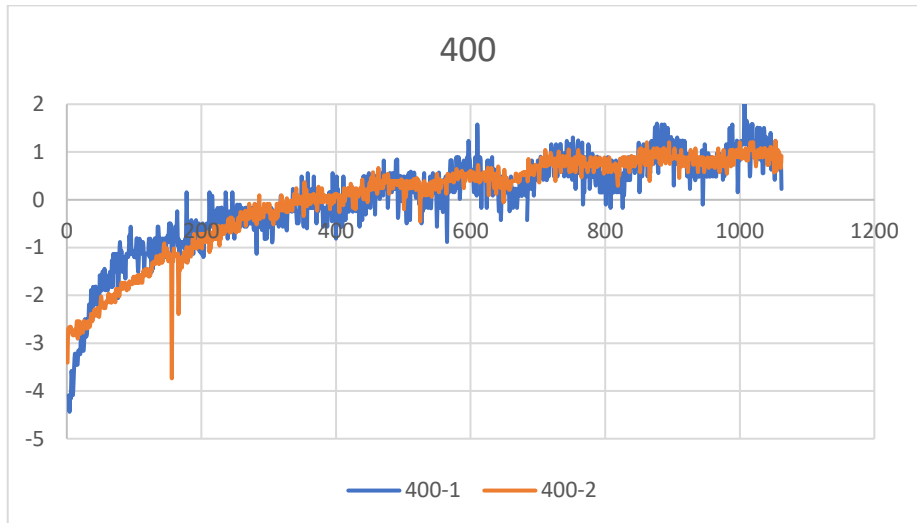
$$y = 0.3323x^{0.3531}$$
$$R^2 = 0.3251$$



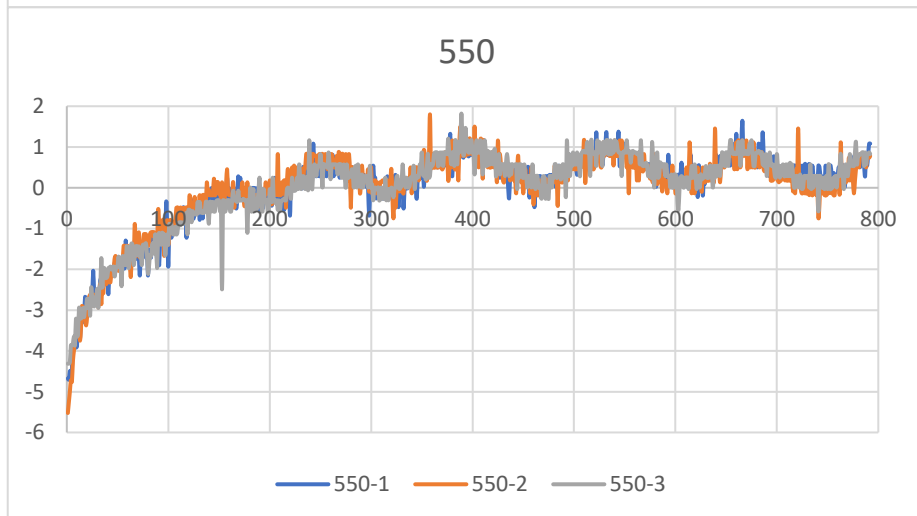
$$y = 0.8436x^{0.326}$$
$$R^2 = 0.5765$$



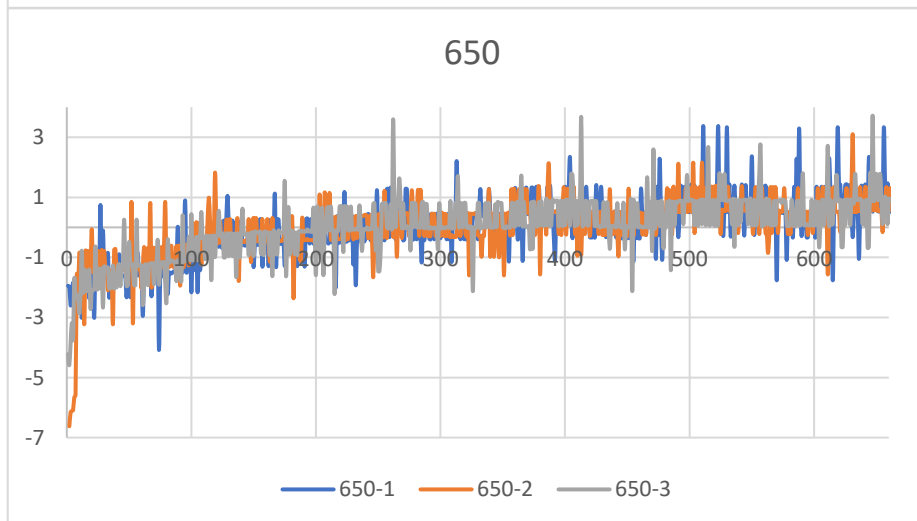
$$y = 1.1334x^{0.2538}$$
$$R^2 = 0.6945$$



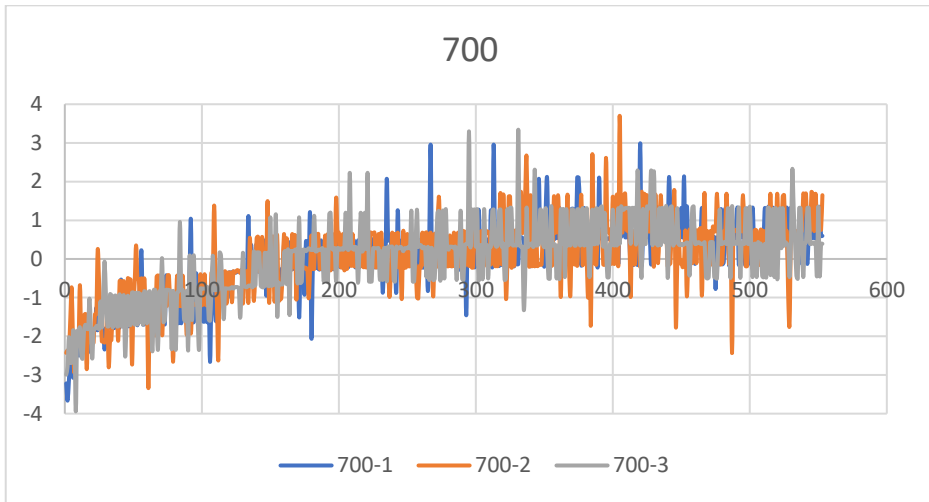
$$y = 0.6842x + 0.3067$$
$$R^2 = 0.6774$$



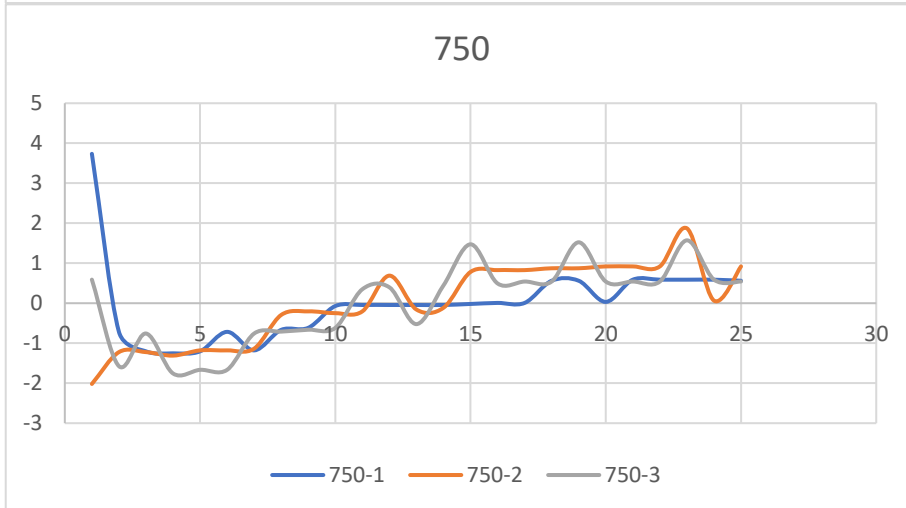
$$y = 0.8493x + 0.2804$$
$$R^2 = 0.5274$$



$$y = 1.1465x + 0.2241$$
$$R^2 = 0.507$$

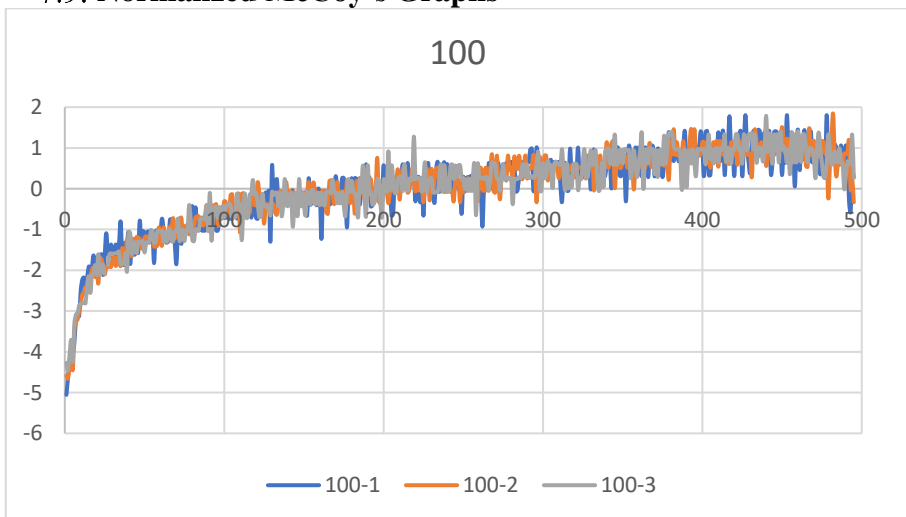


$$y = 0.5898x^{0.3332}$$
$$R^2 = 0.7573$$

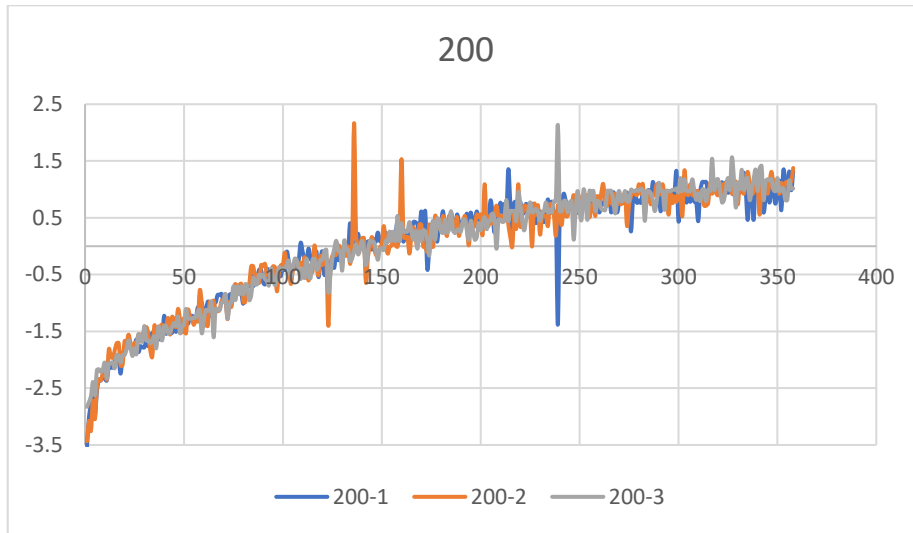


$$y = 0.1253x^{0.7607}$$
$$R^2 = 0.1911$$

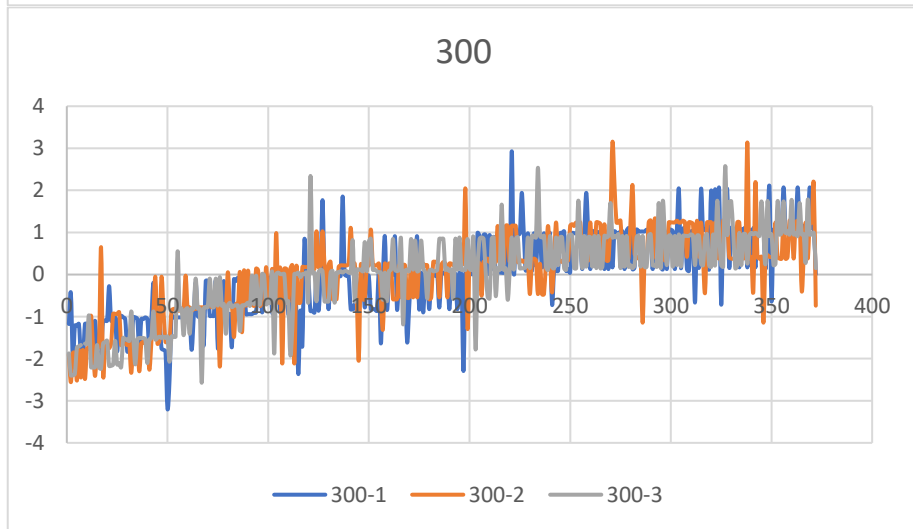
7.9. Normalized McCoy's Graphs



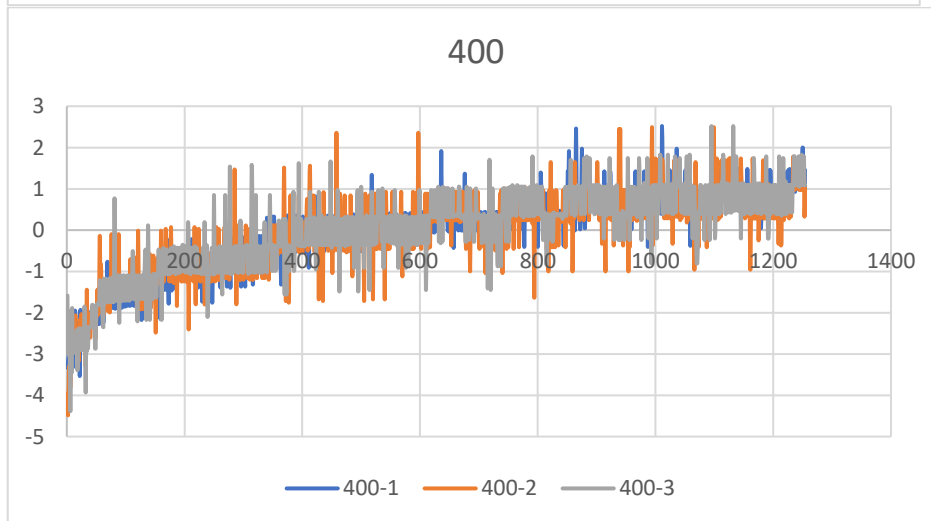
$$y = 0.9905x^{0.306}$$
$$R^2 = 0.6054$$



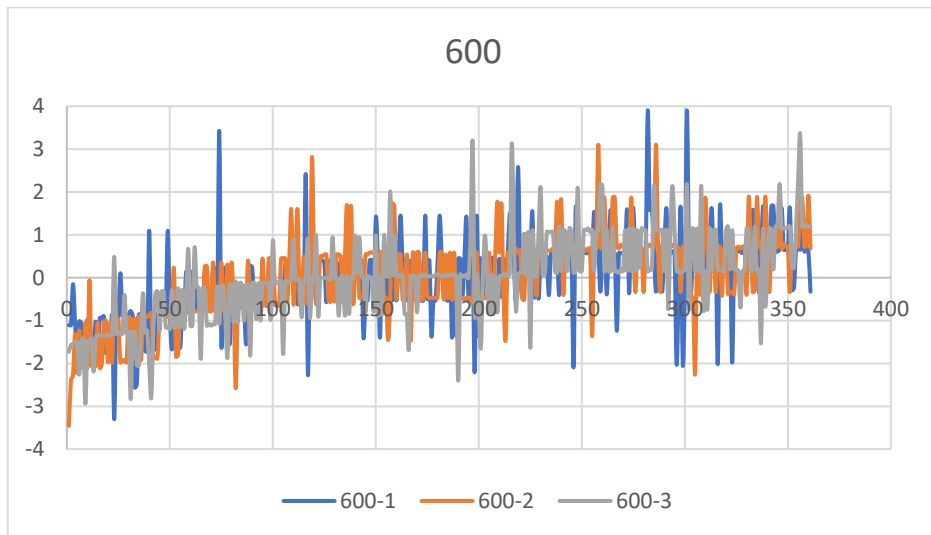
$$y = 0.377x^{0.4432}$$
$$R^2 = 0.8029$$



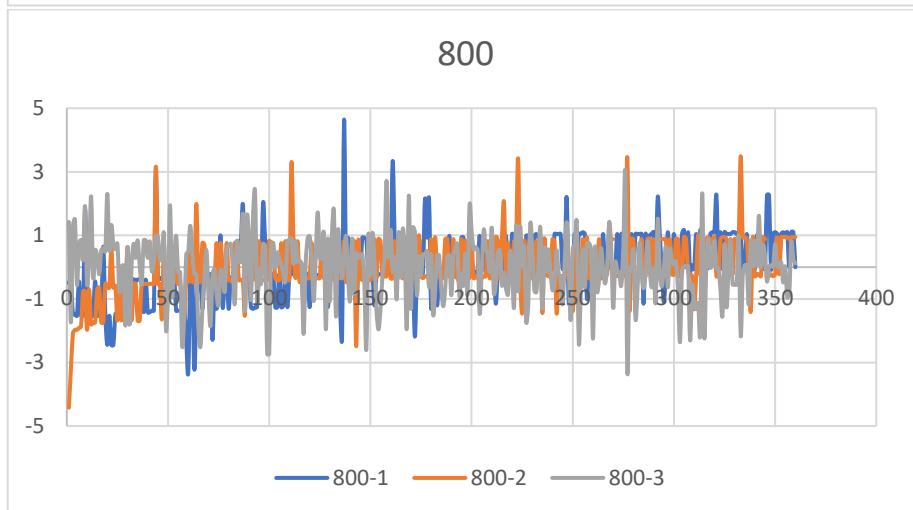
$$y = 0.7596x^{0.2782}$$
$$R^2 = 0.347$$



$$y = 0.3452x^{0.3698}$$
$$R^2 = 0.8246$$



$$y = 1.0366x^{0.2241}$$
$$R^2 = 0.2314$$



$$y = 1.1524x^{0.2026}$$
$$R^2 = 0.1713$$

7.10. **Reviewed Studies on ES of Whole Bone**

Table 4: Reviewed Studies on in vivo Electrical Stimulation on Whole Bone

Model	Stimulation Parameters	Duration of Stimulation	Duration of Experiment [days]	Result	Citation
Mouse	10 μ A	5 min	28	\uparrow number of new blood vessels on day 14 \uparrow number of fibroblasts	[121]
Human	10 μ A 20 μ A	24 hr	14	\uparrow in ALP and Fracture repair	[122]
Rat	10 μ A	5 min	10-90	\uparrow in Collagen Production, Angiogenesis, calcification	[123]
Rabbit	10 μ A 30 μ A	24 hr	35	Improvement of fracture fusion	[124]
Human	10 μ A 20 μ A	24 hr	84	20 μ A helps heal non-union fractures	[125]
Rabbit	100 μ A	24 hr	3-28	Increase BMP-2, BMP-6, BMP-7, TGF-beta	[115]
Rabbit	5-40 μ A	24 hr	21	0-20 μ A \uparrow osteogenesis 50-100 μ A severe damage	[114]
Rabbit	0-100 μ A	24 hr	14	4-6 μ A - no change 15-20 μ A - Periosteal osteogenesis near cathode \uparrow callus formation >100 μ A - destruction to the bone tissue, charring of surrounding tissue	[49]
Rat	5, 10, 20 μ A	24 hr	8	50% thicker (10 μ A) and 80% thicker (20 μ A) bone formation	[34]
OVX Rat	PEMF 40 V PTP 1.5 MHz 1:4 Duty Cycle	20 min	5 x 12 week	Less osteocyte apoptosis Preserves eNOS and iNOS levels	[59]
Rabbit	20 μ A	24 hr	28	Formation of osteoblastic bone	[50]
Dog	10 μ A	24 hr	21	Bone formation around the cathode started poorly organized but improved at 21 days More osteoblasts around the cathode	[57]
Chick Tibia	10 μ A	24 Hours	10	Cathode – thicker periosteum and proliferation of osteoblasts Anode – larger number of osteoclasts and blasts gathered	[29]

7.11. **Reviewed studies on *in vitro* stimulation of cells**

Table 5: Reviewed studies on *in vitro* stimulation of cells

Cell Type	Current Type	Stimulation Parameters	Duration of Stimulation	Duration of Study (days)	Result	Citation
AD MSC	DC	200µA	4 Hours	21	100% more calcium	[116]
MC3T3- E1	CC	60 kHz, 20mV/cm, 50% duty cycle	24 Hours	1	↑ BMP-2, ALP mRNA expression for BMP-2, 4, 5, 6, and 7	[126]
BM MSC	DC	100mV/mm DC Current	1 Hour	3,7,14	↑ osteogenic differentiation, collagen, calcium deposits, expression of Coll1a1, Osteopontin, Osterix and Calmodulin genes 7 days + the results stayed post- testing	[127]
MSC		200mV/mm DC	1 Hour	21	↑ in ERK1/2 phosphorylation, osteopontin (SPP1) expression, and cell proliferation	[100]
	DC	Stimulated Media (200mV/mm DC)	1 Hour	21	↑ osteopontin (SPP1) expression, and cell proliferation	
MC3T3- E1	DC	200mV/mm DC	1 Hour	21	↑ in SPP1 and BMP2, ↓ in cell density around electrodes	
MC3T3-E1	DC	100mV 50-800Hz, square wave 0.1V/cm	1 Hour	1,3,7	200 - 400Hz - max numbers of cells ↑ in ALP, Collagen I ES+IGF – Highest amounts of calcium deposits, RUNX2, collagen 1 and OPN	[110]
Osteoblast- like harvested from rat calvaria	DC	100µA/cm ² through salt bridges connected to stimulated wells	1 Hour	10	↑ in proliferation, calcium entering the cell, calcium is released from the endoplasmic reticulum An Osteocyte network was formed and some osteoblast-like cells transitioned to osteocytes.	[91]
BM-MSCs Chondrocyte s	PEMF	0.7V, 35V/m 1KHz Sine	3x, 45 Minutes, 225 Minutes in between	7	No change in metabolism, ↑ collagen type II	[128]
MLO-Y4	PEMF	15 Hz 0,5,30 G	2 Hours	3	5G – inhibits cellular apoptosis, ↑ dendritic length and OPG mRNA, ↓ RANKL mRNA levels, Media from 5G inhibited osteoclasts and caused apoptosis 30G – Promote Apoptosis of MLO-Y4	[79]

MG63	PEMF	5ms pulses at 15 Hz, 0-18G	8 Hours	4	↑ PGE2, osteocalcin, ALP, ↓ proliferation, more differentiated phenotype	[61]
MLO-Y4	PEMF	5ms pulses at 15 Hz, 0-18G	8 Hours	4	No change in the number of cells, osteocalcin levels, ↑ in PGE2, TGF-Beta 1 initial ↑ then ↓ of cellular activity and Cx43	[78]
ROS 17/23	PEMF	5ms pulses at 15 Hz, 0-18G	24 Hours	3	No change in the number of cells, osteocalcin levels, ↑ in PGE2, TGF-Beta 1 initial ↑ then ↓ of cellular activity and Cx43	[78]
Rat Calvaria	PEMF	25/us width, 3 Hz, varying amplitude	5 Minutes	1	↑ in DNA Synthesis, cAMP Large V drop across the cell membrane	[28]
Rat Calvaria	CC	60-kHz sine capacitively coupled	6 Hours on, 18 off	1	1mV/cm, and 20mV/cm - ↑ proliferation	[30]
Rabbit Osteoclasts	DC	1 V/mm Salt Bridge	17.2 Hours	1	oriented lamellipodia and directed migration toward the cathode	[27]
RCJ 1.20 RCB 2.2A	DC	1 V/mm Salt Bridge	17.2 Hours	1	oriented lamellipodia on their cathodal sides and cellular migration directed toward the cathode	[27]
MC3T3-E1	CC	Cap Coupled 60-Hz sine 44.81 V PTP 2.0 V/m 300 A/cm	30 Minutes- 24 hours	1	↑ in DNA Ca ²⁺ ion movement through voltage-gated channels	[73]
	PEMF	15-Hz burst 20 pulses/burst 4.3 kHz. 22.5 G, and 0.16 V/m.	30 Minutes- 24 hours	1	↑ in DNA cause Ca ²⁺ to be released through intracellular stores	[73]
Rat Calvaria	PEMF	15 Hz 1 G 0.1 mT; 2 mV/cm	14 Hours	1	↑ osteoblast proliferation ↓ in ALP	[71]
Mouse Bone Marrow	PEMF	7.5 Hz 4.8,8.7,12.2 μV/cm	2Hr	9 Days	Osteoclasts appeared after 5 days of stimulation 4.8 μV/cm reduced osteoclast recruitment decreased resorptions area percentage 12 μV/cm increased osteoclast recruitment and bone resorption area percentage	[83]
Mouse Bone Marrow	PEMF	7.5 Hz 3μV/cm	8-16 hours	1	Accelerates apoptosis of osteoclasts	[84]

Mouse Bone Marrow	PEMF	1.6mT 4.8 and 9.6 $\mu\text{V}/\text{cm}$	24 Hours	8 Days	Increased osteoclast-like cell formation Extremely low fields suppressed recruitment of osteoclasts	[85]
-------------------	------	---	----------	--------	--	------